Subsidence Study – Harlingen Upper Cretaceous (Chalk) Reservoir

Vermilion Oil & Gas Netherlands BV.

May, 2007

Addendum September, 2007

Prepared by: Rod Gibbons, P. Eng

Executive Summary

This report was originally submitted to State Supervision of the Mines in May, 2007 and has been refined using their feedback. The results of this review and feedback are contained in Addendum 1: Results of modelling review by SodM, June – September, 2007.

The Harlingen Upper Cretaceous reservoir is a chalk reservoir at a depth of approximately 1000m and has been producing gas since 1988. A total of 1.8 Bcm of gas has been produced (up to September, 2006) with an associated surface subsidence between 9 to 10 cm. The economic limit of the pool is forecasted to be 2016, at which point the ultimate subsidence due to gas extraction is estimated to be 12-13cm.

Geologic and reservoir parameters have been combined in a reservoir model to provide a conceptual model of the pressure depletion of the Harlingen Upper Cretaceous reservoir associated with gas production. This data, along with rock property information from controlled laboratory experiments has been incorporated into a computer simulation to predict gas caused surface subsidence. The model predictions were then compared to actual measured subsidence from survey markers in the area for the years 1997, 2000, 2003, and 2006. The theoretical subsidence model was then iterated until the modelled results had the best statistical fit to the measured data. A review of both surface and deep founded levelling points revealed a wide variety of quality in the foundations of these points and some points were of such suspect quality they had to be excluded.

The subsidence model for the Harlingen Upper Cretaceous reservoir is complete and will be updated periodically when new information is available (pressure surveys, cumulative production) to ensure no major changes are required. The surface subsidence levelling points, and the frequency of

measurement, will be reviewed in detail to generate a measurement plan which provides accurate information in a timely manner.

The results presented in this report are subject to the cumulative statistical uncertainty of the input variables and, as such, are believed accurate to +/- 20%.

Geology and Reservoir Characteristics

The Harlingen calcium formed a deposit during the Upper Cretaceous (Ommelanden). The structure was formed during the Tertiary ("Alpine" compression). The calcium is regionally 200 to 400 metres thick. A geological study shows good homogeneous calcium deposition on the upper side of the thick layers of several meters deep. The deeper situated calcium is more compact with diminished petrophysical qualities. The upper side of the structure is located around 1030 m deep, with a total gas column of approximately 25 metres.

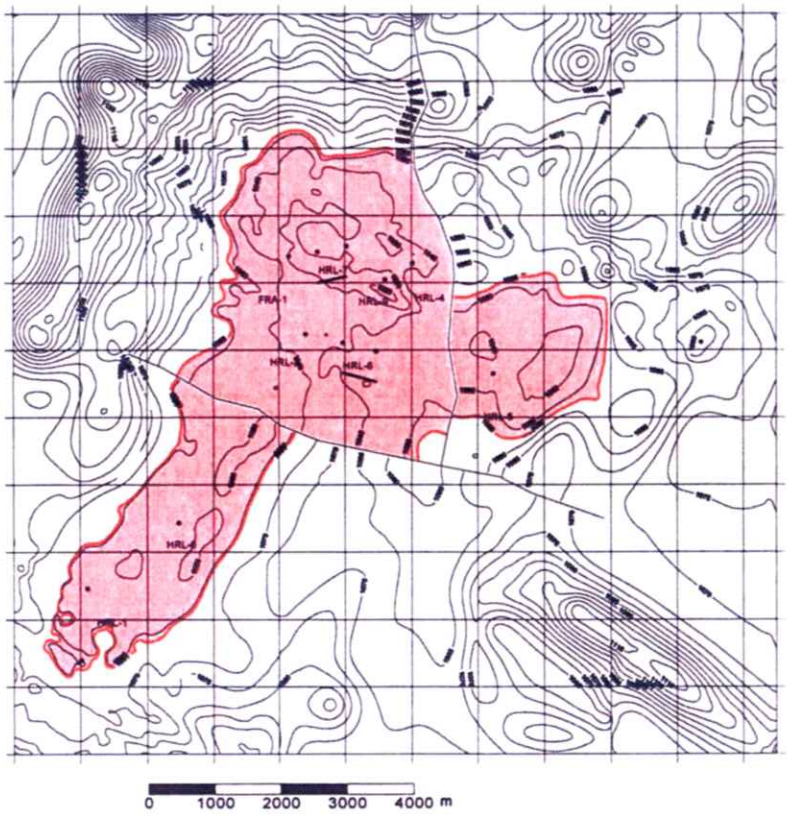

Vermilion Energy Trust	
Harlingen Ommelanden Chalk Structure	
Drawn by DB/VB/DD	

The porosity of the upper side of the layers passes 30%, but the permeability stays around 2 md. The saturations are determined by capillary gravitation

forces and increase along the gas column. The depth of the gas water contact (GWC) seems to be variable, since the capillary pressures differ per place. The depth of the GWC is located at approximately -1053 m/NAP in the northern part of the field. In the southern part of the field, examined by the Harlingen-6 drilling, the upside of the reservoir is located at approximately -1050 m/NAP. The GWC is estimated on -1065 m/NAP. This appears to give an indication of the presence of a barrier between the Northern and Southern parts of the field, even if the seismic profiles do not show a large fault. In the eastern part of the field, examined by the Harlingen-5 drilling, the upside of the reservoir is located at approximately -1030 m/NAP. The GWC is estimated at approximately -1061 m/NAP. This also appears to give an indication of the presence of a barrier between the Northern and Eastern parts of the field, even if the seismic profiles do not show a large fault.

Pool History

The Harlingen Upper Cretaceous reservoir is located in southwest Friesland between the towns of Harlingen and Franeker. The pool was initially discovered in 1964 by well Harlingen-1 which encountered 7m of gas and water but was not deemed economic to develop. In 1988, with the development of the Zuidwal reservoir the gas processing infrastructure was close enough that the development of the Harlingen Upper Cretaceous reservoir was economically possible. The initial development was from wells Harlingen-2, Harlingen-4, Harlingen-5, and Franeker-1 (see Appendix 1: Wellbore Schematics for detailed completion information). The well Harlingen-6 was drilled in 1985 but was not put on production until 1997 (primarily due to the distance from existing infrastructure). A number of wells, including Harlingen-3 and Ried-2, intersected the reservoir, but in the down-dip, non-productive aquifer region. Two horizontal wells, Harlingen-7 and Harlingen-8, were added in 1992 and 1994, respectively. The final well to be brought on production was Harlingen-9 in 2001.

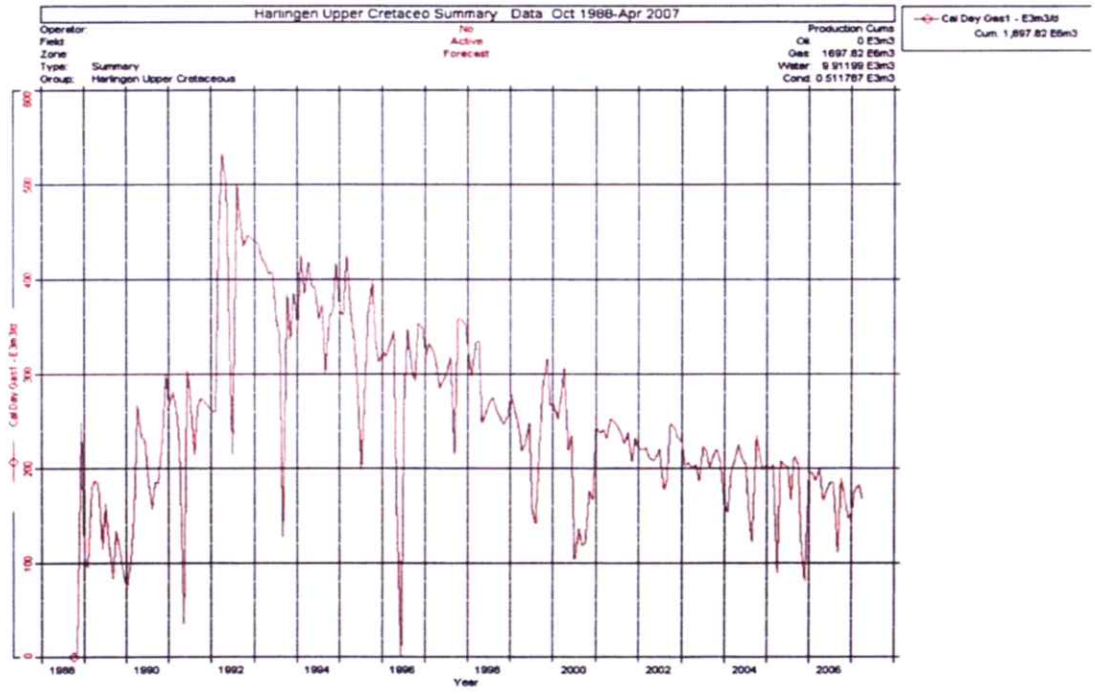

The field has produced a small amount of water from the start of production and the water gas ratio has remained fairly constant. The productive interval

has an increasing gas water contact from the top of structure down to the gas water contact (S_w = 100%) with decreasing reservoir properties (Permeability and porosity) from top to bottom.

The reservoir is composed of three pools, the South pool is produced by well Harlingen-6, the East pool by well Harlingen-5, and the North Pool is produced by the remaining wells in the reservoir. Each of the three pools display a straight line relationship on the P/z plots indicating no aquifer support and a pressure depletion drive mechanism.

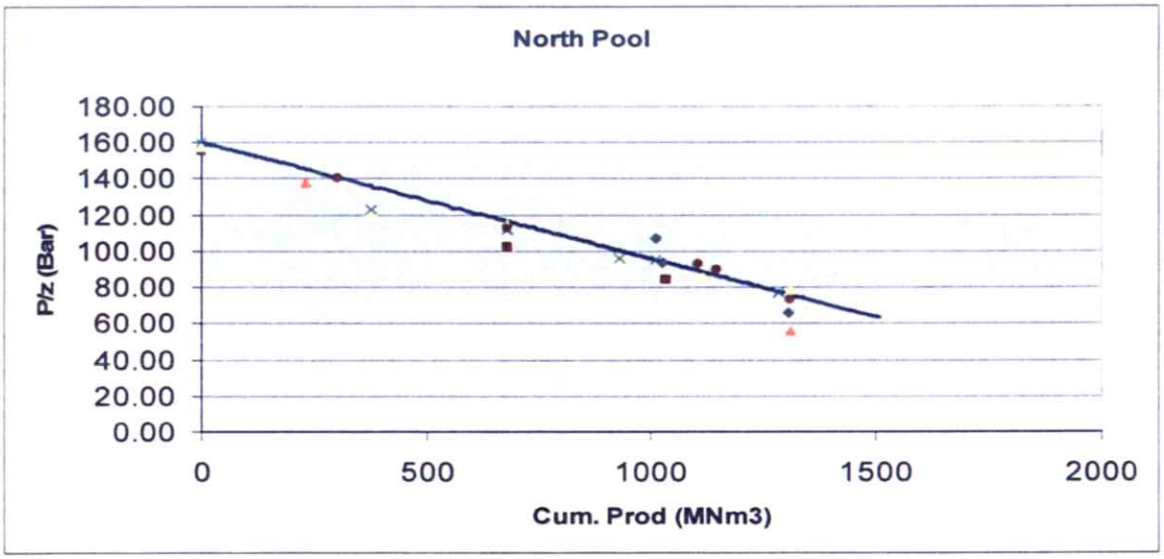

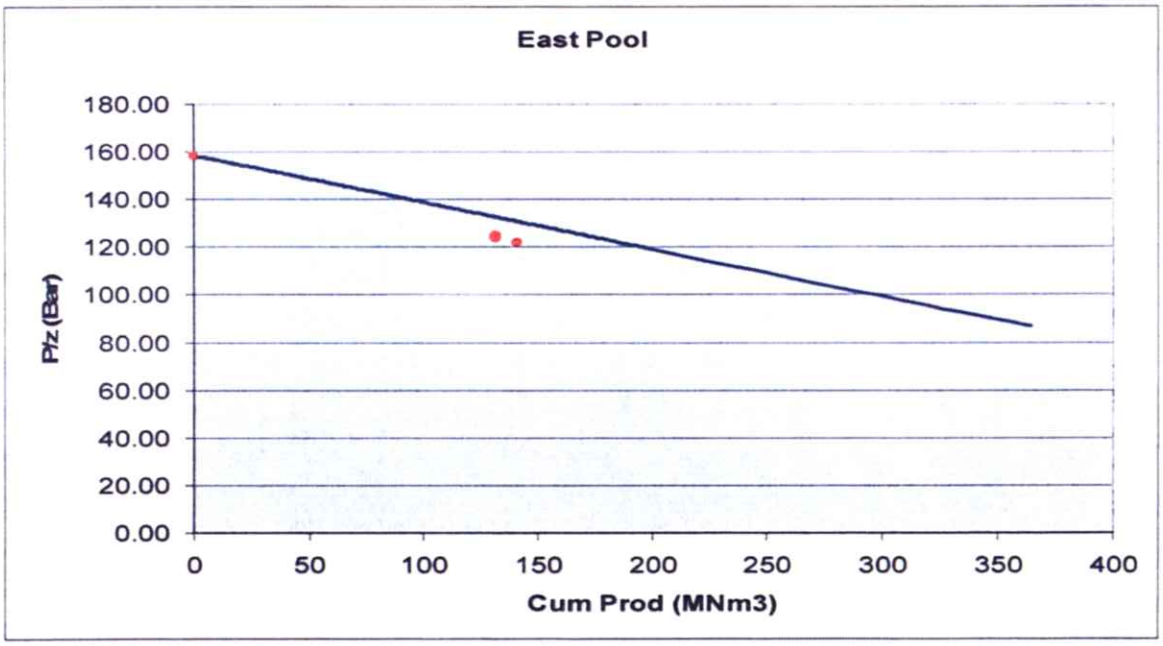

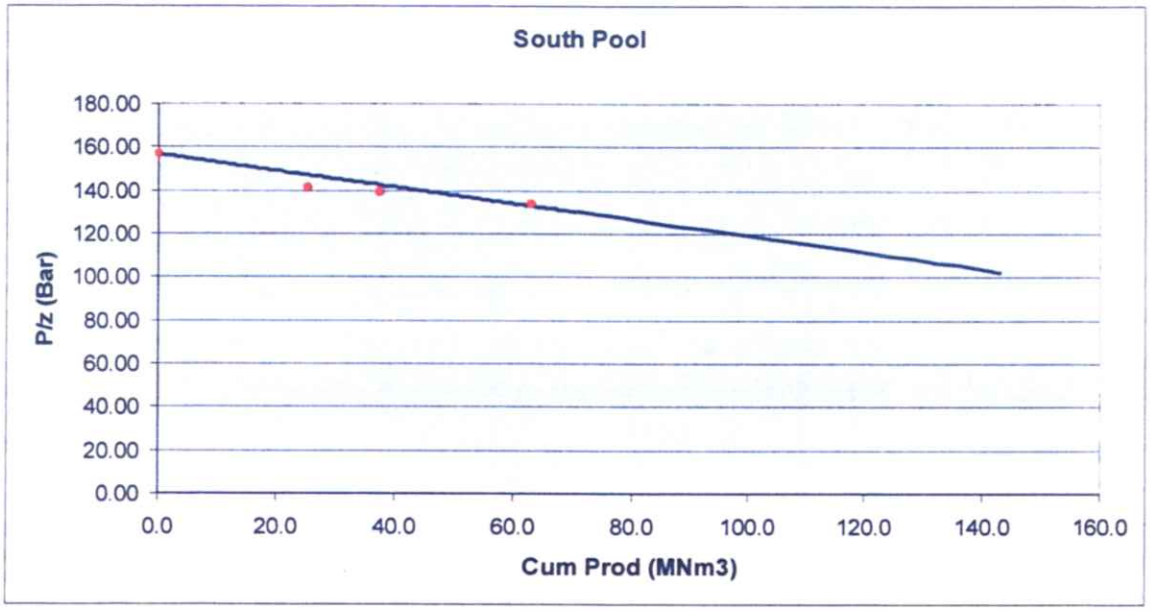

The reservoir is poor quality (average porosity of 25% and average permeability of 2md) and the well productivity is low with current well rates between 15 – 50 e3m3/d.

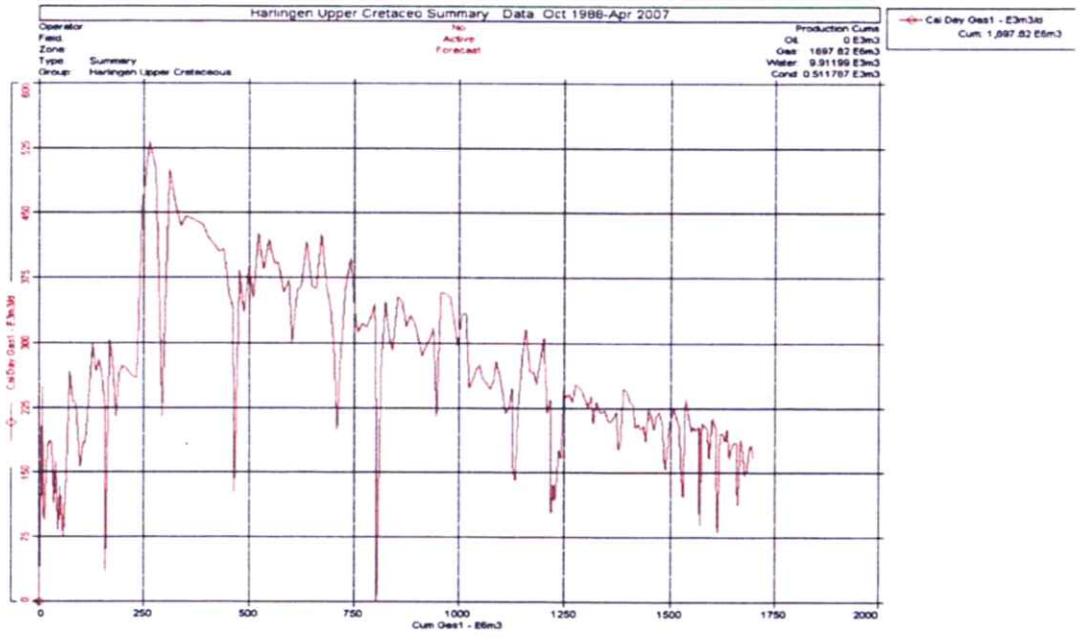

Economic Limit

Future Development

Infill drilling is planned for the Harlingen Upper Cretaceous reservoir in 2007. The primary purpose of the three wellbores in the reservoir is to assist drainage of areas of the reservoir that will not be drained by existing wells before the economic limit is reached due to the tight reservoir properties.

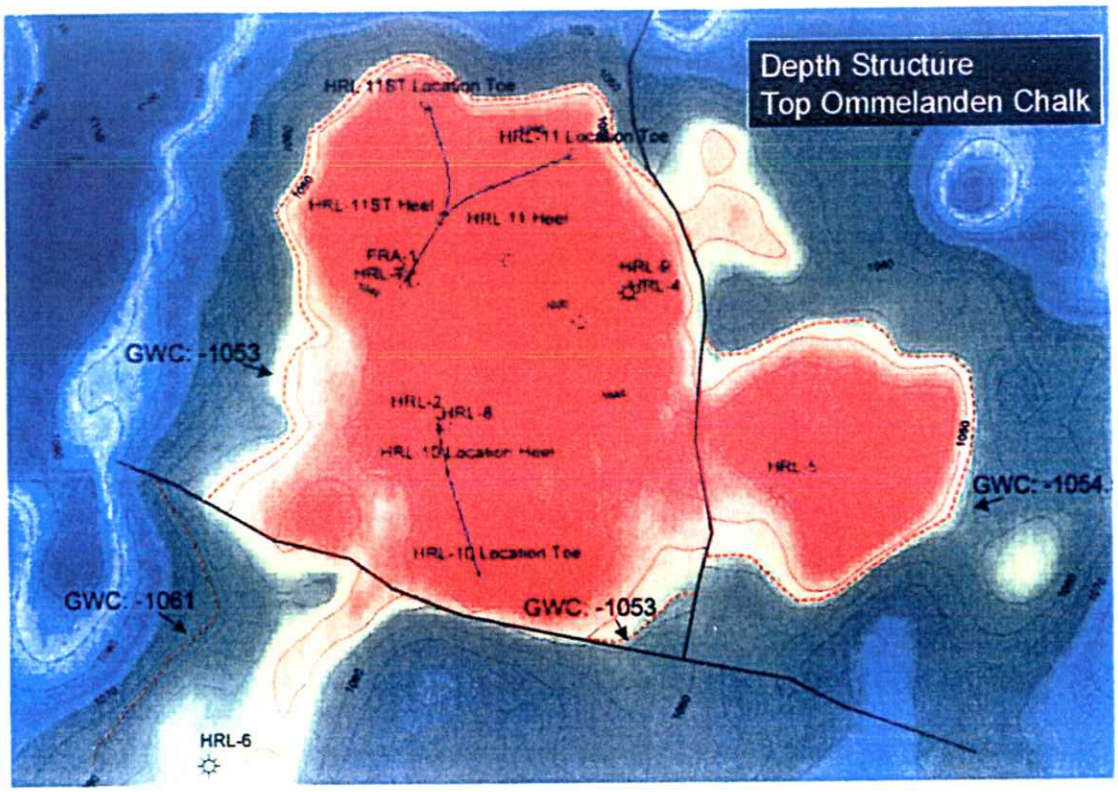

Additional wellbores will allow more uniform pressure depletion and will increase the economically recoverable gas from the reservoir and are targeting the higher pressure parts of the reservoir.

Gas Caused Subsidence Theory and Process

The production of natural gas from a chalk reservoir can cause subsidence at surface. The nature and extent of this subsidence is dependent on a number of factors. Natural gas in a reservoir is contained in the pore space between the rock. As the natural gas is produced from the reservoir, volume is removed, and the remaining gas is at a lower pressure than originally. The reservoir pressure acts on the reservoir rock (from the inside, per se), as does the weight of the overburden. As sediment is deposited on the reservoir rock the pressure acting down on the reservoir increases. When gas is extracted, the internal pressure on the rock is lowered, and then the pressure from the overburden is supported more by the rock than in its pre-development condition. The overburden then compresses the reservoir rock and creates reservoir compaction. This compaction is then transmitted through the layers of the overburden until the surface subsides.

The amount of reservoir compaction is dependant on the amount of pressure drop in the reservoir (DP), the thickness of the rock being depressurized (h), and the strength of the reservoir rock (Cm). The amount (in total depth and aerial extent) of surface subsidence is dependant on the elasticity of the overburden layers and the depth of the compacting reservoir. Surface subsidence is sometimes referred to as the subsidence bowl since the compaction of a single point source will spread to a larger area at surface in a shape similar to a bowl.

Historical Estimation

The estimation of maximum surface subsidence due to gas extraction from the Harlingen Upper Cretaceous reservoir in the existing winningsplan

submitted in 2003 was 10cm (+/- 20%). This estimate was based on pressure depletion from material balance analysis, reservoir thickness from volumetric analysis, and rock compressibility based on laboratory results of core from the well Reid-2 (Cm = ~3 E^{-5}/bar).

In 2006, surface subsidence measurements were recorded that were above this maximum value, prompting a review of the subsidence calculations. The initial estimate of gas caused subsidence utilized the inversion model which calculated rock compressibility from surface subsidence. The result was a rock compressibility of greater than 10 E^{-5}/bar (equivalent to one of the highest values for chalk reservoirs) and associated maximum surface subsidence of 13 – 17cm. This suggested the chalk was in collapse mode which was highly unlikely for the porosities seen in the reservoir. These conclusions prompted further testing of reservoir rock, and, samples from the well Harlingen-7 (in the area of maximum surface subsidence with samples from the productive gas zone) were sent to the Norwegian Geotechnical Institute in Oslo for uniaxial strain compaction testing in a triaxial test cell. A review of the surface subsidence levelling points was also conducted.

Reservoir Model

The Harlingen Upper Cretacous reservoir is modelled as a pure depletion drive with no support from the aquifer. This interpretation is based on the poor reservoir quality below the gas-water contact (cementation of permeability), the low water production rates, and the pressure drop during cumulative production (P/z plot). The material balance equations indicate a linear relationship between the amount of gas produced and the drop in reservoir pressure.

The reservoir simulation uses the correlation between pressure drop and cumulative production in each pool – North, South, and East, to give an average pool pressure for the cumulative production in each pool. The cumulative production is measured from well testing and gas sales volumes monthly, and the reservoir pressure is taken from pressure recorders run in wells at different times. The pressure recorders do show that the actual pool pressure is higher than the pressures measured at the wellbores as evidenced by well pressure still building after a shut-in period. This also indicates a 'tight' reservoir. This is handled in the simulation by taking the average pool pressure from the material balance relationship, the pressure measured at the wellbore as a minimum, and calculating a pressure gradient in the reservoir based on these two points (i.e. as you get further away from the wellbore, the reservoir pressure increases).

The material balance values are history matched to historical pressures and production volumes and then reservoir pressures are forecasted forward based on future production volumes. This is then converted to the time scale by using decline analysis to determine when a well will reach a cumulative volume.

The reservoir model has a grid size of 300m by 300m, and the reservoir thickness is assumed to be constant in each pool from reservoir top down to the gas-water contact (S_w=100%). This gives a thickness of 18 meters, 27 meters, and 34 meters for the South, East, and North pools respectively. The following is an example of pressure distributions in the reservoir (North is to the right of the page in this illustration).

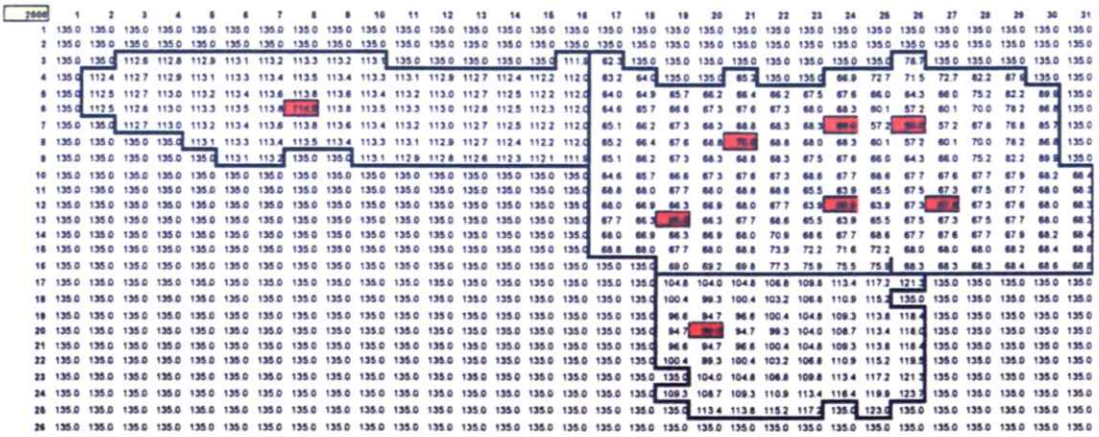

Rock Mechanics

Uniaxial strain compaction experiments were conducted on core samples recovered from the Harlingen-7 well in the North pool of the Harlingen Upper Cretaceous reservoir (see Appendix 2; Uniaxial Compaction Coefficient of Chalk, Compressibility of Harlingen chalk, Norwegian Geotechnical Institute). The purpose of the experiments were to determine the compaction coefficient, C_m, of the Harlingen Upper Cretaceous chalk.

The testing was conducted on both dry and brine saturated samples obtained from the Harlingen-7 well. The dry sample produced a compaction coefficient of $1.70E^{-5}$/Bar and the brine saturated samples produced an average compaction coefficient of $2.58E^{-5}$/Bar and then, with applied stresses increased to simulate abandonment pressure, transitioned to an average of $3.92E^{-5}$/Bar. The maximum value of C_m obtained on these brine saturated samples was $4.86E^{-5}$/Bar in a pressure depleted reservoir condition.

The results of this testing established a range of compaction coefficient that should be applicable to the Harlingen Upper Cretaceous reservoir. Given the relatively high water saturations in the productive interval of the reservoir (i.e. transition zone), the test results from the brine saturated samples are considered more indicative of the average C_m values for the reservoir.

Overburden Model

The layers of sediment overlying the Harlingen Upper Cretaceous reservoir (the overburden) were modelled using TNO's AEsubs subsidence modelling software. The Stratigraphic layers are divided into four distinct layers with varying properties (Young's Modulus and Poissons ratio) and are the Quartenery, Miocene / Oligocene, Bruxxelian, and the Eocene / Paleocene.

Unit No.	Stratigraphic Unit	Thickness (m)	Depth top layer (m)	E (Gpa)	V
1	Quartenery	300	0	0.2	0.4
2	Miocene, Oligocene	320	300	0.5	0.3
3	Bruxxelian	80	620	2.5	0.2
4	Eocene, Paleocene	349	700	1.5	0.25

The elasticity properties for these layers were available from earlier subsidence studies (Elf, 1994). The surface subsidence predictions were run with a number of variations in overburden subdivision and stiffness in this area and had a negligible effect in subsidence calculations.

Subsidence Model

The modelling of gas caused subsidence from the Harlingen Upper Cretaceous reservoir was done with AEsubs subsidence modelling software, developed by TNO (reference to Fokker, 2002; and Fokker and Orlic, 2006). Using reservoir parameters from the reservoir model and compaction coefficients from the rock mechanics experiments, the AEsubs program calculates reservoir compaction at a number of point sources in the compacting reservoir. A solution is found for each point source and then integrated over each grid block (in this case a 250 meter x 250 meter surface grid) to calculate the resulting subsidence pattern at surface.
The initial subsidence model run used parameters calculated from reservoir modelling and uniaxial strain experiments and was compared to levelling data from the deep founded levelling points 0A2750, 0A2752, and 0A2756 for the years 1997, 2000, 2003, and 2006.

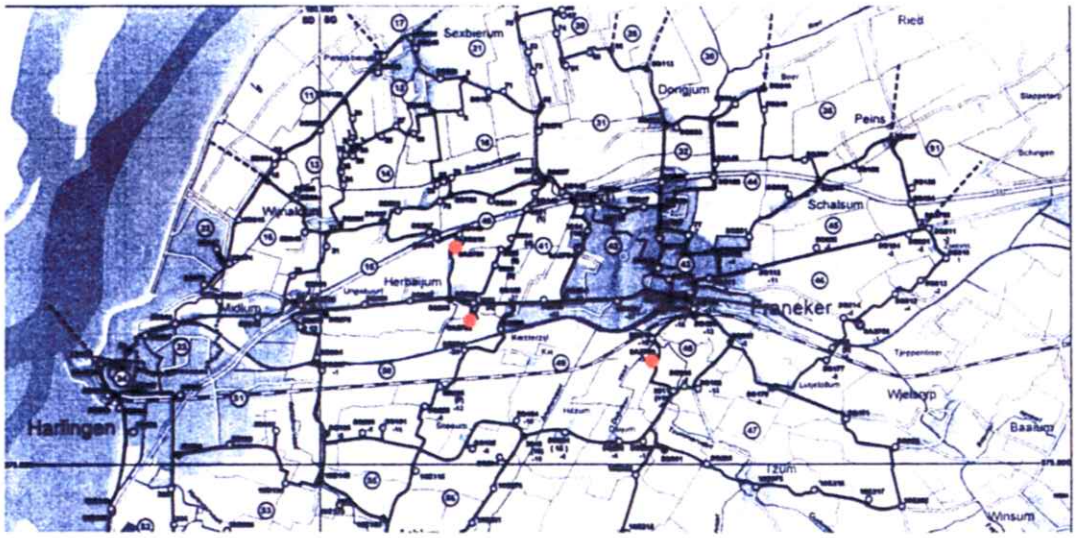

Reservoir pressures and compaction coefficients were then iterated to generate a solution that best matched the surface subsidence measurements of these deep founded points.

Once a reasonable match for these points was found for the four years of surveying data (spread over nine years), the prediction was then compared to

shallow founded subsidence markers for the same years. Further model iterations were conducted until the final simulation provided a best fit to the surface and deep founded survey markers (levelling points are addressed in the following section).

Levelling Points

Surface subsidence is measured by surveying ~60 levelling points every three years. These levelling points, or benchmarks, are a combination of deep founded and surface founded. Seven of the points are deep founded and the remainder are surface founded. The surface founded points are bolts connected to surface structures such as houses, barns, sheds, etc. and are dependant on the foundations and construction quality of these structures to provide accurate measurements of subsidence. The deep founded levelling points are specifically constructed to measure subsidence without the influence of shallow compaction forces such as ground dewatering, peat compaction, and faulty building construction.

These deep founded points are composed of a metal rod inside a driven metal tube (see Appendix 3; Grondmechanica Delft construction report). The tube is driven through the soft surface layer until it reaches a hard ground layer which prevents it from being driven further (this is monitored by both the pressure required to drive the rod and the friction pressure). Five of these deep founded levelling points were driven and landed in what appears to be the hard Pleistocene layer and could be expected to give reliable results. One deep founded point (0A2754) was driven to 37 meters searching for this hard layer, but not encountering high friction pressure, the survey tube was finally located at 31 meters. The absence of a deep hard layer combined with the fact the survey rod was landed above the already pre-driven hole would suggest this point is not a reliable survey point. This could also imply a shallow surface geology (such as a potential peat layer) not continually present in this part of the province of Friesland. The deep founded levelling point 0A2750 also did not see the friction pressure response in the other five reliable deep founded points but the survey point was located at the bottom of the driven hole, making it more reliable than 0A2754 but one would expect it to be less reliable than the other five points (this may also suggest a shallow subsurface condition different than seen regionally).

The following graph shows the variance in the modelled values when compared to the measurements of the deep founded points 0A2750, 0A2752, and 0A2756 for 1997, 2000, 2003, and 2006.

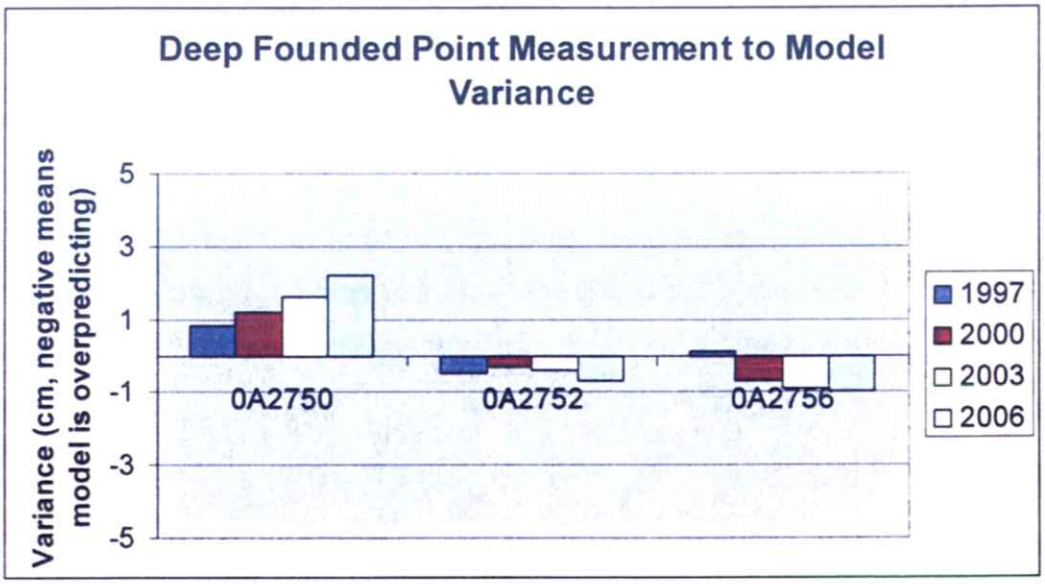

The measured values of points 0A2752 and 0A2756 are less than the model predicted values for all but one sample. Point 0A2750 has a trend of increasing variance over time which is not reflected in the other two deep founded levelling points. This variance between modelled and measured readings could be due to the construction quality of point 0A2750 (as previously noted) and the influence of salt modelling on this point. Points 0A2750 and 0A2752 have similar reservoir depletion, thickness and resulting gas caused subsidence, however salt modeled subsidence for 0A2752 is 15% of measured, while for 0A2750 it is 50% of measured (2006 data). A breakdown of salt and gas modelled subsidence for all points is provided later in the table on page 23.

The surface levelling points, as mentioned earlier, are mounted on existing structures, and therefore, can be affected by surface compaction and building techniques. A field inspection of points 3004 and 3005 showed them to be connected to structures subject to localized subsidence or questionable foundations.

Surface levelling point 5G219, located only ~50 meters from deep founded point 0A2750 showed an difference of 3.4cm in 2006 indicating this point is affected by localized surface subsidence. Levelling point 5G165 also demonstrates high variation to it's neighbouring levelling point 5G208 which is located closer to the gas reservoir.

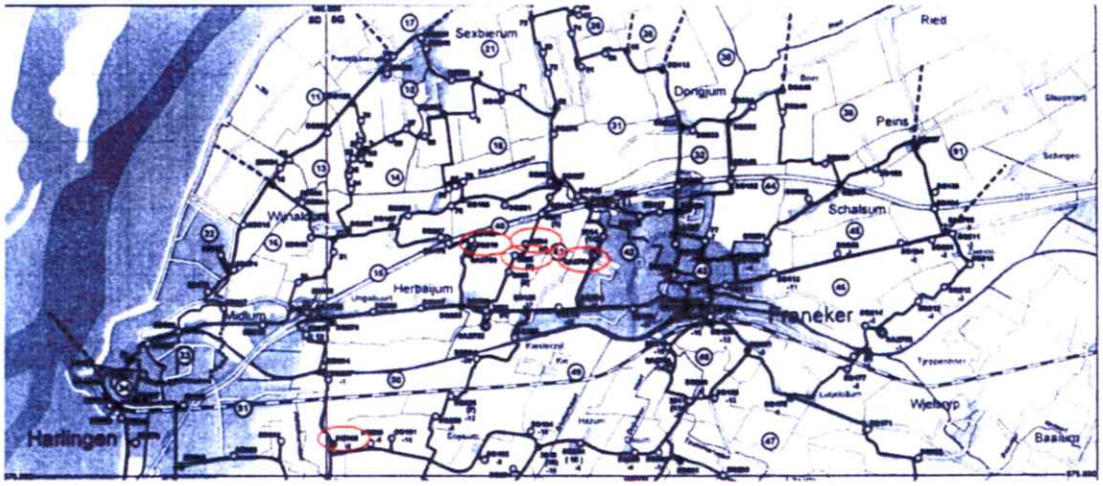

When compared to the modelled surface subsidence, the 2006 modelled surface subsidence matched the reliable survey points to within +2.2cm / -3.3cm with a mean difference of –0.5cm (on average, the model is predicting 0.5cm more subsidence than the measured values). Using the deep founded survey points 0A2750, 0A2752, and 0A2756 the modelled values matched the measured points to within +2.2cm / -1.0cm with a mean difference of 0.2cm. The following plot shows the distribution of model results compared to

measured data for 2006 (negative values indicate the model is predicting more subsidence than measured).

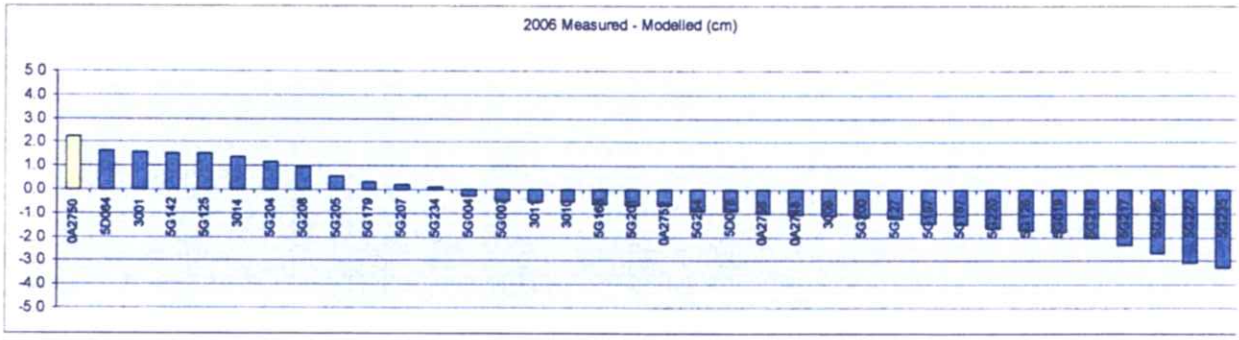

This variation is displayed in map view in the following graphic;

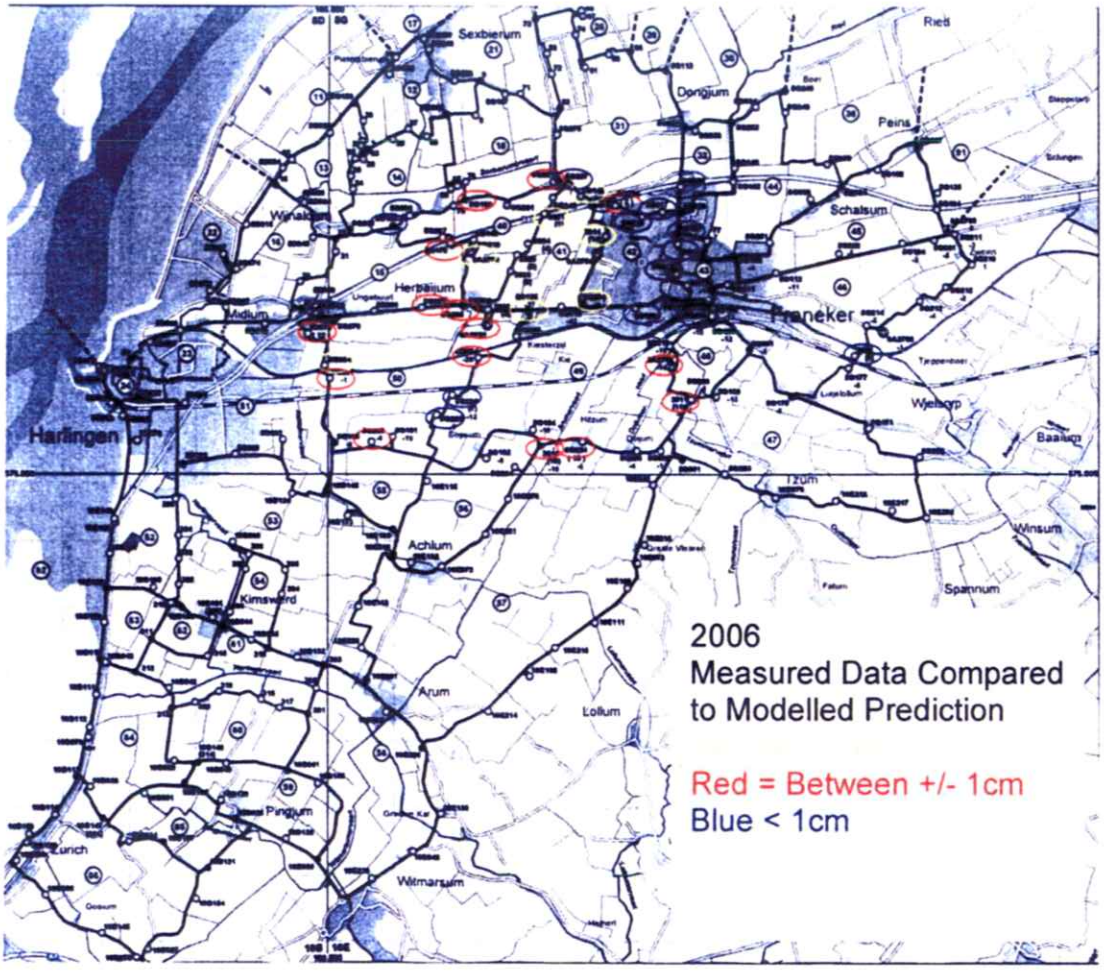

The above figures were generated from the output of the subsidence model and the measured surface data subtracting the theoretical salt model subsidence.

Levelling Point	x	y	Gas Model Value	Total Salt Model	Total Modelled	Total measured subs 2006	Measured - Modelled (cm)	Comments
5G219	162160	578400	-0.0753	0.0777	0.1530	0.208	5.5	Excluded based on variation to 0A2750.
0A2754	164020	578300	-0.0871	0.0056	0.0927	0.143	5.0	Excluded based on construction problesm.
3004	162990	578515	-0.0910	0.0361	0.1271	0.171	4.4	Excluded based on evidence of localized settling.
3005	162820	578290	-0.0907	0.0352	0.1259	0.162	3.6	Excluded due to building structural collapse.
5G165	160120	575510	-0.0015	0.0006	0.0021	0.027	2.5	Indicates possible 2.5cm surface compaction.
0A2750	162160	578380	-0.0756	0.0761	0.1517	0.174	2.2	Included but questionable construction.
5D064	159950	576630	-0.0005	0.0074	0.0079	0.024	1.6	
3001	163230	578916	-0.0933	0.0380	0.1313	0.147	1.6	
5G142	163760	579150	-0.0870	0.0217	0.1087	0.124	1.5	
5G125	162980	577420	-0.0868	0.0089	0.0957	0.111	1.5	
3014	164150	578580	-0.0842	0.0062	0.0904	0.104	1.4	
5G204	163820	577570	-0.0884	0.0030	0.0914	0.103	1.2	
5G208	160650	575470	0.0000	0.0006	0.0006	0.01	0.9	
5G205	162030	577510	-0.0750	0.0276	0.1026	0.108	0.5	
5G179	161800	578460	-0.0631	0.1072	0.1702	0.173	0.3	
5G207	160010	576450	-0.0010	0.0052	0.0062	0.008	0.2	
5G234	163820	575480	-0.0091	0.0000	0.0092	0.01	0.1	
5G004	162250	576750	-0.0786	0.0060	0.0846	0.082	-0.3	
5G007	161400	577510	-0.0288	0.0395	0.0684	0.064	-0.4	
3011	165540	576150	-0.0148	0.0000	0.0148	0.01	-0.5	
3010	163200	575450	-0.0168	0.0001	0.0169	0.012	-0.5	
5G168	162060	579130	-0.0759	0.1521	0.2281	0.222	-0.6	
5G201	163260	579330	-0.0803	0.0503	0.1305	0.124	-0.7	
0A2752	162390	577240	-0.0778	0.0130	0.0908	0.084	-0.7	
5G254	164304	579035	-0.0823	0.0078	0.0901	0.081	-0.9	
5D078	159770	577110	-0.0033	0.0169	0.0202	0.011	-0.9	
0A2756	165220	576610	-0.0502	0.0000	0.0502	0.04	-1.0	
0A2748	159820	577420	-0.0001	0.0293	0.0295	0.019	-1.0	
3009	167950	576850	-0.0133	0.0000	0.0133	0.002	-1.1	
5G200	161230	578900	-0.0182	0.2013	0.2196	0.208	-1.2	
5G127	165250	578450	-0.0524	0.0005	0.0529	0.041	-1.2	
5G197	165250	578600	-0.0466	0.0006	0.0471	0.033	-1.4	
5G167	160950	578730	-0.0102	0.1864	0.1966	0.182	-1.5	
5G220	161620	575890	-0.0317	0.0014	0.0331	0.017	-1.6	
5G126	164600	577490	-0.0847	0.0005	0.0853	0.068	-1.7	
5G019	165240	578000	-0.0676	0.0003	0.0679	0.05	-1.8	
5G218	164620	578890	-0.0834	0.0036	0.0870	0.067	-2.0	
5G217	165020	578930	-0.0649	0.0016	0.0665	0.043	-2.3	
5G285	165815	577525	-0.0375	0.0000	0.0376	0.011	-2.7	
5G227	163320	579350	-0.0807	0.0472	0.1280	0.097	-3.1	
5G235	162000	576140	-0.0547	0.0020	0.0567	0.024	-3.3	

The 2006 data can be described by the following statistics;

Mean	-0.54
Standard Error	0.23
Median	-0.67
Standard Deviation	1.40
Sample Variance	1.95
Kurtosis	-0.55
Skewness	0.14
Range	5.50
Minimum	-3.27
Maximum	2.23
Sum	-19.35
Count	36.00
Confidence Level(95.0%)	0.47

The modelling results give similar results for years 2003, 2000, and 1997 shown in the following graphs and figures.

2003;

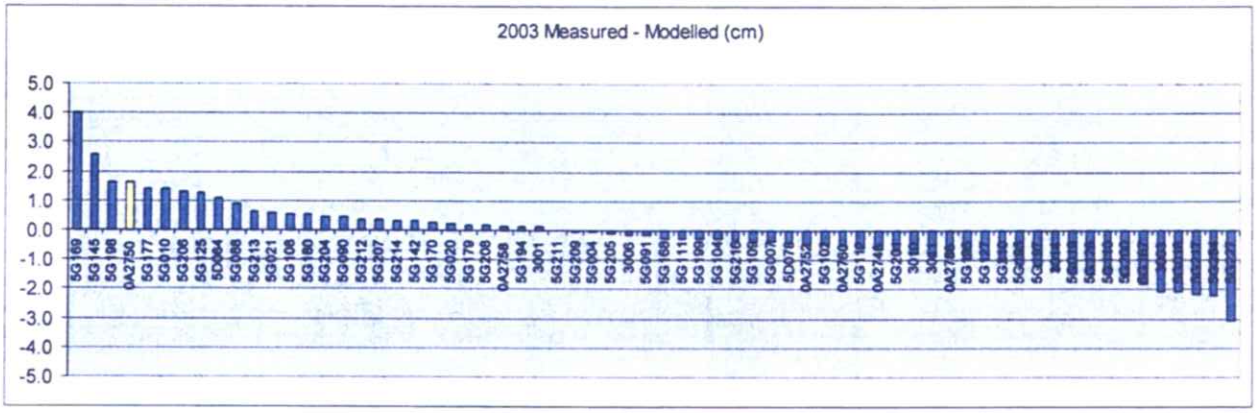
2003 Measured - Modelled (cm)
5.0
4.0
3.0
2.0
1.0
0.0
-1.0
-2.0
-3.0
-4.0
-5.0

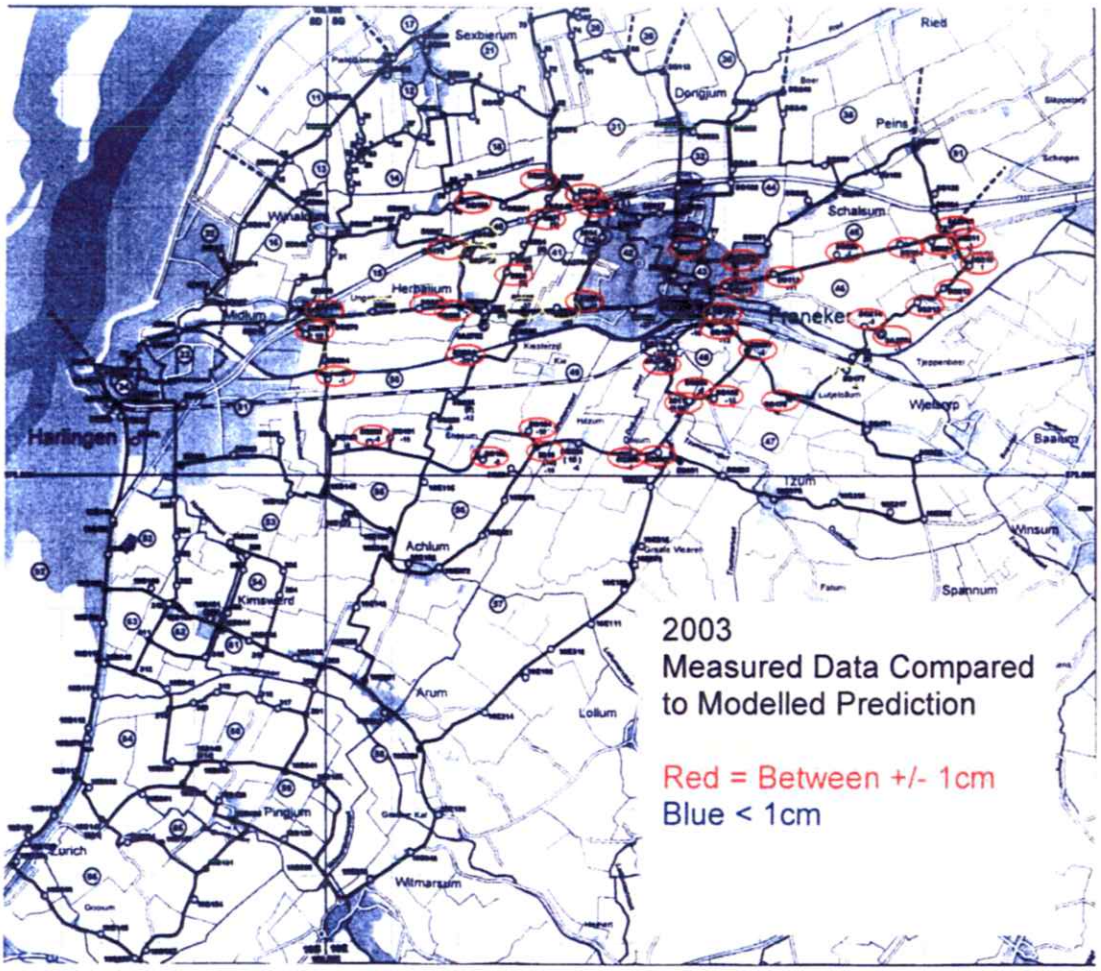
Sexbierum
Dongjum
Ried
Peins
Schalsum
Franeker
Wjelsrp
Baaium
Harlingen
Achlum
Kimswerd
Arum
Lollum
Pingjum
Zurich
Witmarsum
Winsum
Spannum
2003
Measured Data Compared
to Modelled Prediction
Red = Between +/- 1cm
Blue < 1cm

2000;

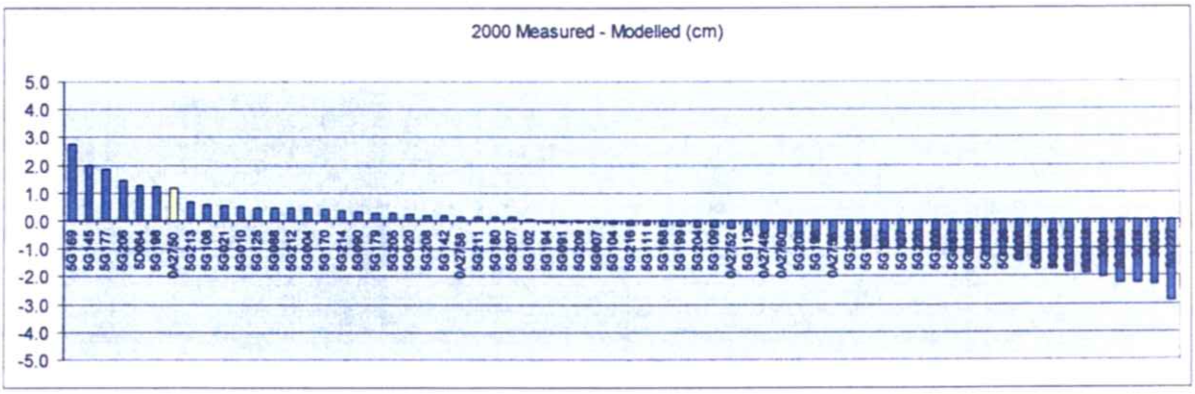
2000 Measured - Modelled (cm)
5.0
4.0
3.0
2.0
1.0
0.0
-1.0
-2.0
-3.0
-4.0
-5.0

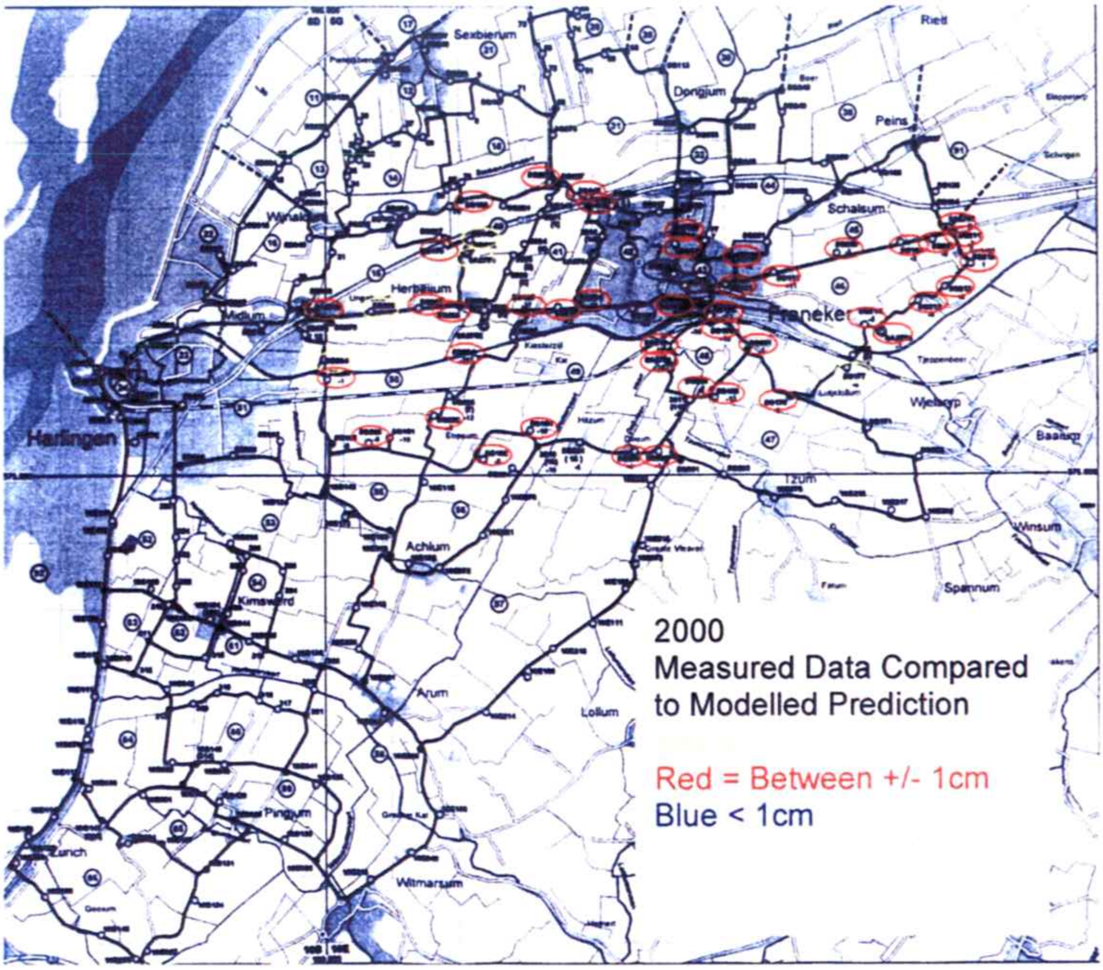
Sexbierum
Peins
Schalsum
Harlingen
Achlum
Arum
Lollum
Witmarsum
Spannum
2000
Measured Data Compared
to Modelled Prediction
Red = Between +/- 1cm
Blue < 1cm

1997;

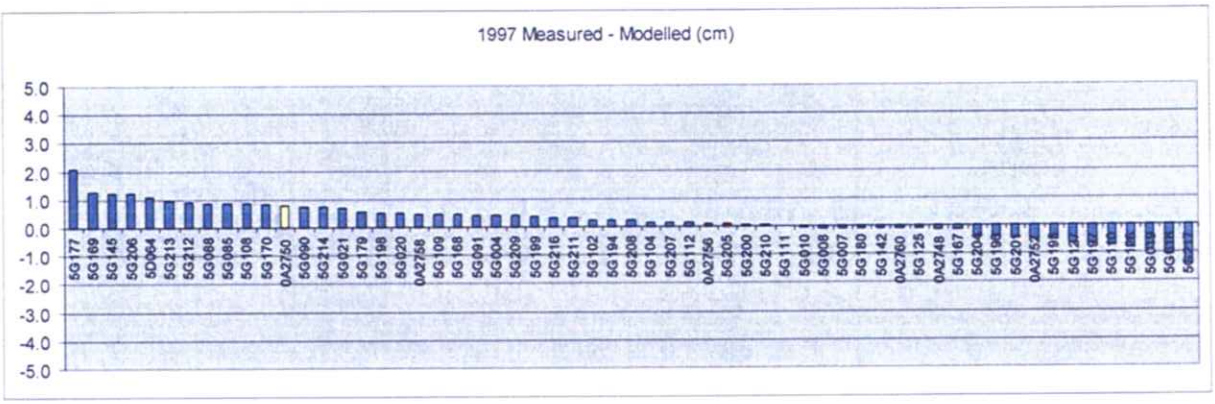

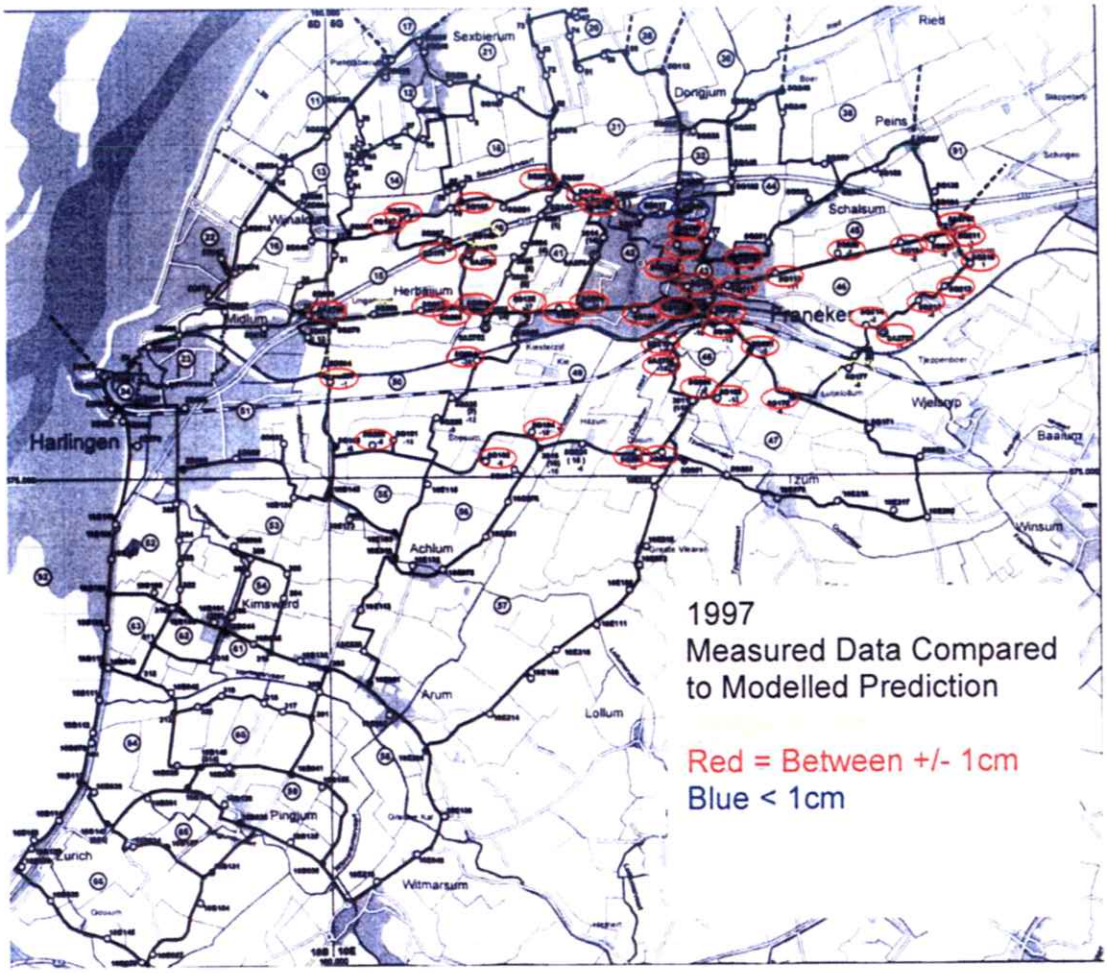

The majority of surface levelling points show a good correlation to deep founded levelling points when both are of quality construction, but care should be taken to select appropriately founded structures, and, in regions with potential surface compaction, deep founded levelling points should be constructed to provide accurate measurements.

Subsidence Prediction

The AEsubs program was used to generate subsidence contours for the historical subsidence measurements once a statistical fit to the data had been achieved. The following plots show the gas caused subsidence contours for the years 1997, 2000, 2003, and 2006, respectively.

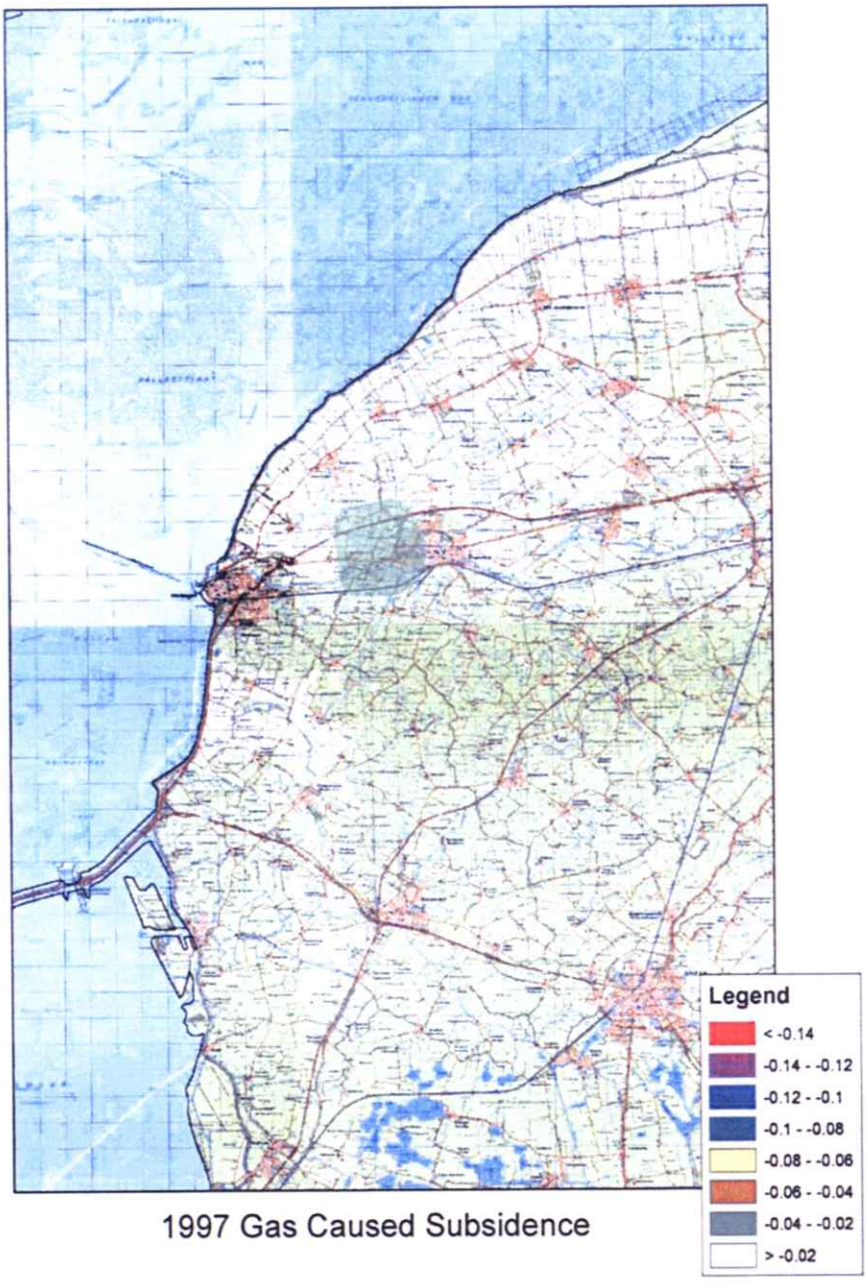

1997 Gas Caused Subsidence

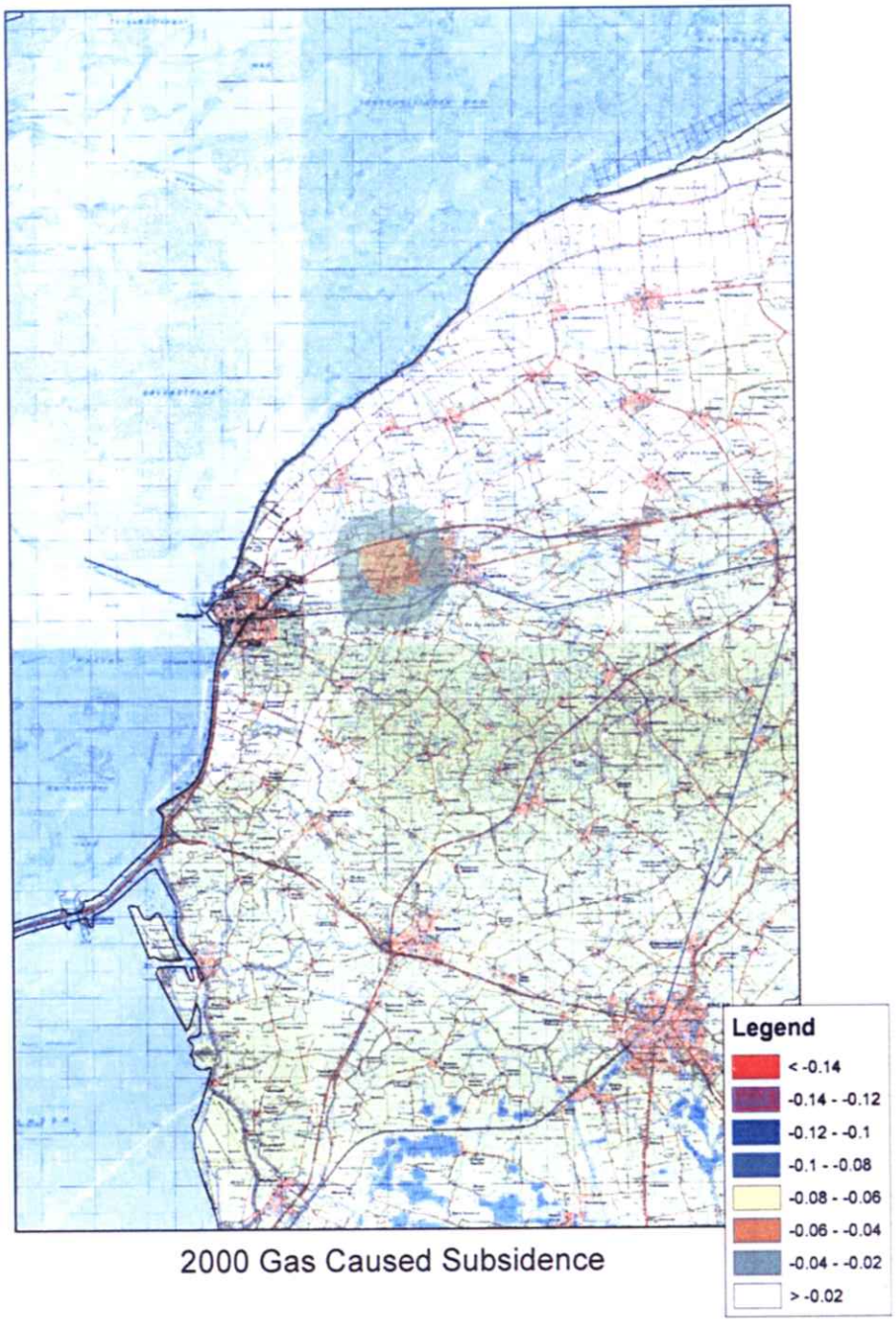

2000 Gas Caused Subsidence

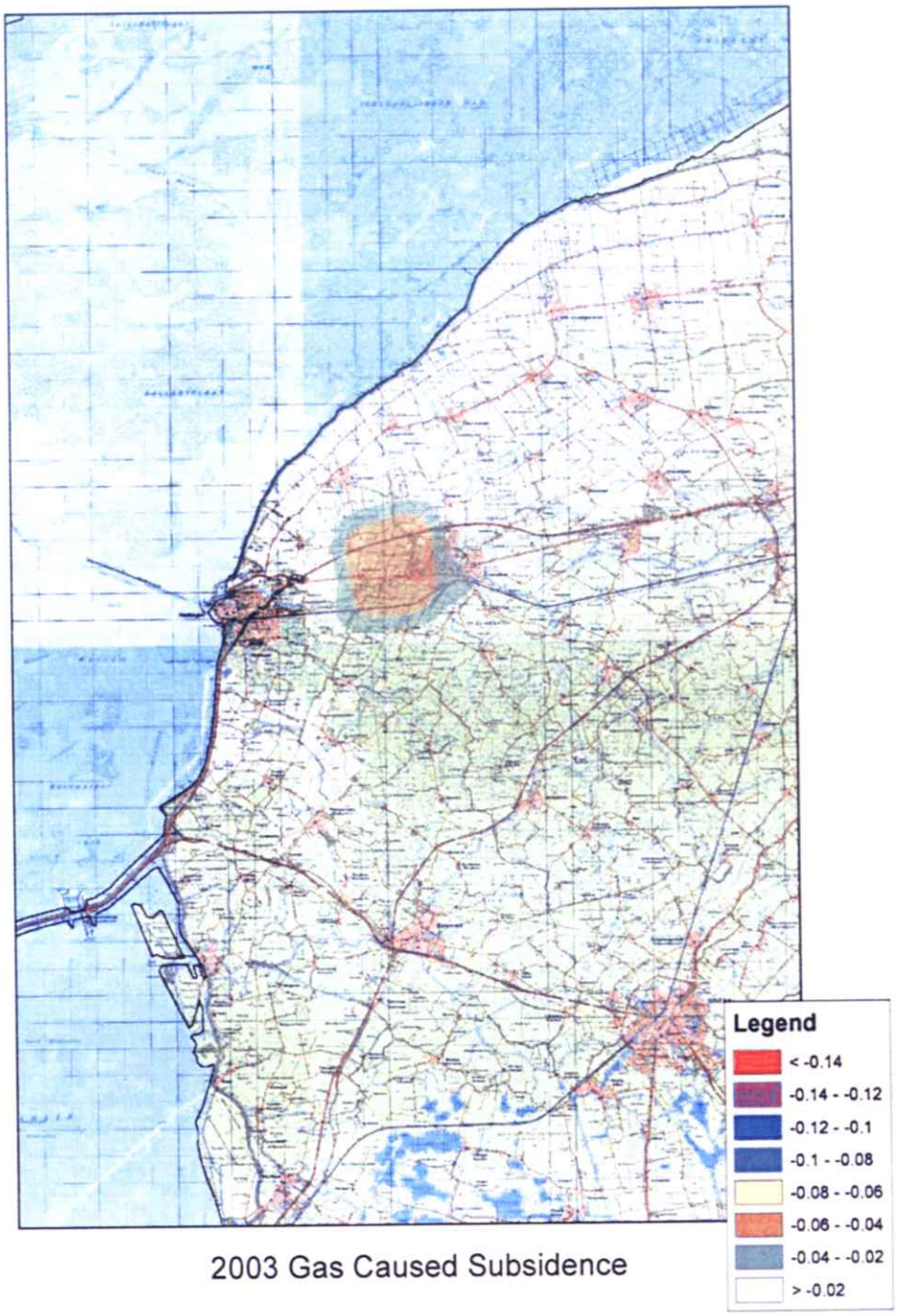

2003 Gas Caused Subsidence

Technical Limit - 2025 Gas Caused Subsidence

The same model was also used to predict the impact infill drilling would have on ultimate subsidence, as this would increase the amount of gas produced before reaching the economic limit of gas production from the Harlingen Upper Cretaceous reservoir.

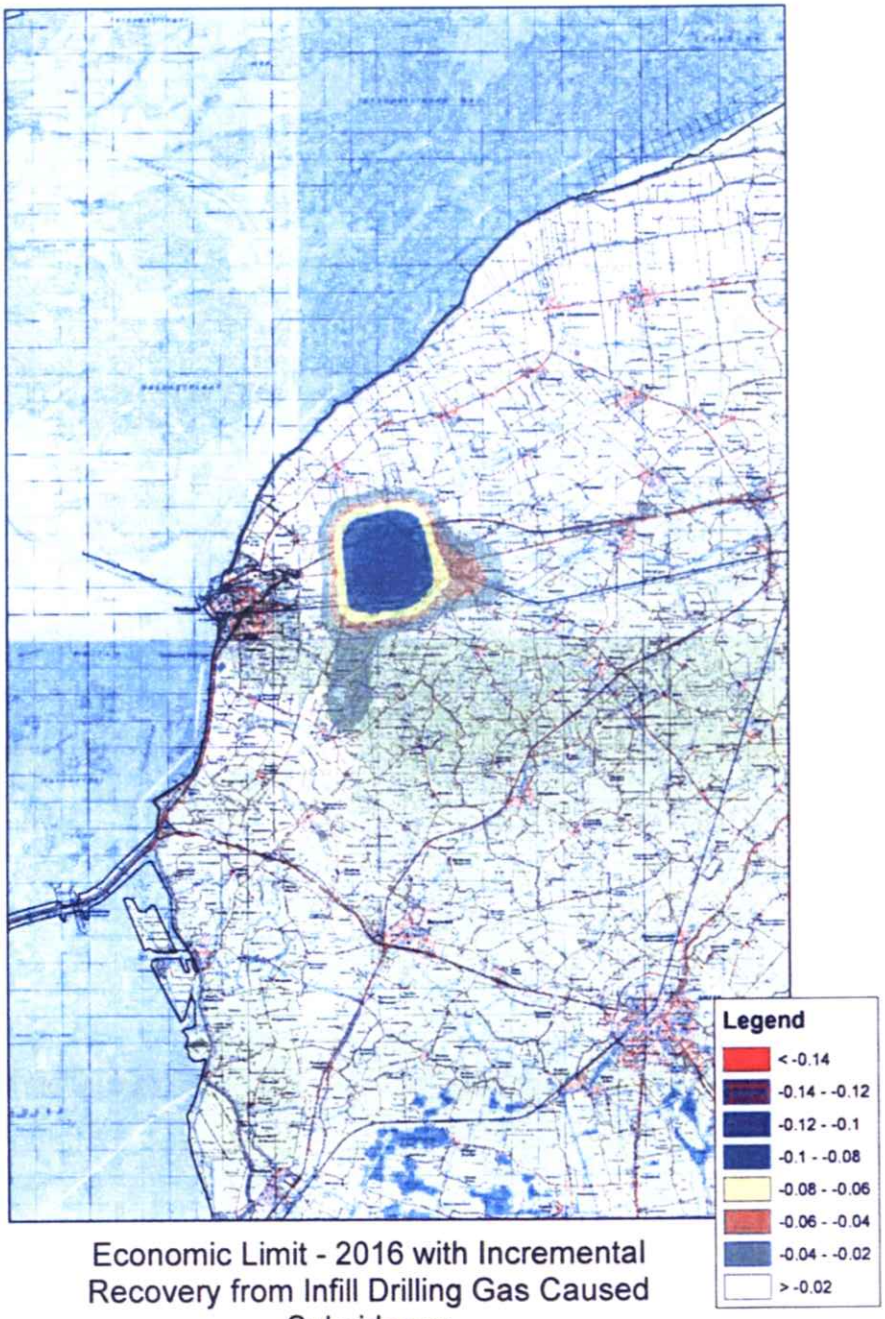

Economic Limit - 2016 with Incremental Recovery from Infill Drilling Gas Caused Subsidence

The contours above indicate it is reasonable to expect subsidence of 10 to 12cm in the future, but statistical variation in surface measured data compared to model data (see Levelling Points section) suggest that the expected maximum gas caused surface subsidence from the Harlingen Upper Cretaceous reservoir could be as high as 12 to 13cm.

Study Conclusions

Laboratory tests and computer simulations have been compared to actual measurements to provide a realistic interpretation of gas caused subsidence from the Harlingen reservoir.

Estimation of gas caused subsidence can be erroneously affected by acceptance of surface levelling data that is of suspect quality. Data that is significantly different than the conceptual model should be rigorously scrutinized before being incorporated.

Current (2006) maximum subsidence caused by gas extraction from the Harlingen Upper Cretaceous reservoir is 9 – 10cm.

The expected maximum subsidence caused by gas extraction from the Harlingen Upper Cretaceous reservoir is 12 – 13cm.

There is potentially shallow compaction in areas of the Harlingen field that are not accurately mapped.

Appendix 1: Wellbore Schematics

VERMILION FIELD : LW WEST WELL : FRA 1

NORM CLASSIFIED : NO

N°	Bottom hole equipment	ID	OD	Depth	Length
	ITAG 110 elevation to tubing head spool top flange			5.84	5.84
1	Tubing hanger FMC type 7"TC1AEN - 3.50"EUE box up 3.50"NVAM box down w/ 3" CIW "H" BPV profile	2.992	7.000	5.99	0.15
2	Pup joint 3.50" New Vam 9.20# L80	2.992	3.500	7.26	1.27
3	Tubings @ Pup joint 3.50"New Vam 9.20# L80	2.992	3.500	37.12	29.86
4	Flow coupling 3.50" New Vam 9.20# L80	2.970	3.890	38.87	1.75
5	Baker B 2.81" Safety nipple 3.50" New vam 9.20# L80	2.810	5.060	39.42	0.55
6	Flow coupling 3.50" New Vam 9.20# L80	2.970	3.890	41.17	1.75
7	Tubings @ Pup joints 3.50" New Vam 9.20# L80	2.992	3.500	986.63	945.46
8	Flow coupling 3.50" New Vam 9.20# L80	2.960	3.890	988.38	1.75
9	Baker SSD 2.75" CMU 3.50" New Vam 9.20# L80	2.750	4.280	989.62	1.24
10	Flow coupling 3.50" New Vam 9.20# L80	2.960	3.890	991.37	1.75
11	Pup joints 3.50" New Vam 9.20# L80 (0.99m + 1.49m)	2.992	3.500	993.85	2.48
12	Baker KC-22s anchor size 81-47 3.50" New Vam 9.20#	2.992	5.500	994.60	0.75
13	Baker SC2PAH size 70B, 47x38 pkr 5" New Vam box 1	3.875	6.000	996.56	1.96
14	Baker Millout Extension 5" New Vam pin x pin 15#	4.408	5.020	998.16	1.60
15	X-over 5" New Vam box 15# x 3.50" New vam pin 9.20#	2.992	5.583	998.54	0.38
16	Pup joint 3.50" New Vam 9.20# L80	2.992	3.500	1000.03	1.49
17	Tubings 3.50" New Vam 9.20# L80	2.992	3.500	1686.29	686.26
18	Pup joint 3.50" New Vam 9.20# L80	2.992	3.500	1687.78	1.49
19	Baker SSD 2.56" CMU 3.50" New Vam 9.20# L80	2.560	4.280	1689.05	1.27
20	Pup joint 3.50" New Vam 9.20# L80	2.992	3.500	1690.54	1.49
21	Baker L-22 locator seal assembly (3.5m long) 3.50" Nva	2.992	5.000	1692.39	1.85
22	Baker FB-1 size 87-40 pkr	4.000	5.992	1693.15	0.76
23	Baker seal bore extension 5" - 4.75" stub Acme connec	4.000	5.010	1696.00	2.85
24	X-Over 4.75" stub Acme x 2.875" New Vam pin 6.40#	2.441	5.670	1696.20	0.20
25	Pup joint 2.875"New Vam 6.40# L80	2.441	2.875	1697.21	1.01
26	Tubing 2.875" New Vam 6.40# L80	2.441	2.875	1706.75	9.54
27	Baker 2.31" F landing ported nipple 2.875"New Vam 6.4	2.312	3.244	1707.06	0.31
28	Perforated tube 2.875" New Vam 6.40# L80	2.441	2.875	1716.59	9.53
29	Baker 2.31" R landing ported nipple 2.875"New Vam 6.4	2.259	3.244	1716.92	0.33
30	Tubing 2.875" New Vam 6.40# L80	2.441	2.875	1726.44	9.52
31	Wire Line Entry Guide 2.875" New Vam 6.40# L80	2.374	3.244	1726.65	0.21

	Miscellaneous (Casing, Plug, Fish...)	ID	Lbs/ft	Bot depth	Top depth
I	24" CP			27.00	
II	13 3/8" BTC C75 surface casing		68.00	317.00	
III	9 5/8" BTC N80 protection casing		43.50	1027.00	
IV	7" VAM N80 production casing	6.366	23.00	1833.00	
V	Bridge plug				1749.00

	Perforation intervals Depth		Type	Status
A	1038.00	1047.00		cement
B	1738.50	1746.00		open

Comments: Ref. for perforation depths : log from 06/1978 with rig N80
29/09/1997 - 5spf 4"1/2 HMX

Max inclination	5.5 deg at 1659m (totco)
Packer fluid Type	DRW
SG	1.00
Completion type	Simple
Weight ↗	22 tons
↘	22 tons
Weight/Height on PKR	no weigth on packer
Rig	ITAG RIG 110
Reference depth	ITAG RIG 110 RKB
Final depth	

Type of SCSSV	Wire line retrievable valve
Type of Packer	Retrievable
Bottom gauge	○ Yes ◉ No
Tubing OD	3.500
Production casing OD	7.000
Activation type	Eruptive

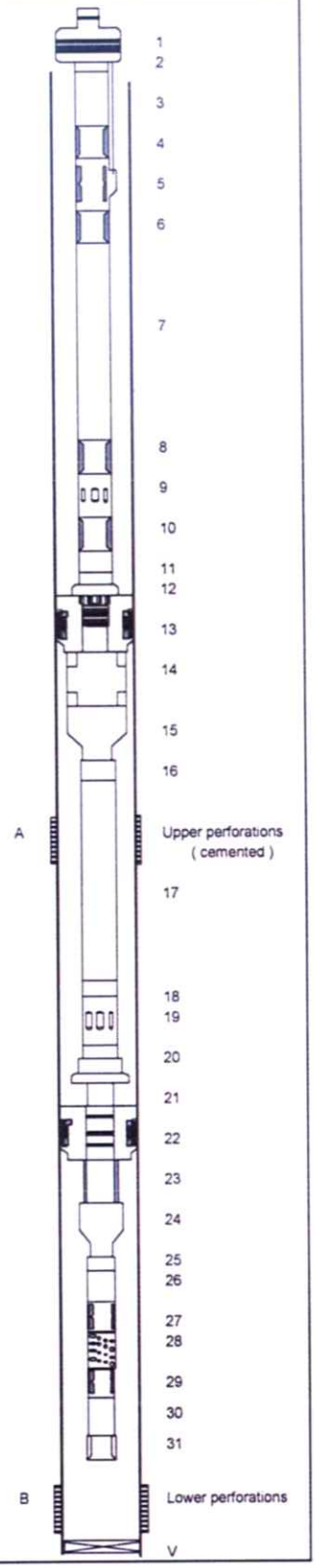

VERMILION

FIELD : LW WEST

WELL : HARLINGEN 2

RT/TH : 5.10 m.
COMPLETION DATE : 4/65

ANNULUS FLUID :
INHIBITED CACL2 BRINE S.G. 1.35

VOLUMES	DRILLING DEPTHS
TUBING : 3.1 m3	7" CSG SHOE : 1131 m.
ANNULUS : 15.5 m3	9 5/8 " CSG SHOE : 1015 m.
HOLE : 20.7 m3	13 3/8" CSG SHOE : 300 m.

Xmas TREE

TUBING HEAD	OCT 10"-3000 X 6"-3000
TUBING HANGER	FMC 6" SPECIAL WITH 3" CAMERON BPV PROF.
L MASTER VALVE	FMC 3 1/8"-3000
U MATER VALVE	FMC 3 1/8"-3000
SWAB VALVE	FMC 3 1/8"-3000
WING VALVES	FMC 3 1/8"-3000
TOP CAP	6 1/2"-4 ACME QUICK UNION.

STRING

ITEM	QTY	DESIGNATION	Depth/Th	ID/in
1	1	TUBING HANGER WITH 3" CAMERON BPV PROFILE	0.22	3.000
2	3	PUP JOINT 3 1/2" VAM 9.2# N80	5.41	2.992
3	3	TUBING 3 1/2" VAM 9.2# N80	33.94	2.992
4	1	PUP JOINT 3 1/2" VAM 9.2# N80	35.85	2.992
5	1	FLOW COUPLING 3 1/2" VAM	36.78	2.992
6	**1**	**CAMCO B6 SCSSSV NIPPLE 3 1/2" VAM**	**37.59**	**2.813**
7	1	FLOW COUPLING 3 1/2" VAM	38.43	2.992
8	1	PUP JOINT 3 1/2" VAM 9.2# N80	38.94	2.992
9	1	TUBING 3 1/2" VAM 9.2# N80	48.53	2.992
10	1	PUP JOINT 3 1/2" VAM 9.2# N80	50.45	2.992
11	1	XOVER 3 1/2" VAM BOX X 2 7/8" VAM PIN	50.69	2.441
12	1	PUP JOINT 2 7/8" VAM 6.4# N80	51.63	2.441
13	101	TUBING 2 7/8" VAM 6.4# N80	992.55	2.441
14	1	PUP JOINT 2 7/8" VAM 6.4# N80	994.49	2.441
15	1	K22 ANCHOR 80 SA 40	994.77	
16	1	BAKER 84 X 40 SAB PACKER	996.25	
17	1	5" MILLOUT EXTENSION	997.87	
18	1	XOVER 5" VAM B X 2 7/8" VAM P	998.12	2.441
19	1	PUP JOINT 2 7/8" VAM 6.4# N80	999.06	2.441
20	**1**	**BAKER 2.25" F NIPPLE**	**999.35**	**2.250**
21	1	PUP JOINT 2 7/8" VAM 6.4# N80	1000.29	2.441
22	1	TUBING 2 7/8" VAM 6.4# N80	1009.55	2.441
23	1	PUP JOINT 2 7/8" VAM 6.4# N80	1011.49	2.441
24	**1**	**BAKER 2.25" R NIPPLE**	**1011.77**	**2.197**
25	2	PUP JOINT 2 7/8" VAM 6.4# N80	1015.65	2.441
26	1	WIRELINE ENTRY GUIDE	1015.85	2.441

PERFORATIONS / RKB

1039 TO 1043 m. 2 1/8" UNIJET

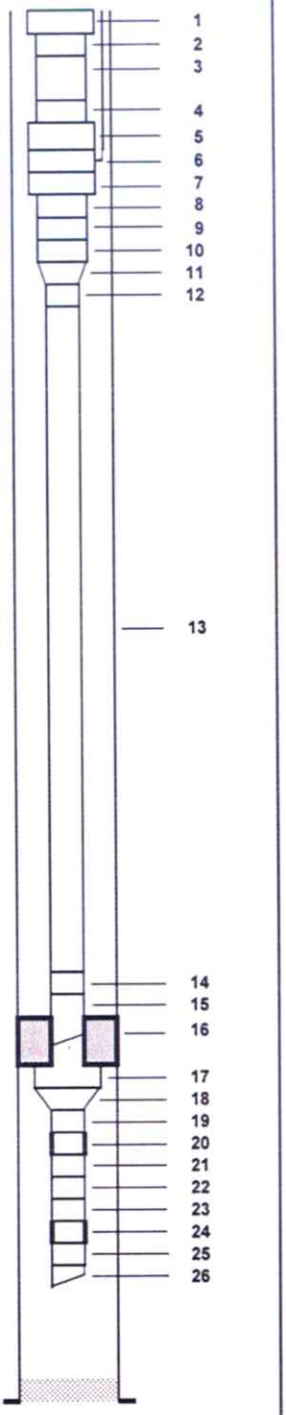

NORM CLASSIFIED : NO

Vermilion

FIELD : LW WEST

WELL : HAR 4

RT/TH : 5.66 m.
COMPLETION DATE : 01/85

ANNULUS FLUID :
1.35 S.G. CaCl2 BRINE

VOLUMES	DRILLING DEPTHS / RKB
TUBING : 2.5m3	7 " CSG SHOE @ 1011 m.
ANNULUS : 13 m3	4 1/2" LINER HANGER @ 827 m.
HOLE : 17.5m3	4 1/2" LINER SHOE @ 1101 m.

Xmas TREE

TUBING HEAD	OCT TCMOO 11"-3000 X 7 1/16"-3000
TUBING HANGER	OCT TC1A WITH 3" CAMERON H BPV PROFILE
L MASTER VALVE	OCT GATE VALVE 3 1/8"-3000
U MATER VALVE	OCT GATE VALVE 3 1/8"-3000
SWAB VALVE	OCT GATE VALVE 3 1/8"-3000
WING VALVES	OCT GATE VALVE 3 1/8"-3000
TOP CAP	MOTI OTIS TYPE 6 1/2"-4 ACME QUICK UNION

STRING

ITEM	QTY	DESIGNATION	Depth/Th	ID/IN
1	1	TUBING HANGER WITH 3" CAMERON H BPV PROFILE	0.15	3.000
2	1	PUP JOINT 3 1/2" VAM N80 9.2#		2.992
3	3	TUBINGS 3 1/2" VAM N80 9.2#		2.992
4	1	PUP JOINT 3 1/2" VAM N80 9.2#		2.992
5	**1**	**CAMCO B6 SCSSSV NIPPLE**	**31.47**	**2.813**
6	3	PUP JOINT 3 1/2" VAM N80 9.2#		2.992
7	1	X OVER 3 1/2" VAM X 2 7/8" VAM	34.63	2.441
8	1	PUP JOINT 2 7/8" VAM N80 6.4#		2.441
9	63	TUBINGS 2 7/8" VAM N80 6.4#		2.441
10	1	PUP JOINT 2 7/8" VAM N80 6.4#		2.441
11	1	BAKER K22 ANCHOR		3.250
12	1	BAKER SAB PACKER	806.66	3.250
13	1	MILLOUT EXTENSION 5" VAM		4.400
14	1	X OVER 5" VAM X 2 7/8" VAM	808.47	2.441
15	1	PUP JOINT 2 7/8" VAM N80 6.4#		2.441
16	**1**	**BAKER 2.25" " F " NIPPLE**	**810.51**	**2.250**
17	1	PUP JOINT 2 7/8" VAM N80 6.4#		2.441
18	21	TUBINGS 2 7/8" VAM N80 6.4#		2.441
19	1	PUP JOINT 2 7/8" VAM N80 6.4#		2.441
20	**1**	**BAKER 2.25" " R " NIPPLE**	**1006.80**	**2.197**
21	1	PUP JOINT 2 7/8" VAM N80 6.4#		2.441
22	1	WIRELINE ENTRY GUIDE	1008.11	2.441

PERFORATIONS / RKB

1038 TO 1043 m. 2 1/8" ENERJET

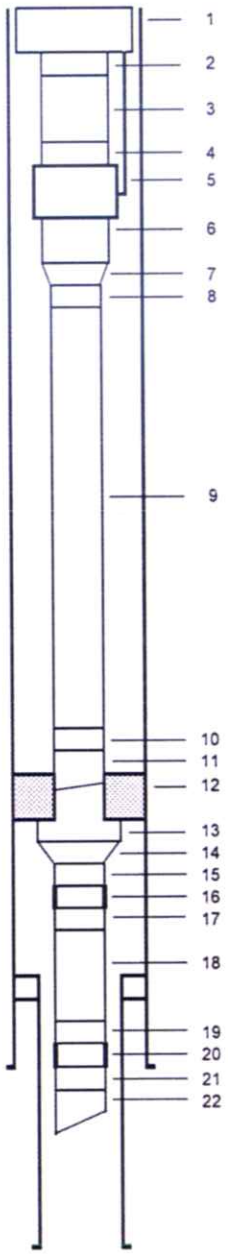

NORM CLASSIFIED : NO

Vermilion

FIELD : LEEUWARDEN WEST

WELL : HAR 5

RT/TH : 5.72 m.
COMPLETION DATE : 01/85

ANNULUS FLUID :
1.35 S.G. KCL BRINE

VOLUMES

TUBING : 3 m3
ANNULUS : 13 m3
HOLE : 18 m3

DRILLING DEPTHS / RKB

7 " CSG SHOE @ 1029.3 m.
4 1/2" LINER HANGER @ 824.01 m.
4 1/2" LINER SHOE @ 1111.38 m.

Xmas TREE

TUBING HEAD	OCT TCMOO 11"-5000 X 7 1/16"-3000
TUBING HANGER	OCT TC1A WITH 3" CAMERON H BPV PROFILE
L MASTER VALVE	OCT GATE VALVE 3 1/8"-3000
U MATER VALVE	OCT GATE VALVE 3 1/8"-3000
SWAB VALVE	OCT GATE VALVE 3 1/8"-3000
WING VALVES	OCT GATE VALVE 3 1/8"-3000
TOP CAP	MOTI OTIS TYPE 6 1/2"-4 ACME QUICK UNION

STRING

ITEM	QTY	DESIGNATION	Depth/Th	ID/IN
1	1	TUBING HANGER WITH 3" CAMERON H BPV PROFILE	0.18	3.000
2	1	X OVER 3 1/2" VAM X 2 7/8" VAM	0.35	2.441
3	1	PUP JOINT 2 7/8" VAM N80 6.4#	1.79	2.441
4	3	TUBINGS 2 7/8" VAM N80 6.4#	29.85	2.441
5	1	PUP JOINT 2 7/8" VAM N80 6.4#	31.29	2.441
6	**1**	**BAKER 2.31" "B" TYPE SCSSSV NIPPLE**	**31.79**	**2.312**
7	1	PUP JOINT 2 7/8" VAM N80 6.4#	32.79	2.441
8	82	TUBINGS 2 7/8" VAM N80 6.4#	794.38	2.441
9	1	PUP JOINT 2 7/8" VAM N80 6.4#	795.82	2.441
10	1	BAKER K22 ANCHOR	796.86	3.250
11	1	BAKER SAB PACKER	797.56	4.000
12	1	MILLOUT EXTENSION 5" VAM	789.17	4.400
13	1	X OVER 5" VAM X 2 7/8" VAM	799.47	2.441
14	1	PUP JOINT 2 7/8" VAM N80 6.4#	800.92	2.441
15	**1**	**BAKER 2.25" " F " NIPPLE**	**801.21**	**2.250**
16	1	PUP JOINT 2 7/8" VAM N80 6.4#	802.21	2.441
17	22	TUBINGS 2 7/8" VAM N80 6.4#	1017.51	2.441
18	1	PUP JOINT 2 7/8" VAM N80 6.4#	1018.95	2.441
19	**1**	**BAKER 2.25" " R " NIPPLE**	**1019.23**	**2.197**
20	1	PUP JOINT 2 7/8" VAM N80 6.4#	1020.19	2.441
21	1	WIRELINE ENTRY GUIDE	1020.49	2.441

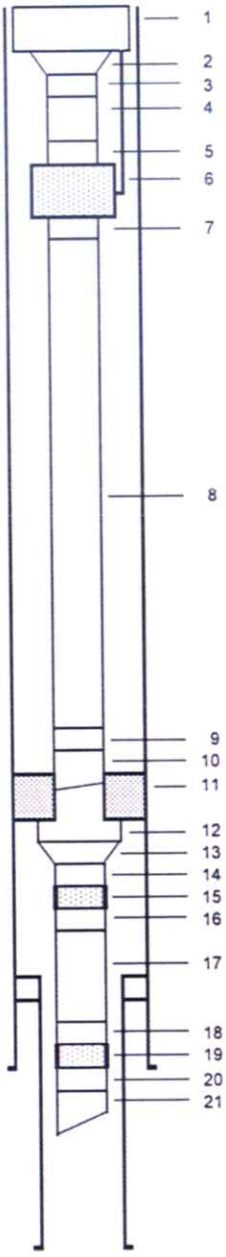

PERFORATIONS / RKB

1050.5 TO 1053.5 m. 2 1/8" ENERJET

NORM CLASSIFIED : NO

Vermilion

FIELD : LW WEST

WELL : HAR 6

RT/TH : 5.72 m.
COMPLETION DATE : 2/85

ANNULUS FLUID :
1.35 S.G. KCL BRINE

VOLUMES

TUBING : 3 m3
ANNULUS : 13 m3
HOLE : 18 m3

DRILLING DEPTHS / RKB

7 " CSG SHOE @ 1028 m.
4 1/2" LINER HANGER @ 833.60 m.
4 1/2" LINER SHOE @ 1117m.

Xmas TREE

TUBING HEAD	OCT TCMOO 11"-5000 X 7 1/16"-3000
TUBING HANGER	OCT TC1A WITH 3" CAMERON H BPV PROFILE
L MASTER VALVE	OCT GATE VALVE 3 1/8"-3000
U MATER VALVE	OCT GATE VALVE 3 1/8"-3000
SWAB VALVE	OCT GATE VALVE 3 1/8"-3000
WING VALVES	OCT GATE VALVE 3 1/8"-3000
TOP CAP	MOTI OTIS TYPE 6 1/2"-4 ACME QUICK UNION

STRING

ITEM	QTY	DESIGNATION	Depth/Th	ID/IN
1	1	TUBING HANGER WITH 3" CAMERON H BPV PROFILE	0.16	3.000
2	1	X OVER 3 1/2" VAM X 2 7/8" VAM	0.36	2.441
3	1	PUP JOINT 2 7/8" VAM N80 6.4#	1.90	2.441
4	3	TUBINGS 2 7/8" VAM N80 6.4#	29.76	2.441
5	1	PUP JOINT 2 7/8" VAM N80 6.4#	31.21	2.441
6	**1**	**BAKER 2.31" "B" TYPE SCSSSV NIPPLE**	**31.71**	**2.312**
7	1	PUP JOINT 2 7/8" VAM N80 6.4#	32.72	2.441
8	82	TUBINGS 2 7/8" VAM N80 6.4#	796.00	2.441
9	1	PUP JOINT 2 7/8" VAM N80 6.4#	797.43	2.441
10	1	BAKER K22 ANCHOR	797.65	3.250
11	1	BAKER SAB PACKER	799.15	4.000
12	1	MILLOUT EXTENSION 5" VAM	800.78	4.400
13	1	X OVER 5" VAM X 2 7/8" VAM	801.08	2.441
14	1	PUP JOINT 2 7/8" VAM N80 6.4#	802.58	2.441
15	**1**	**BAKER 2.25" " F " NIPPLE**	**802.88**	**2.250**
16	1	PUP JOINT 2 7/8" VAM N80 6.4#	803.88	2.441
17	23	TUBINGS 2 7/8" VAM N80 6.4#	1015.23	2.441
18	1	PUP JOINT 2 7/8" VAM N80 6.4#	1016.68	2.441
19	**1**	**BAKER 2.25" " R " NIPPLE**	**1016.98**	**2.197**
20	1	PUP JOINT 2 7/8" VAM N80 6.4#	1017.98	2.441
21	1	WIRELINE ENTRY GUIDE	1018.28	2.441
22	1	SPES PLUS-PLUG	1064.00	

PERFORATIONS / RKB

1066 TO 1068 m. 2 1/8" ENERJET

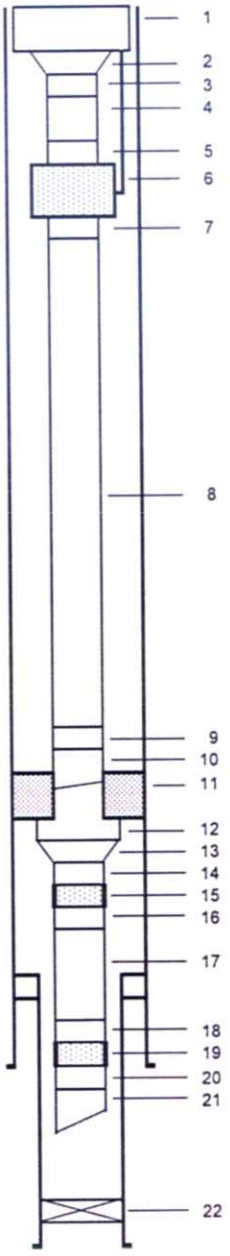

NORM CLASSIFIED : NO

VERMILION

FIELD : LEEUWARDEN WEST

WELL : HARLINGEN 7

RT/TH : 6.36 m.
COMPLETION DATE : EARLY 92

ANNULUS FLUID : INH. WATER

VOLUMES	DRILLING DEPTHS
TUBING : 7.6 m3	
ANNULUS : 12 m3	7 " CASING 1000 m.
HOLE : 25.8 m3	4.5" SLOTTED LINER FROM 1000 TO 1600 m

Xmas TREE

TUBING HEAD	FMC 11" - 5000
TUBING HANGER	FMC 11"- 4.5"
L MASTER VALVE	4 1/16 " FMC GATE VALVE
U MATER VALVE	4 1/16" FMC GATE VALVE WITH BAKER CSWC ACTUATOR
SWAB VALVE	4 1/16" FMC GATE VALVE
WING VALVES	4 1/16" FMC GATE VALVE (ONE WITH BAKER ACTUATOR)
TOP CAP	FMC ZUIDWAL TYPE

STRING

ITEM	QTY	DESIGNATION	Depth/Th	ID/in
1	1	TUBING HANGER WITH 4" CAMERON BPV PROFILE	0.20	4.000
2	1	XOVER 5"VAM X 4.5" VAM	0.40	3.921
3	1	PUP JOINT 4.5" VAM N80 13.5#	1.65	3.921
4	3	TUBING 4.5"VAM N80 13.5#	36.06	3.921
5	1	PUP JOINT 4.5" VAM N80 13.5#	37.93	3.921
6	1	4.5" VAM FLOW COUPLING	39.77	3.921
7	**1**	**SAFETY VALVE NIPPLE 3.81" BAKER B (DEV. 0dg)**	**40.31**	**3.813**
8	1	4.5" VAM FLOW COUPLING	42.14	3.921
9	1	PUP JOINT 4.5" VAM N80 13.5#	52.75	3.921
10		TUBING 4.5"VAM N80 13.5#	944.43	3.921
11	1	PUP JOINT 4.5" VAM N80 13.5#	945.83	3.921
12	1	4.5" VAM FLOW COUPLING	947.66	3.921
13	1	XOVER 4.5" VAM X 3.5" VAM	947.96	2.992
14	1	PUP JOINT 3.5" VAM N80 9.2#	949.44	2.992
15	1	TUBING 3.5" VAM N80 9.2#	958.93	2.992
16	1	PUP JOINT 3.5" VAM N80 9.2#	960.40	2.992
17	1	3.5" VAM FLOW COUPLING	962.23	2.992
18	**1**	**BAKER 2.81" TYPE "L" SSD (DEV. 37 dg)**	**963.14**	**2.812**
19	1	PUP JOINT 3.5" VAM N80 9.2#	964.61	2.992
20	1	TUBING 3.5" VAM N80 9.2#	974.18	2.992
21	1	PUP JOINT 3.5" VAM N80 9.2#	975.64	2.992
22	1	BAKER KC22 ANCHOR	976.59	
23	1	BAKER PACKER SC-2PAH 7"	978.22	
24	1	4.5"VAM MILLOUT EXTENSION	979.24	3.921
25	1	XOVER 4.5" VAM x 2 7/8" VAM	979.48	2.441
26	1	PUP JOINT 2 7/8" VAM N80 6.4#	980.99	2.441
27	1	TUBING 2 7/8" VAM N80 6.4#	990.51	2.441
28	1	PUP JOINT 2 7/8" VAM N80 6.4#	991.96	2.441
29	**1**	**BAKER 2.31" "F" NIPPLE (DEV. 42 dg)**	**992.24**	**2.312**
30	1	PUP JOINT 2 7/8" VAM N80 6.4#	993.75	2.441
31	1	TUBING 2 7/8" VAM N80 6.4#	1003.22	2.441
32	1	PUP JOINT 2 7/8" VAM N80 6.4#	1004.20	2.441
33	**1**	**BAKER 2.25" "R" NIPPLE (DEV. 45 dg)**	**1004.57**	**2.250**
34	1	PUP JOINT 2 7/8" VAM N80 6.4#	1006.55	2.441
35	1	W.E.G.	1006.76	2.441

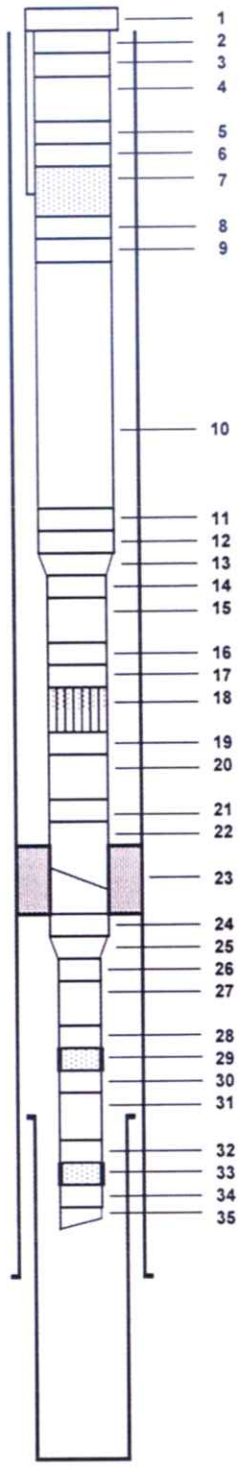

PERFORATIONS

SLOTS OF SLOTTED 4.5" LINER FROM 1601 TO 1205 M/RKB

NORM CLASSIFIED : NO

VERMILION

FIELD : LEEUWARDEN WEST

WELL : HARLINGEN 8

RT/TH : 6.78 m.
COMPLETION DATE : AUTUM 93

ANNULUS FLUID : INH. WATER

VOLUMES	DRILLING DEPTHS (RKB)
TUBING : 7.6 m3	9 5/8" CSG 791.3m TO SURFACE
ANNULUS : 24.2 m3	TOP 7" LINER 791.3 m
HOLE : 48.4 m3	4 1/2" SLOTTED LINER 1012.4-1830 m

Xmas TREE

TUBING HEAD	COOPER TYPE AP 11"-5000
TUBING HANGER	COOPER TYPE F-FBB 11'-5000 X 4 1/2" VAM
L MASTER VALVE	COOPER GATE VALVE TYPE FL 4 1/16"-5000
U MATER VALVE	FMC MODEL 120 4 1/16"-5000 WITH AVA OOW ACTUATOR
SWAB VALVE	COOPER GATE VALVE TYPE FL 4 1/16"-5000
WING VALVES	COOPER GATE VALVE TYPE FL 4 1/16"-5000
TOP CAP	FMC ZUIDWAL TYPE

STRING

ITEM	QTY	DESIGNATION	Depth/Th	ID/in
1	1	COOPER F-FBB TBG HGR WITH 4" CAMERON BPV PROFILE	0.40	4.000
2	5	TUBING 4.5"VAM N80 12.6#	32.20	3.957
3	1	4.5" VAM FLOW COUPLING	34.00	3.957
4	1	**SAFETY VALVE NIPPLE 3.81" BAKER B**	**34.50**	**3.813**
5	1	4.5" VAM FLOW COUPLING	36.40	3.957
6	98	TUBING 4.5"VAM N80 12.6#	939.00	3.957
7	1	4.5" VAM FLOW COUPLING	940.90	3.957
8	1	XOVER 4.5" VAM X 3.5" VAM	941.20	2.992
9	1	3.5" VAM FLOW COUPLING	943.00	2.992
10	3	TUBING 3.5" VAM N80 9.2#	954.80	2.992
11	1	3.5" VAM FLOW COUPLING	956.60	2.992
12	1	**BAKER 2.81" TYPE "L" SSD (DEV. 46 DG.)**	**957.50**	**2.813**
13	2	TUBING 3.5" VAM N80 9.2#	960.00	2.992
14	1	KBH 80/40 ANCHOR	960.80	
15	1	BAKER SAB PACKER	961.80	3.250
16	1	5"VAM MILLOUT EXTENSION	964.00	3.921
17	1	XOVER 5" VAM x 2 7/8" VAM	964.40	2.441
18	4	TUBING 2 7/8" VAM N80 6.4#	985.80	2.441
19	1	**BAKER 2.31" "F" NIPPLE (DEV. 50 DG.)**	**986.00**	**2.313**
20	1	TUBING 2 7/8" VAM N80 6.4#	995.50	2.441
21	1	**BAKER 2.25" "R" NIPPLE (DEV. 51 DG.)**	**995.90**	**2.250**
22	3	PUP JOINT 2 7/8" VAM N80 6.4#	1007.90	2.441
23	1	W.E.G.	1008.10	2.441

PERFORATIONS

SLOTS OF LINER 1820-1317 m/RKB

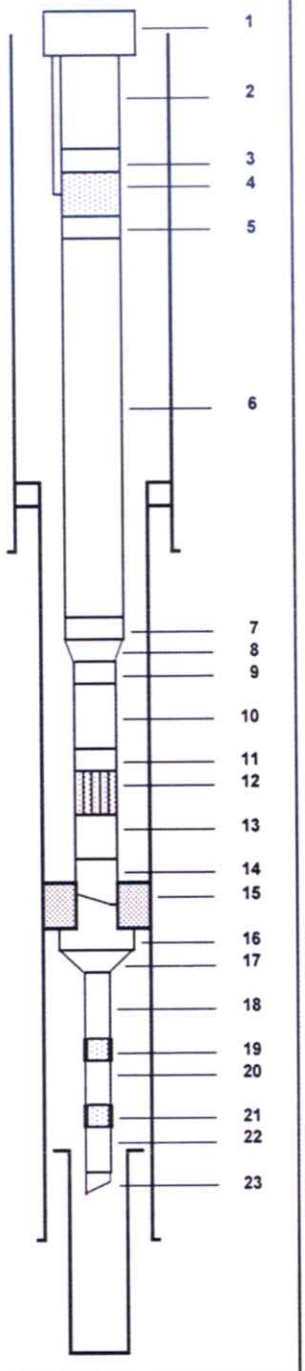

NORM CLASSIFIED : NO

Vermilion FIELD : LW WEST - WELL : HAR9

NORM CLASSIFIED : NO

N°	Bottom hole equipment	ID	OD	Depth	Length
	DEUTAG T103 elevation to tubing head spool top flange			5.05	5.05
1	Tubing hanger FMC type 7"TC1AEN 3"5 EUE box up x 3"5 New Vam 12.7# box down w/3" CIW BPV profile	2.894	7.000	5.20	0.15
2	3"5 pup joint New Vam 9.20# L80	2.952	3.500	6.47	1.27
3	5x 3"5 tubing joint New Vam 9.20# L80	2.88	3.500	53.86	47.39
4	3"5 pup joint New Vam 9.20# L80	2.992	3.500	55.35	1.49
5	Baker model "B" Safety Valve Nipple size 2"812	2.812	4.3898	55.90	0.55
6	3"5 pup joint New Vam 9.20# L80	2.992	3.500	57.39	1.49
7	X-over 3"5 New Vam box x 2"7/8 New Vam pin	2.3819	3.8976	57.58	0.19
8	2"7/8 pup joint New Vam 6.4# L80	2.441	2.875	59.01	1.43
9	94x 2"7/8 tubing joint New Vam 6.4# L80	2.441	2.875	949.03	890.02
10	2"7/8 pup joint New Vam 6.4# L80	2.441	2.875	951.02	1.99
11	Baker model "CMU" Sliding Sleeve size 2"312	2.312	3.74	952.22	1.20
12	2"7/8 pup joint New Vam 6.4# L80	2.441	2.875	954.19	1.97
13	1x 2"7/8 tubing joint New Vam 6.4# L80	2.441	2.875	963.69	9.50
14	2"7/8 pup joint New Vam 6.4# L80	2.441	2.875	965.14	1.45
15	Baker model "KBH-22" Anchor size 80-40	2.992	4.4862	965.88	0.74
16	Baker model "SAB-3" Packer size 84-40x32	3.252	5.67	967.38	1.50
17	Baker Millout Extension 5" New Vam pin x pin 15#	4.488	5.039	968.97	1.59
18	X-over 5" New Vam box x 2"7/8 New Vam pin	2.992	5.591	969.35	0.38
19	2"7/8 pup joint New Vam 6.4# L80	2.441	2.875	970.79	1.44
20	1x 2"7/8 tubing joint New Vam 6.4# L80	2.441	2.875	980.29	9.50
21	2"7/8 pup joint New Vam 6.4# L80	2.441	2.875	982.21	1.92
22	Baker model "F" top no-go Seating Nipple size 2"25	2.25	3.248	982.56	0.35
23	1x 2"7/8 tubing joint New Vam 6.4# L80	2.441	2.875	992.06	9.50
24	2"7/8 pup joint New Vam 6.4# L80	2.441	2.875	993.56	1.50
25	Baker model "R" bottom no-go Seating Nipple size 2"25	2.25	3.248	993.89	0.33
26	2"7/8 pup joint New Vam 6.4# L80	2.441	2.875	995.89	2.00
27	wireline entry guide w/2"7/8 New Vam box	2.3622	3.248	996.09	0.20

	Miscellaneous (Casing, Plug, Fish...)	ID	Lbs/ft	Bot depth	Top depth
I	24" CP			53.00	6.44
II	9 5/8" 43.5# casing New Vam P110/K55	8.756	43.50	765.00	6.06
III	7" 32# casing New Vam P110	6.366	32	1111.00	5.71
IV	4 1/2" liner NVam N80 12.6# w. tieback packer above	3.701	12.6	1305.00	987.05
V	EZ drill squeeze packer(=cement retainer)				1154.00

Perforation intervals				
	Depth		Type	Status
A	1126m/log	1131m/log		open
	1130m/log	1135m/log		open

Comments

wireline entry guide 9m inside liner tieback PBR

Length of PBR = 10 feet

Slack off on packer = 0.30 m

Type of SCSSV	Wire line retrievable valve
Type of Packer	Permanent
Bottom gauge	○ Yes ◉ No
Tubing OD	2 7/8 - 3 1/2
Production casing OD	7.000
Activation type	Eruptive

Max inclination 27

Packer fluid Type DRW **SG** 1.02

Completion type Simple

Weight ↗ 11 ↘

Weight/Height on PKR 4 T / 0.30 m slack off

Rig DEUTAG T103

Reference depth RKB deutag T103

Final depth 1306.00

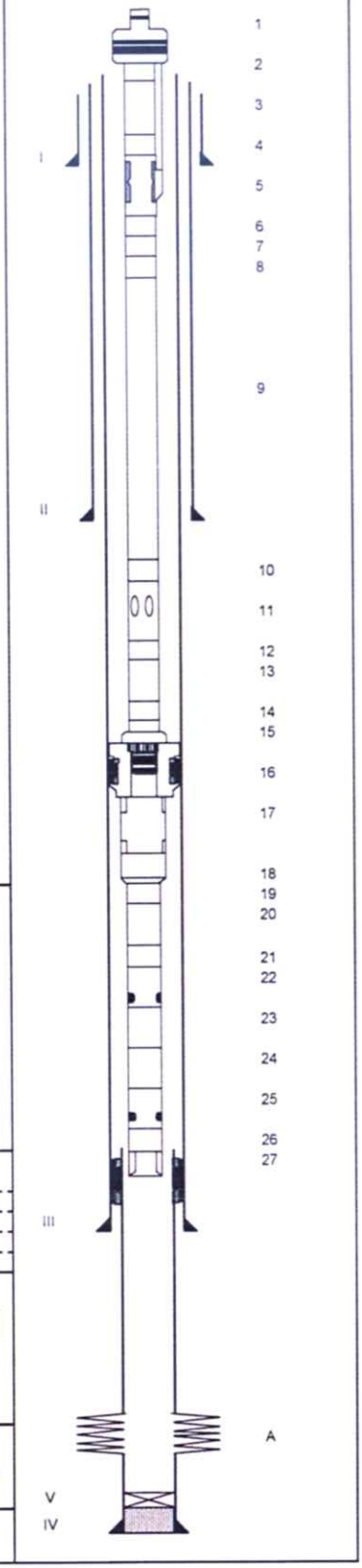

Appendix 2: Uniaxial Compaction Coefficient of Chalk

INGEKOMEN 28 MAART 2007

NORGES GEOTEKNISKE INSTITUTT
NORWEGIAN GEOTECHNICAL INSTITUTE
NGI

Vermillion Oil & Gas BV
Zuidwalweg 2
8861 NV Harlingen
The Netherlands

Attn: Rod Gibbons

Oslo, 22 March 2007
-/ms

20071135 Uniaxial Compaction Coefficient of Chalk

Please find enclosed two paper copies of our report 20071135-1 "Compressibility of Harlingen chalk" dated 22 March 2007.

Please also find enclosed reports we have received from you and one article (Havmøller & Foged).

Sincerely yours
for NORWEGIAN GEOTECHNICAL INSTITUTE

Fabrice Cuisiat
Project Manager

Enclosure

f:\p\2007\11\20071135\10-admin\div\report.doc

Postal address: P.O. Box 3930 Ullevaal Stadion, N-0806 OSLO, NORWAY
Street address: Sognsveien 72, OSLO
Internet: http://www.ngi.no
Telephone: (+47) 22 02 30 00
Telefax: (+47) 22 23 04 48
e-mail: ngi@ngi.no
IBAN: NO26 5096 0501 281
Bank account: 5096 05 01281
Business No. 958 254 318 MVA

Sk: 047

NGI

Uniaxial Compaction Coefficient of Chalk

Compressibility of Harlingen chalk

20071135-1 22 March 2007

NGI rapport

Uniaxial Compaction Coefficient of Chalk

Compressibility of Harlingen chalk

20071135-1 22 March 2007

Client: **Vermilion Oil & Gas BV**

Contact person: Rod Gibbons
Contract reference: Order confirmation dated 20.02.2007

For the Norwegian Geotechnical Institute

Project Manager: Fabrice Cuisiat

Report prepared by: Fabrice Cuisiat

Work also carried out by: Trude Ørbech, Sven Vangbæk, Toralv Berre

Postal address: P.O. Box 3930 Ullevaal Stadion, N-0806 OSLO, NORWAY
Street address: Sognsveien 72, OSLO
Internet: http://www.ngi.no
Telephone: (+47) 22 02 30 00
Telefax: (+47) 22 23 04 48
e-mail: ngi@ngi.no
IBAN: NO26 5096 0501 281
Bank account 5096 05 01281
Business No. 958 254 318 MVA

Summary

Three uniaxial strain compaction experiments have been carried out on chalk plugs drilled from available core material from Well Harlingen-7, Harlingen field (Ommelanden chalk) for Vermilion Oil & Gas BV. The tests have been performed for dry and brine saturated chalk with an initial porosity around 31%. The compressibility values are summarised in the following table:

Fluid Type	Effective axial stress σ'_v (MPa)	Bulk compressibility C_{bm} (/MPa)	Pore compressibility C_{pp} (/MPa)
dry	6-40 MPa	1.70E-04	5.49E-04
dry	>40 MPa	2.67E-04	8.61E-04
brine*	6-23 MPa	2.58E-04	8.38E-04
brine*	23-30 MPa	3.92E-04	1.27E-03
brine*	>30 MPa	7.02E-04	2.28E-03

*average value of two identical tests

The main findings of the study are:

1. The compressibility depends on the fluid in place. Higher compressibility values are obtained in brine saturated chalk, especially beyond pore collapse.
2. The onset of pore collapse starts at circa 40 MPa effective axial stress for dry chalk, and circa 23 MPa for brine saturated chalk. Given the initial stress conditions at Harlingen (effective vertical stress of 90 bars or 9 MPa, initial reservoir pressure of 135 bars or 13.5 MPa) and expected final reservoir pressure at abandonment (30 bars or 3 MPa, corresponding to 19.5 MPa effective vertical stress), pore collapse is not expected for the porosity intervals of 31% and below. Pore collapse may occur in the higher porosity chalk intervals if existing in the reservoir.
3. Available trendlines for North Sea chalk have been used to assess the variation of compressibility throughout the reservoir section. Based on a porosity log from Harlingen-2, a maximum reservoir compaction of roughly 3 to 9 cm is predicted. The upper and lower ranges correspond to different pore pressure depletion scenarios. The predictions are much lower than current surface measurement. Discrepancy between the two values could be due to the assumptions used in the current study (e.g. intact chalk, representative vertical porosity distribution from Harlingen-2), as well as other effects related to the interpretation of the subsidence measurements (natural shallow compaction, contribution from salt mining).

Contents

1 INTRODUCTION

The Harlingen field, onshore gas reservoir in Northern Netherlands (Franeker, Harlingen), is operated by Vermilion Oil & Gas BV after take over from Total. The initial development plan was based on a subsidence prognosis of 10cm. The current measurements indicate 13cm. Current prognosis gives a maximum subsidence of 17cm at the end of 2025. Given this discrepancy, the authorities have requested a revised production plan with updated prognosis.

Subsidence prognosis is complicated by deep solution salt mining in the neighbourhood. The measured subsidence is a cumulative of reservoir induced subsidence from the Harlingen field, as well as salt mining from beneath. Numerical analyses must be done to predict the impact of the different industrial activities (gas production, salt exploitation) on subsidence. Subsidence is modelled by TNO on the behalf of the mining industry. Input data to their model are the pressure changes predicted by Vermilion's reservoir simulator. In Vermilion's reservoir simulation, gas production is modelled without aquifer support. Water is not mobile in the water bearing zones of the reservoir. Elastic and plastic compressibility values have been used in subsidence prediction, as well as an "Ekofisk- compressibility". The values range from 2.1 10^{-5} /bar (elastic), 3.1 10^{-5} /bar (plastic) to 9 10^{-5} /bar (Ekofisk).

The chalk reservoir is divided into three "pools": Northern (NP), Eastern (EP) and Southern (SP) pools. NP and EP are separated by a sealing fault. NP and SP are distinguished on the basis of a different GWC. The gas bearing chalk reservoir has a porosity varying between circa 25-36%, and permeability between 1 and 2 mD.

In connection with a revision of the subsidence prognosis, Vermilion Oil and Gas BV requested NGI's assistance in the set-up of the appropriate laboratory program to measure and suggest representative reservoir chalk compressibility values for the stress changes expected during production life. The scope of work is specifically:

1) to prepare core samples for testing from existing core material
2) to measure in the laboratory chalk compressibility on the core samples
3) to compare the values to other chalk data
4) to calculate an equivalent compressibility for whole reservoir section, given the vertical variation of chalk porosity
5) to assess the need for further laboratory testing and chalk cores from new wells.

2 PREPARATION OF SAMPLES FOR TESTING

The chalk material was provided by Rod Gibbons during his visit to NGI on Monday, 12th february 2007. The chalk was cored from Harlingen-7, horizontal well in the Ommelanden Chalk formation (Upper Cretaceous). Due to the bad quality of the core, only 7 intact samples could be drilled at NGI. Based on assumed grain density (2.68 g cm^{-3}) and measured weight and dimensions, the porosity can be estimated for all samples. It is fairly uniform between 30-31% (Table 2.1).

The three samples which are tested are all selected from Sample 1. Coring was not oriented. However by assuming that the geological features visible in Sample 1 could be related to the horizontal top unconformity, the most probable orientation of the core could be inferred. Three vertical plugs were then drilled from Sample 1 (Figure 2.1).

Table 2.1 List of chalk samples prepared for testing

Sample ID	Depth (MD)	Test ID	Weight (g)	Diameter (cm)	Height (cm)	Porosity (%)
1A	1309.56	T1609	109.640	3.803	5.188	30.6
1B	1309.56	T1610	108.990	3.803	5.188	31.0
1C	1309.56	T1612	109.020	3.803	5.188	31.0
2	1308.30	-	85.770	3.804	4.100	31.3
3	1307.00	-	76.470	3.804	3.596	30.2
4	1311.00	-	63.110	3.803	2.983	30.5
8	1303.80	-	83.030	3.804	3.965	31.2

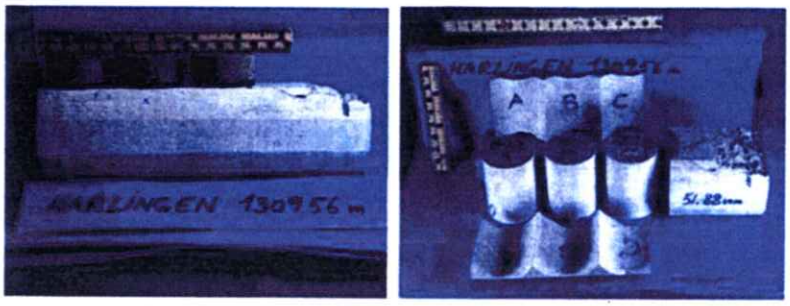

Figure 2.1 Photographs of sample 1 and plugs for laboratory experiments

Due to the lack of porosity variation in the samples selected, it is not possible to measure the variation of chalk compressibility with porosity in the reservoir. The variation will be estimated on the basis of published correlations.

Once the plugs are cored, they are mounted with small pins for deformation measurement and sprayed with an external membrane to isolate the pore fluid from the confining fluid during testing.

Chalk is water sensitive and its mechanical properties are greatly affected by the fluid in place. Water (brine) saturated chalk is weaker and more compressible than oil or gas saturated one. Full weakening is obtained when water saturation exceeds circa 15%.

In the following testing has been carried out on brine saturated and dry chalk. For in situ water saturation below 15%, the properties of the dry chalk sample should be representative of in situ conditions. Above 15% water saturation, the properties of the brine saturated sample should be used. The brine composition is taken from Elf (1993):

Table 2.2 Brine composition (from Elf, 1993)

Salt	Concentration (g/l)
NaCl	58
KCl	-
CaCl2, 6 H2O	55.6
MgCl2, 6 H2O	8.5

3 TRIAXIAL TESTING

3.1 Experimental set-up

Each plug is mounted between end-caps and instrumented with LVDTs for measuring strains in the axial and radial directions. The instrumented plug is placed inside a pressure vessel equipped with an internal load cell. The pressure vessel is filled with oil to apply confining pressure to the specimen. Confining pressure, axial stress, axial strain, and radial strain (in two perpendicular directions) are measured and/or controlled during each test. The axial strain is measured between the two radial cantilevers mounted ca 24mm from each other and 14mm from the end faces of the plug.

Recorded data is corrected for false deformation of the membrane, end-caps and other parts of the triaxial cell. The tests are performed either dry (T1609) or saturated with brine (T1610 and T1612) in drained conditions. For dry testing, no back-pressure is used. Back-pressure is used for brine saturated tests. Appropriate loading rates are used to ensure that no pressure build-up occurs during loading due to limited drainage of the pore fluid.

The tests are carried out at ambient temperature. The effect of temperature on chalk behaviour is noticeable especially above 70°C, i.e. for temperatures higher than the relevant reservoir temperature. At higher temperature creep rates increase and weakening due to water – chalk interaction is more pronounced.

3.2 Compressibility measurement by effective stress method under uniaxial strain

The uniaxial strain condition is usually representative of reservoir deformation during production, especially for thin elongated reservoirs. The condition yields for most of the reservoir, except close to the reservoir boundaries.

The sample is loaded to in situ stress conditions, by increasing simultaneously the confining pressure and axial stress to the target stresses (initial effective horizontal and vertical stresses). The pore pressure is held constant to the atmospheric condition (dry) or equal to 1 MPa for brine saturated tests.

The total vertical stress is the maximum principal stress and equals the weight of the overburden. The horizontal stress is unknown. Previous testing carried out by Elf (1993) assumed a ratio between total horizontal and vertical stresses K of 0.8. The same stress conditions have been used in this study. The initial stress conditions defined in Elf (1993) are given in Table 3.1.

Table 3.1 Initial stress conditions for laboratory experiments

Stress / Pore pressure	Value (bars)
Total vertical stress σ_V	225
Initial total horizontal stress σ_H	180
Initial octahedral stress σ_{oct}	195
Initial Reservoir Pressure p_o	135
Initial Effective vertical stress σ'_V	90
Initial Effective horizontal stress σ'_H	45
Initial Effective octahedral stress σ'_{oct}	60

After loading to initial stress conditions, the effective vertical stress is increased under imposed uniaxial strain boundary conditions (or so called Ko conditions). During this type of loading, the horizontal stress will change to maintain the condition of no lateral deformation.

In the tests, the effective vertical stress was increased far beyond the value corresponding to full reservoir depletion. The aim was to estimate the onset of pore collapse for Harlingen chalk. The final effective vertical stress for a depleted reservoir (abandon reservoir pressure of 30 bars) is equal to 195 bars.

3.3 Results from the experiments

The constrained modulus M (i.e inverse of bulk compressibility) is calculated from the applied vertical stress changes and recorded vertical deformation during uniaxial conditions (Ko-loading):

$$M = \left.\frac{d\sigma'_v}{d\varepsilon_v}\right|_{d\varepsilon_h=0} \qquad \text{Equation 3.1}$$

The bulk compressibility under uniaxial loading conditions C_{bm} is equal to the inverse of the constrained modulus M. The pore volume compressibility C_{pp} is calculated from the constrained modulus M and initial sample porosity at in-situ conditions:

$$C_{pp} = \frac{1}{M\phi_o} \qquad \text{Equation 3.2}$$

Note that the pore volume compressibility is often required for reservoir simulation, where as the bulk compressibility is the parameter required for a compaction analysis.

Porosity is updated from initial porosity and volumetric strain, assuming incompressible grains:

$$d\phi = -(1-\phi)d\varepsilon_v \qquad \text{Equation 3.3}$$

For chalk, one usually distinguishes between the elastic compressibility, before yielding or onset of pore collapse, and the plastic compressibility after pore collapse.

3.3.1 Test T1609 – dry

The results from the test are shown in Figure 3.1 and Figure 3.2. Additional plots are given in Appendix A. Pore collapse occurs from circa 40 MPa (400 bars) effective vertical stress. The compressibility values are summarised in the following table:

Table 3.2 T1609 (dry) - Measured bulk and pore compressibilities

Test ID	Effective axial stress	C_{bm} (/MPa)	C_{pp} (/MPa)
T1609	6-40 MPa	1.70E-04	5.49E-04
T1609	>40 MPa	2.67E-04	8.61E-04

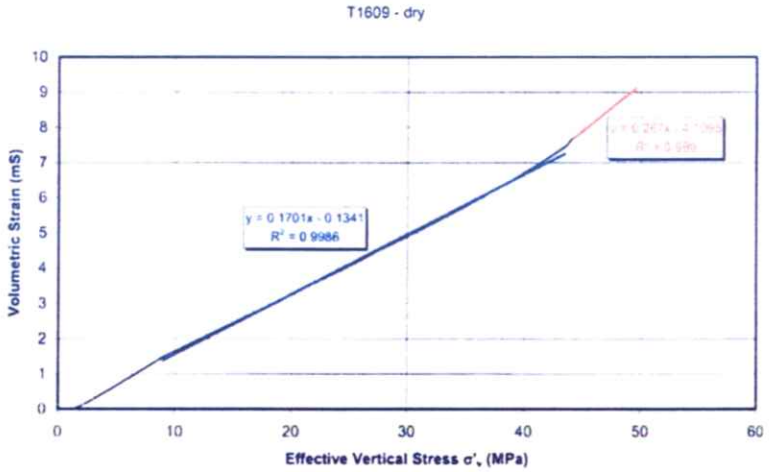

Figure 3.1 T1609 (dry) - Volumetric strain versus effective vertical stress during testing

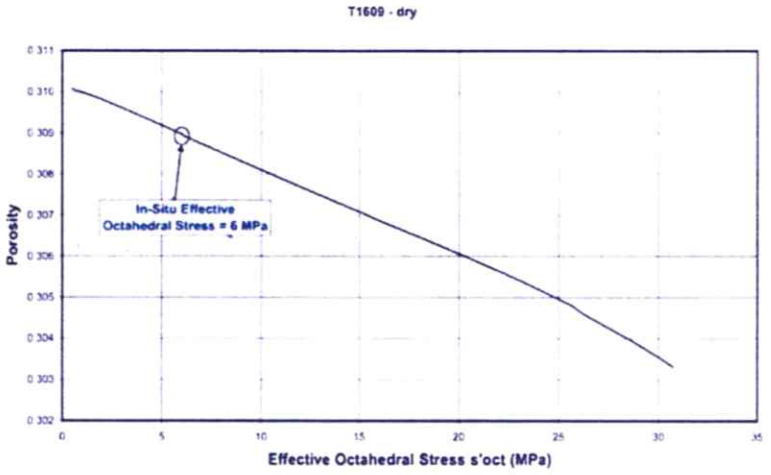

Figure 3.2 T1609 (dry) - Updated porosity during testing

3.3.2 Test T1610 – brine saturated

The results from the test are shown in Figure 3.3 and Figure 3.4. Additional plots are given in Appendix A. Pore collapse occurs from circa 23 MPa (230 bars) effective vertical stress. The compressibility values are summarised in the following table:

Table 3.3 T1610 (brine) - Measured bulk and pore compressibilities

Test ID	Effective axial stress	C_{bm} (/MPa)	C_{pp} (/MPa)
T1610	6-23 MPa	2.34E-04	7.60E-04
T1610	23-30 MPa	2.98E-04	9.66E-04
T1610	>30 MPa	4.08E-04	1.32E-03

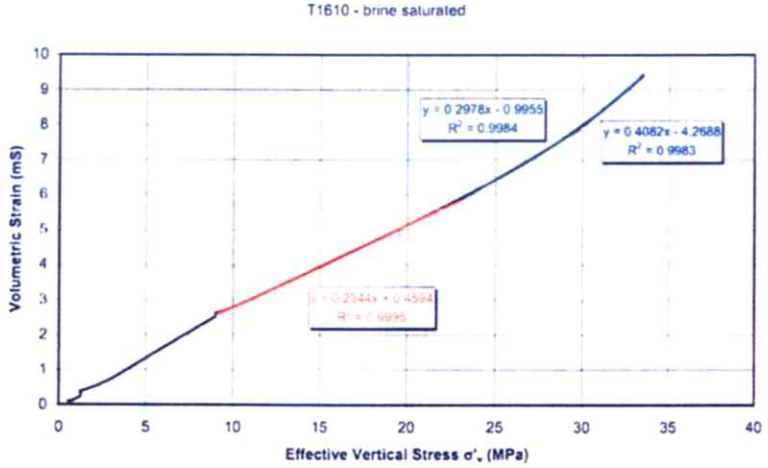

Figure 3.3 T1610 (brine) - Volumetric strain versus effective vertical stress during testing

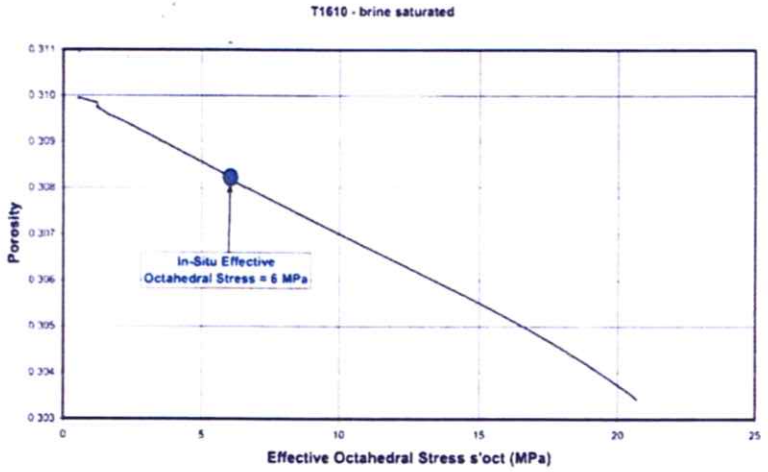

Figure 3.4 T1610 (brine) - Updated porosity during testing

3.3.3 Test T1612 – brine saturated

The results from the test are shown in Figure 3.5 and Figure 3.6. Additional plots are given in Appendix A. Pore collapse occurs from circa 23 MPa (230 bars) effective vertical stress. The compressibility values are summarised in the following table:

Table 3.4 T1612 (brine) - Measured bulk and pore compressibilities

Test ID	Effective axial stress	C_{bm} (/MPa)	C_{pp} (/MPa)
T1612	6-23 MPa	2.81E-04	9.16E-04
T1612	23-30 MPa	4.86E-04	1.58E-03
T1612	>30 MPa	9.95E-04	3.24E-03

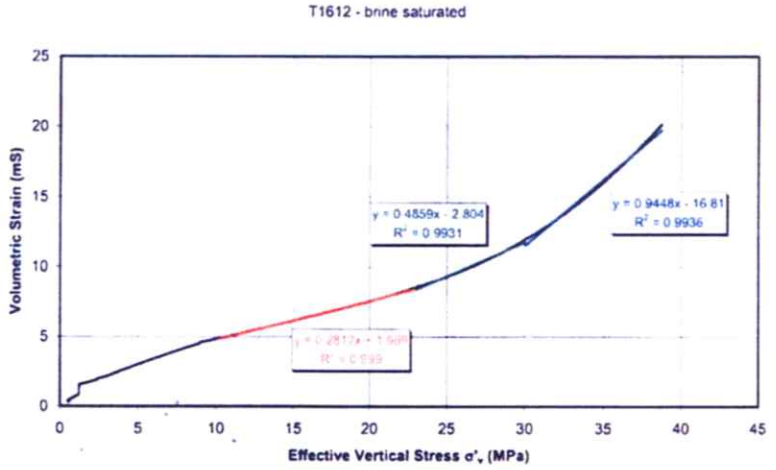

Figure 3.5 T1612 (brine) - Volumetric strain versus effective vertical stress during testing

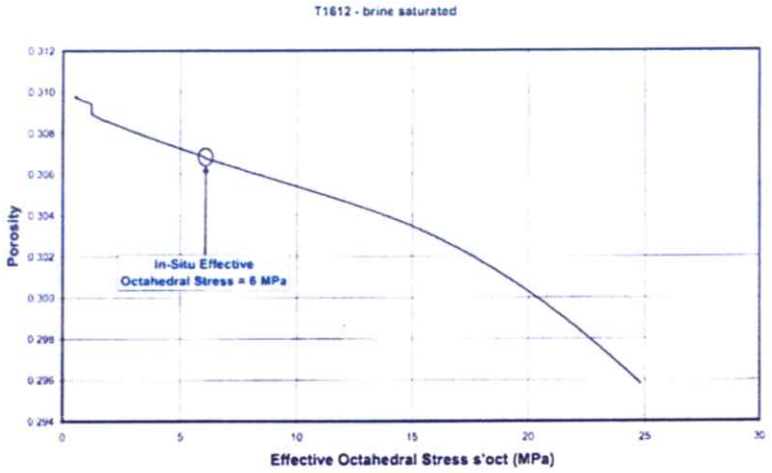

Figure 3.6 T1612 (brine) - Updated porosity during testing

3.4 Comparison with available correlations

The compressibility values inferred from the laboratory experiments are plotted in Figure 3.7 together with two trendlines proposed by Havmøller and Foged (1996) for the elastic and plastic compressibilities (i.e. before and after pore collapse) versus porosity. The compressibility values are fairly well bounded and in good agreement with the elastic and plastic trendlines defined by Havmøller and Foged (1996).

The initial uniaxial yield stress, i.e. stress at which the stress strain curve exhibits a first deviation from linear elastic behaviour, is plotted in Figure 3.8 together with the trendline proposed by Havmøller and Foged (1996). Note that the trendline does not explicitly distinguish between saturating fluid conditions and loading rate, although it is more representative of lower water saturations. The initial yield stress inferred from test T1609 (dry) is more or less in agreement with the value predicted by the trendline.

According to Figure 3.8, the yield stress reduces dramatically with increasing porosity. Yielding may occur at the end of field life (i.e. effective vertical stress of 19.5 MPa) in dry (or gas saturated) chalk for porosity intervals above 40%, and in brine saturated chalk[1] for lower porosity values (circa 33-35%).

[1] assuming that pressure is also reduced during production in water saturated chalk

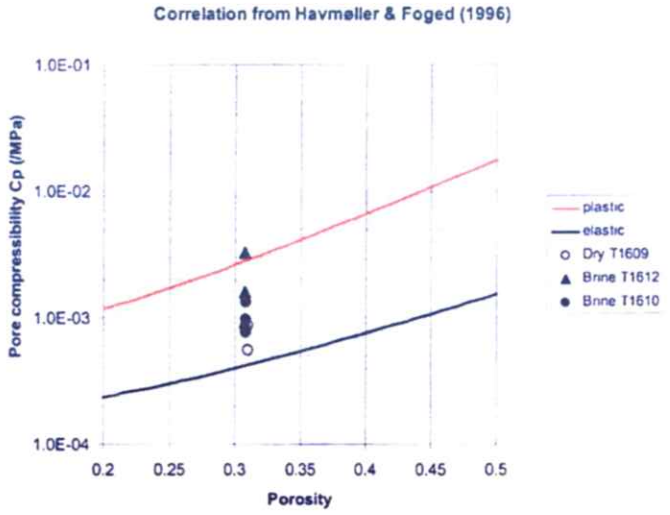

Figure 3.7 *Compressibility inferred from testing and compared to trendlines*

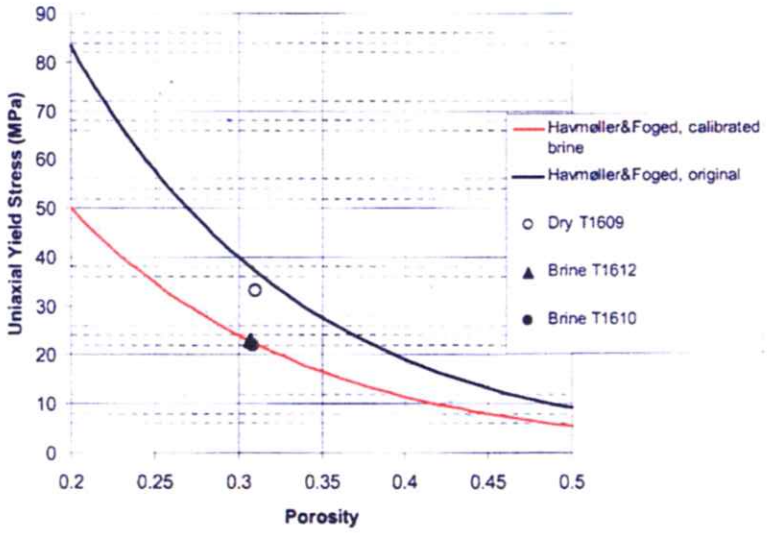

Figure 3.8 *Uniaxial yield stress for tests performed and trendline from Havmøller and Foged (1996)*

4 EQUIVALENT COMPRESSIBILITY FOR WHOLE RESERVOIR SECTION

Data material and testing from the Ommelanden chalk is limited. Hence it is highly improbable that the plugs tested will give a representative variation of chalk behaviour within the reservoir.

The vertical porosity variation through the reservoir is shown in Figure 4.1 from Well Harlingen – 2. The porosity decreases with depth. In the gas bearing chalk, porosities are usually greater than 28% with maximum values above 35%. In the water bearing zone, porosities are lower, between 25 and 30%.

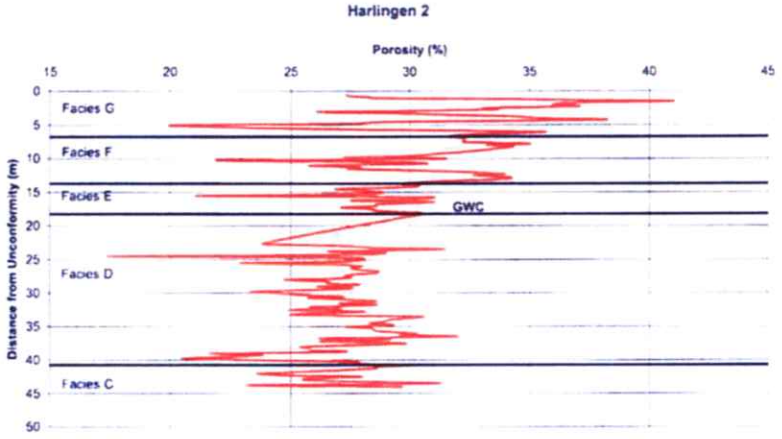

Figure 4.1 Porosity log from Harlingen-2 (vertical well). Distance from top cretaceous unconformity

Reservoir compaction and associated sea-bed subsidence are calculated by TNO based on average reservoir compressibility for the depleting interval. It is assumed that water is immobile in the water bearing formation, and the pore pressure is only reduced in the gas bearing zone during production (Gibbons, personal communication). It is important to take into account the variation of porosity in the calculation of an equivalent compressibility coefficient for compaction prognosis.

A first order analysis of the effect of porosity variation on reservoir compressibility is shown hereafter. Two calculations are performed:

1) Assuming that pressure is reduced only in the gas bearing chalk. The compressibility is defined from the elastic trendline (Figure 3.7) calibrated to the dry test.

2) Assuming that pressure is reduced in both gas and water bearing chalk. The compressibility is defined from the elastic trendline calibrated to the dry test for the gas bearing zone, and from the elastic trendline calibrated to the brine saturated tests for the water bearing zone.

The elastic compressibility is used since pore collapse is not expected within the effective vertical stress range experienced during production for gas saturated chalk below 40% porosity and brine saturated chalk below 33-35% porosity.

The equivalent compressibility is calculated for the porosity log shown in Figure 4.1 assuming homogenous pore pressure depletion throughout the relevant interval (i.e. gas bearing zone or whole chalk formation). Expected reservoir compaction is also calculated. The results are given in the following table.

Table 4.1 Estimate of reservoir compaction due to pore pressure depletion

Depleting interval	Thickness (m)	Maximum depletion (bars)	Compaction (m)	Equivalent bulk compressibility C_{bm} (/MPa)
gas bearing zone (facies E,F,G)	18.25	105	0.031	1.68 E-04
gas and water bearing zones (facies C,D,E,F,G)	44	105	0.086	1.88 E-04

The results of the analysis indicate very limited compaction, with a maximum of 8.6 cm for pore pressure reduction in the whole chalk formation. Assuming full transfer to surface, a maximum subsidence of 8.6cm is predicted at the end of production. This value is much lower than current surface measurement (in the order of 14cm). The discrepancy between surface measurements and current prediction could be due to the assumptions used in the current study (e.g. intact chalk without fractures, representative vertical porosity distribution from Harlingen-2), as well as other effects related to the interpretation of the subsidence measurements (natural shallow compaction, contribution from salt mining).

5 REFERENCES

Elf Aquitaine Production Report No PhC/AN/No632/93 (1993)
Measurements under stress on wellbore HAR7 (Harlingen – Elf Petroland)

Havmøller O. Foged N. (1996)
Review of rock mechanical data for chalk. Proceedings of the 5th North Sea Chalk Symposium, Reims, France

Appendix A - Results from Laboratory Tests

CONTENTS

A1 TEST T1609 – DRY

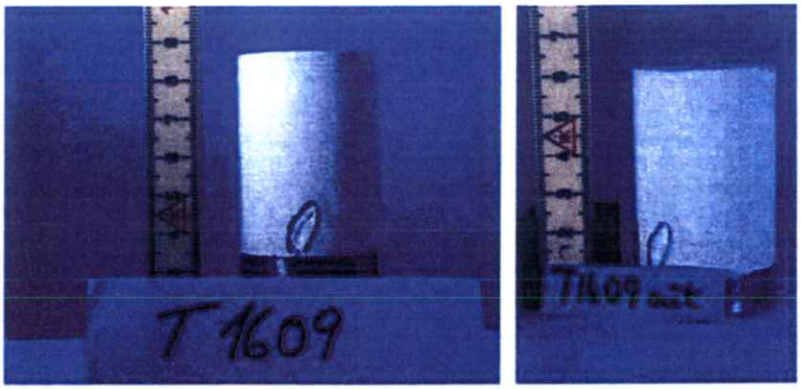

Figure 1.1 T1609 - Photograph before and after testing. The tiny void outlined in blue was filled with gypsum before testing

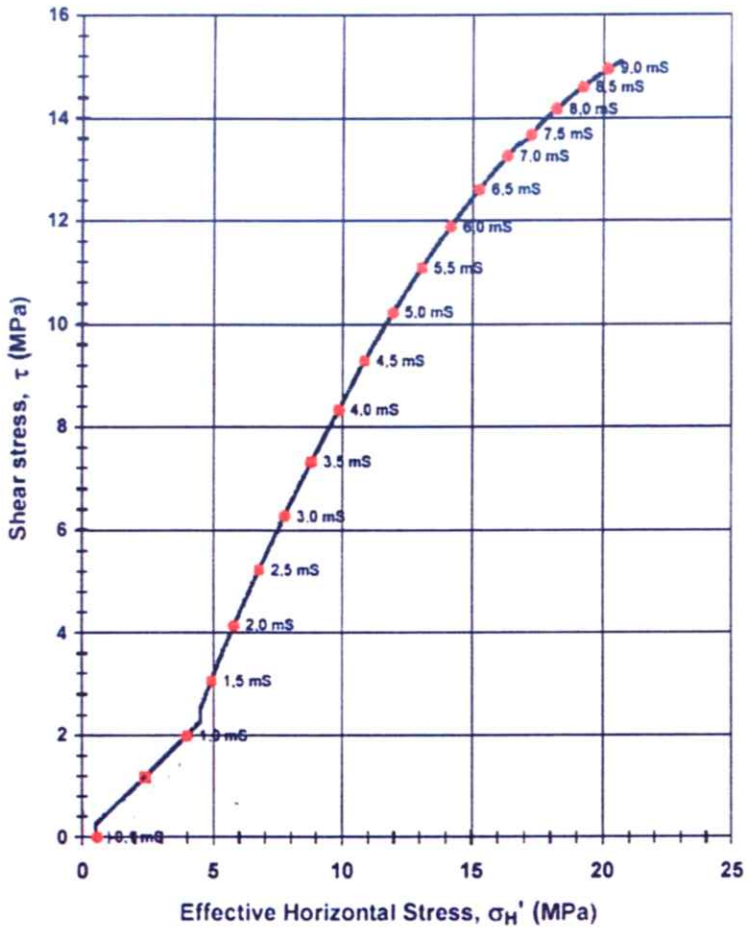

Figure 1.2 T1609 – Shear stress versus effective horizontal stress

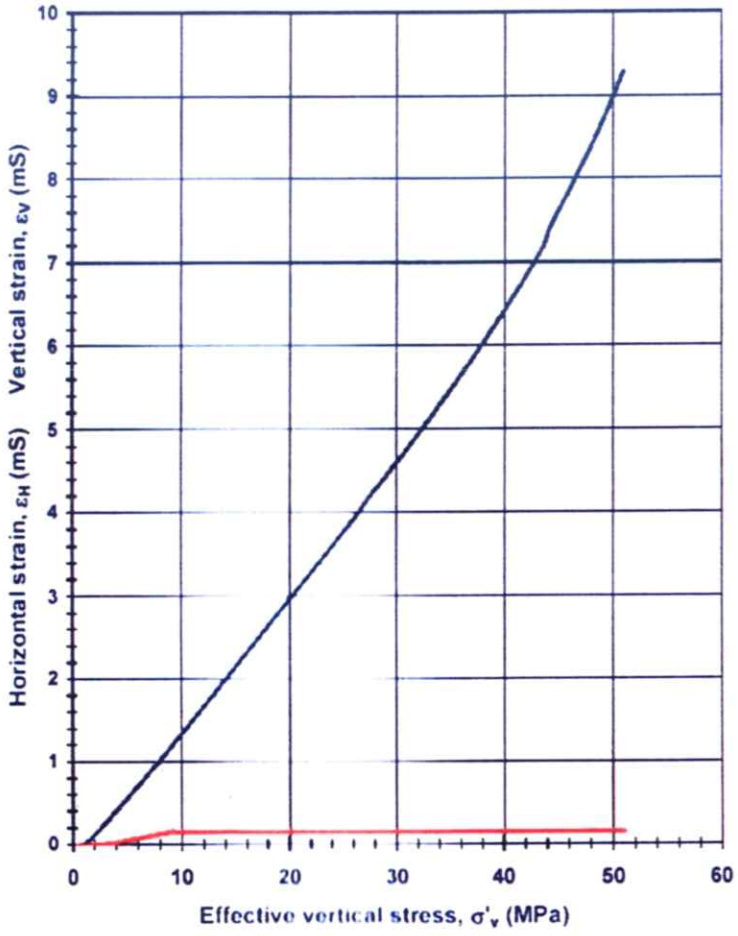

Figure 1.3 *T1609 - Vertical and average horizontal strain versus effective vertical stress*

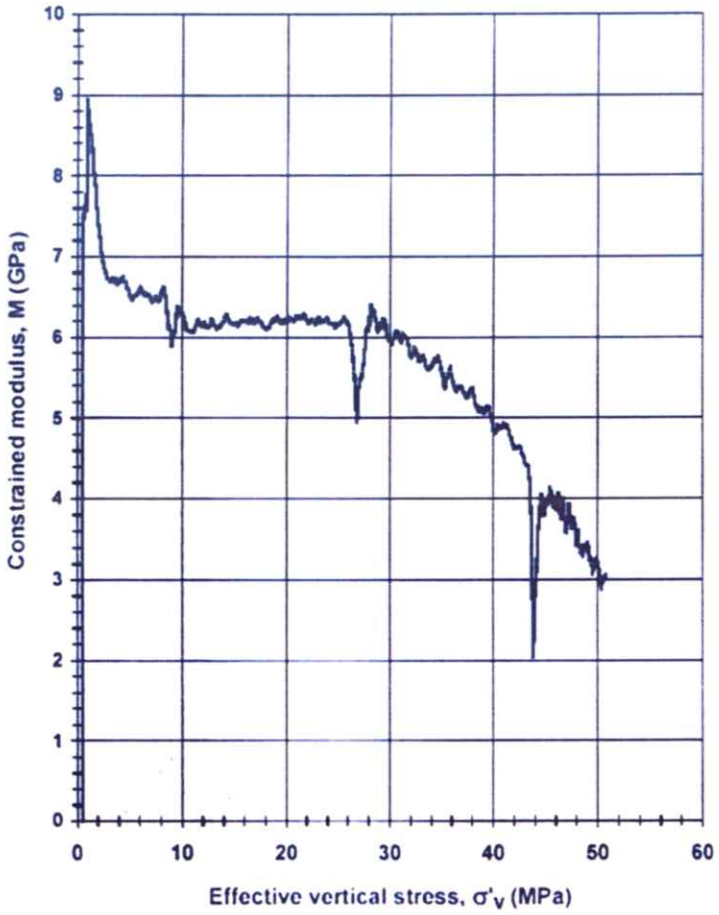

Figure 1.4 T1609 – Tangent constrained modulus versus effective vertical stress

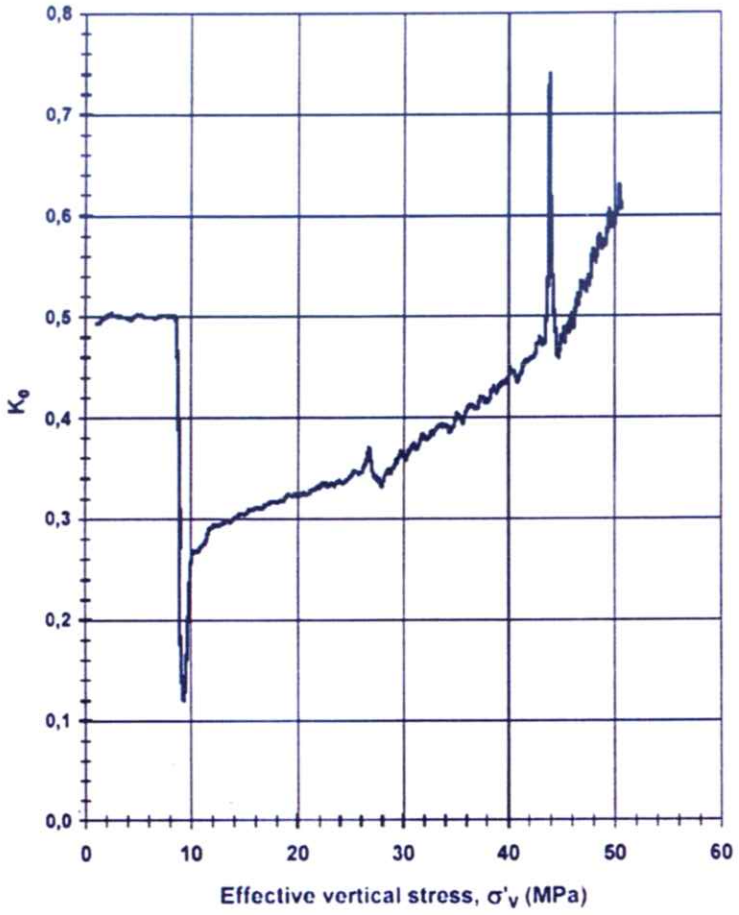

Figure 1.5 *T1609 – Stress ratio K (effective horizontal to vertical stress) versus effective vertical stress*

A2 TEST T1610 – BRINE SATURATED

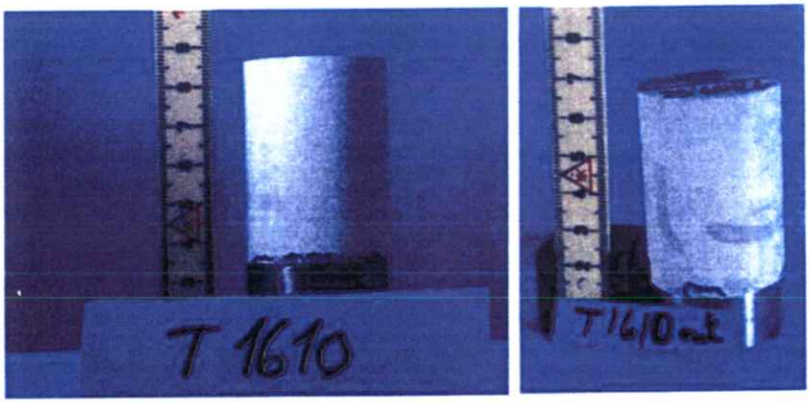

Figure 2.1 *T1610 - Photograph before and after testing. The tiny void outlined in blue was filled with gypsum before testing.*

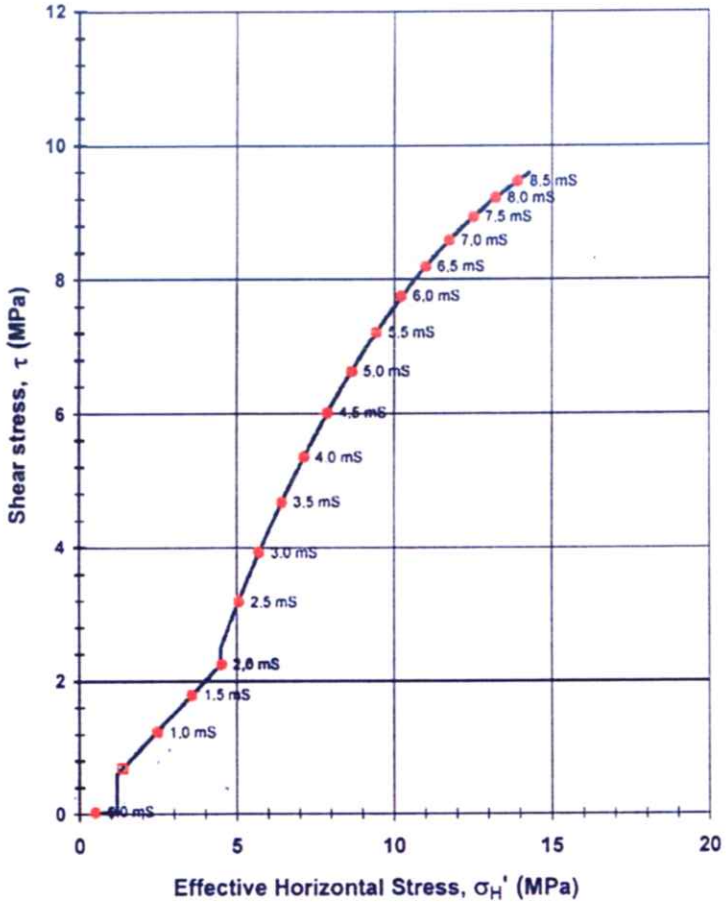

Figure 2.2 T1610 – Shear stress versus effective horizontal stress

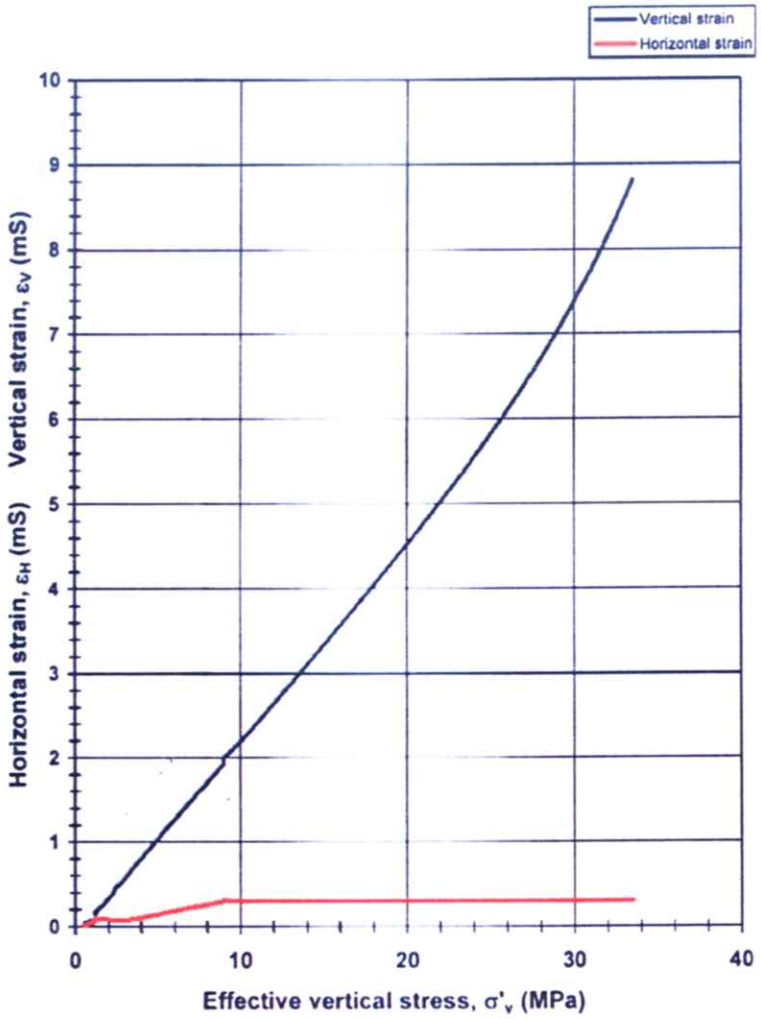

Figure 2.3 *T1610 – Vertical and average horizontal strain versus effective vertical stress*

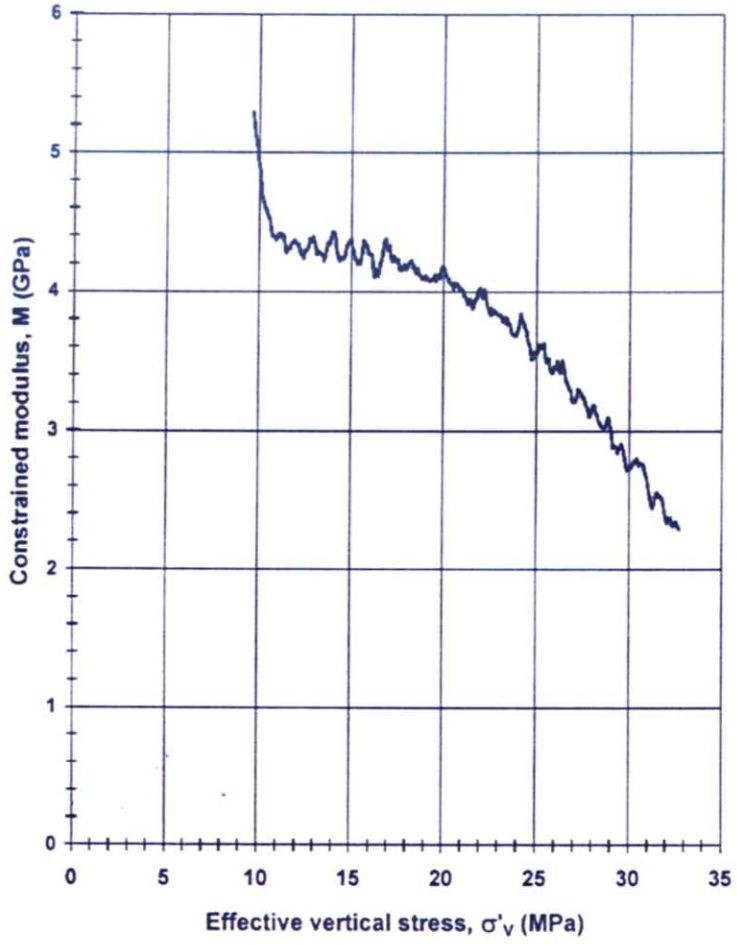

Figure 2.4 T1610 – Tangent constrained modulus versus effective vertical stress

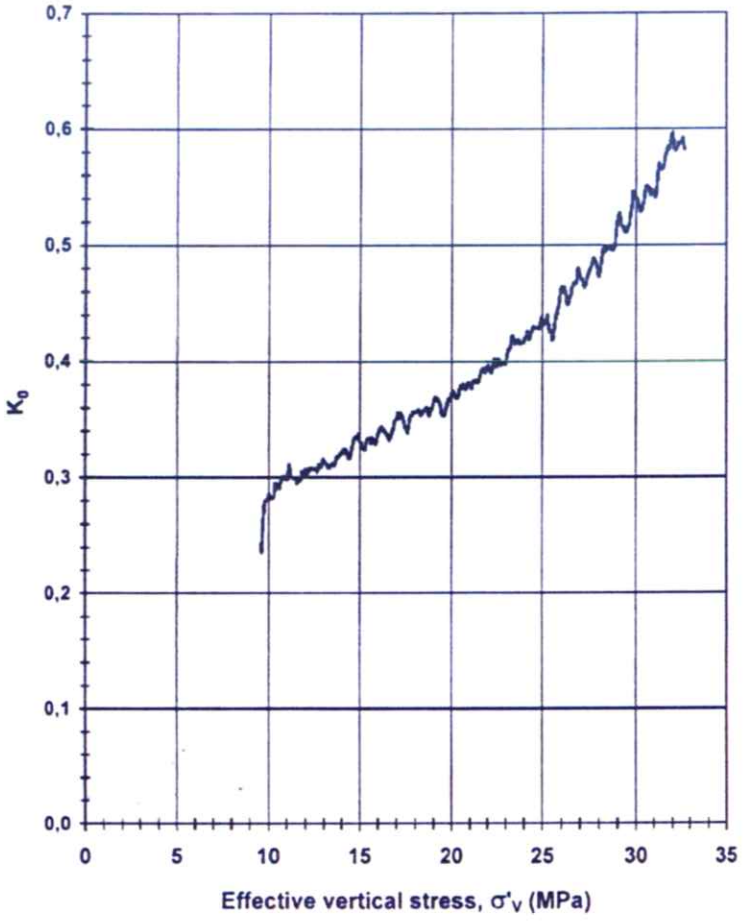

Figure 2.5 T1610 – Stress ratio K (effective horizontal to vertical stress) versus effective vertical stress

A3 TEST T1612 – BRINE SATURATED

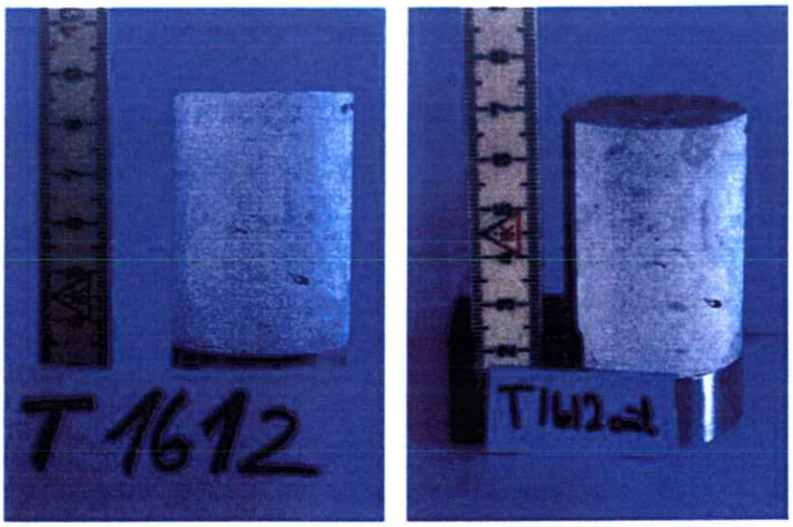

Figure 3.1 T1612 - Photograph before and after testing

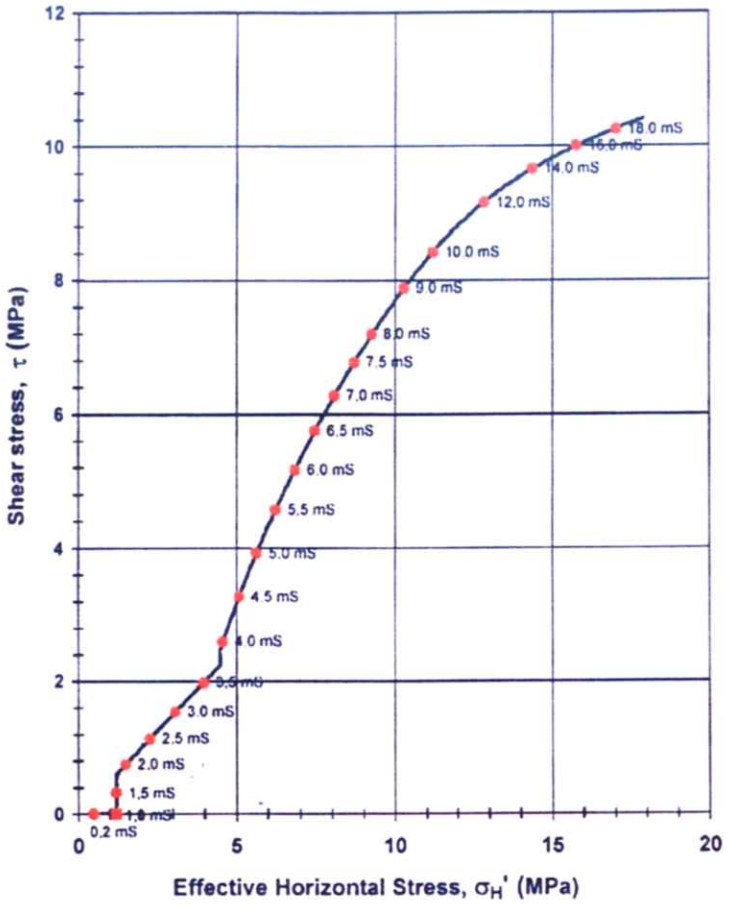

Figure 3.2 T1612 – Shear stress versus effective horizontal stress

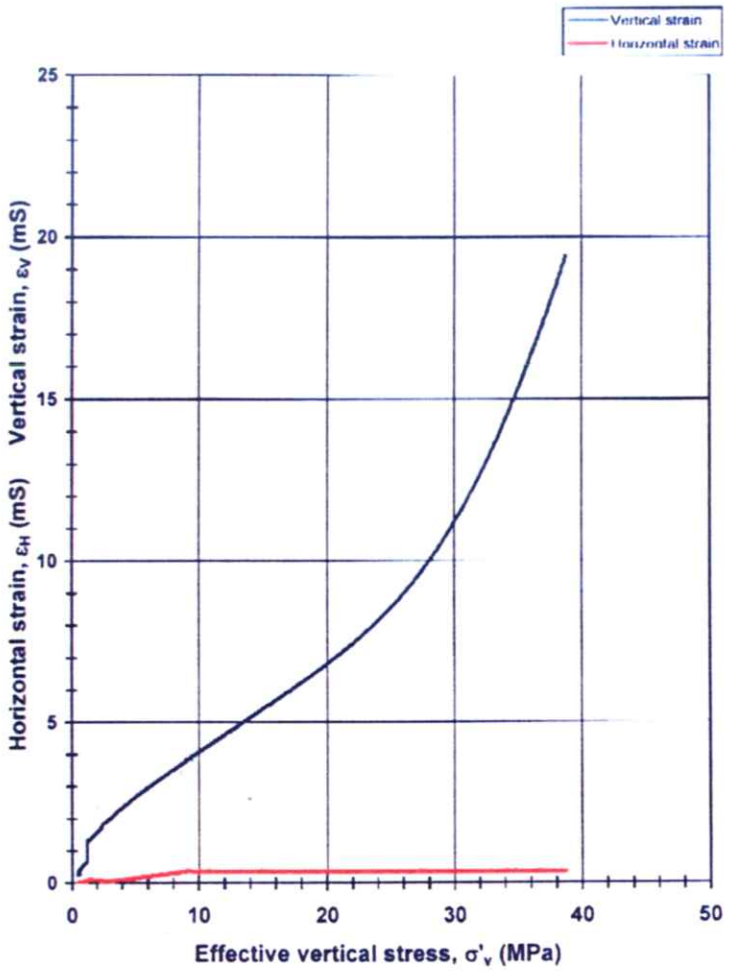

Figure 3.3 T1612 – Vertical and average horizontal strain versus effective vertical stress

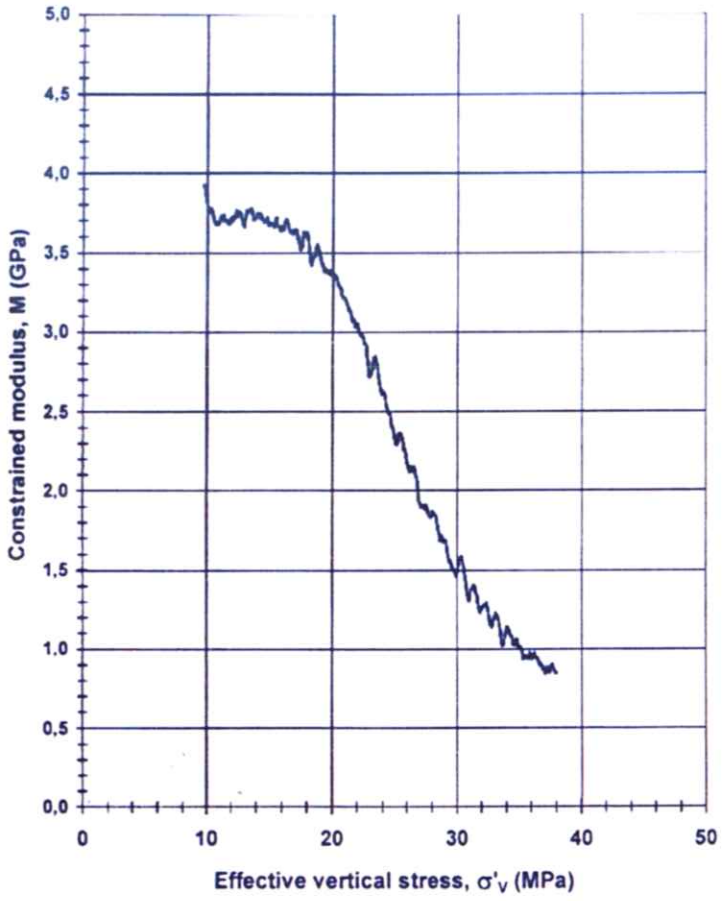

Figure 3.4 T1612 – Tangent constrained modulus versus effective vertical stress

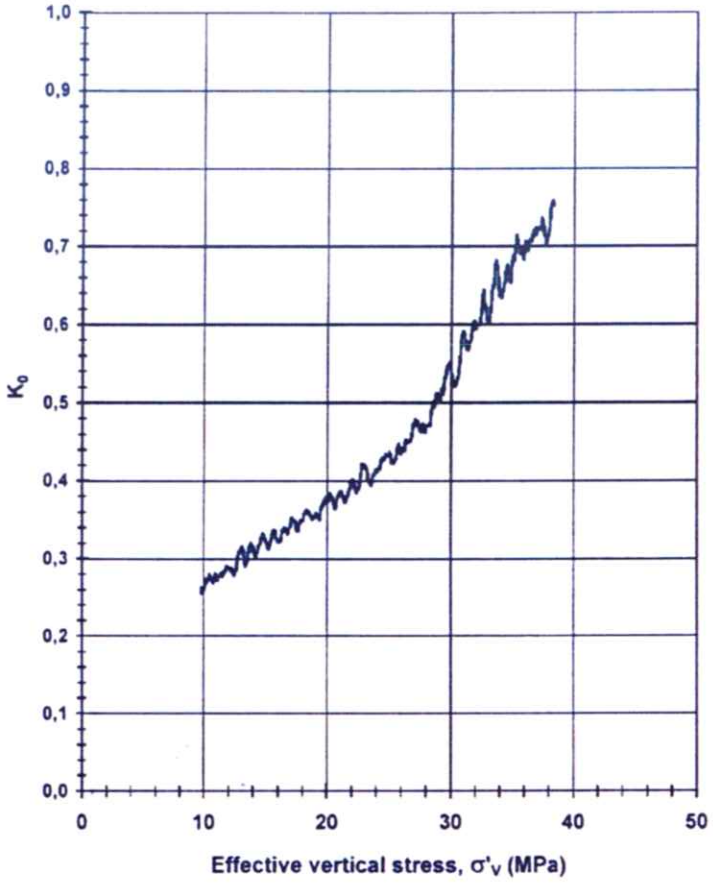

Figure 3.5 T1612 – Stress ratio K (effective horizontal to vertical stress) versus effective vertical stress

Kontroll- og referanseside/ *Review and reference page*

NGI

Dokumentinformasjon/*Document information*		
Dokumenttittel/*Document title* Uniaxial Compaction Coefficient of Chalk Compressibility of Harlingen chalk		**Dokument nr/*Document No.*** 20071135-1
Dokumenttype/*Type of document* ☒ Rapport/*Report* ☐ Teknisk notat/*Technical Note*	**Distribusjon/*Distribution*** ☐ Fri/*Unlimited* ☒ Begrenset/*Limited* ☐ Ingen/*None*	**Dato/*Date*** 22 March 2007 **Rev.nr./*Rev.No.***
Oppdragsgiver/*Client* Vermilion Oil & Gas BV		
Emneord/*Keywords* compressibility, chalk, subsidence, compaction		

Stedfesting/*Geographical information*	
Land, fylke/*Country, County*	**Havområde/*Offshore area***
Kommune/*Municipality*	**Feltnavn/*Field name*** Harlingen
Sted/*Location*	**Sted/*Location*** The Netherlands
Kartblad/*Map*	**Felt, blokknr./*Field, Block No.***
UTM-koordinater/*UTM-coordinates*	

Dokumentkontroll/*Document control*

Kvalitetssikring i henhold til/*Quality assurance according to* NS-EN ISO9001

Rev./ *Rev.*	**Revisjonsgrunnlag/*Reason for revision***	**Egen-kontroll/ *Self review* av/*by:***	**Sidemanns-kontroll/ *Colleague review* av/*by:***	**Uavhengig kontroll/ *Independent review* av/*by:***	**Tverrfaglig kontroll/ *Inter-disciplinary review* av/*by:***
0	Original document	FC FC	LaG LG		

Dokument godkjent for utsendelse/ *Document approved for release*	**Dato/*Date***	**Sign. Prosjektleder/*Project Manager***
	23/03/07	Fabrice Cuisiat

Skj.nr. 043

Appendix 3: Grondmechanica Delft Construction Report

CONSTRUCTIE VAN 7
ONDERGRONDSE MERKEN IN DE
OMGEVING VAN FRANEKER TEN
BEHOEVE VAN PETROLAND

Stieltjesweg 2
Postbus 69, 2600 AB Delft
Telefoon 015-693500
Telex 38234 soil nl
Telefax 015-610821

Postgiro 234342
Bank Mees en Hope NV
Reknr. 25.92.35.911

K.v.K. S 145040 Delft

GRONDMECHANICA DELFT

CONSTRUCTIE VAN 7 ONDERGRONDSE MERKEN IN DE OMGEVING VAN FRANEKER TEN BEHOEVE VAN PETROLAND

CO-300770/13
januari 1988
Hma/Abg/1/184/petro

Opgesteld in opdracht van:
Ingenieursburo Oranjewoud BV

AFDELING GRONDCONSTRUCTIES
projectleider: ir. J. Heemstra
afdelingshoofd: ir. J.W. Sip

GRONDMECHANICA DELFT

INHOUD:

GRONDMECHANICA DELFT

BIJLAGEN:

1	Situatie
2 t/m 8	Sonderingen
9 t/m 15	Doorsnede vast punt

GRONDMECHANICA DELFT

1. INLEIDING

Op 18 juli jl. werd aan Grondmechanica Delft door Ingenieursburo Oranjewoud BV telefonisch opdracht gegeven zeven ondergrondse merken in de omgeving van Franeker te installeren ten behoeve van het waterpasnetwerk van Petroland. Deze opdracht werd op 4 augustus 1988 bij schrijven 71-03825 bevestigd.

GRONDMECHANICA DELFT

2. VOORONDERZOEK

Het betreft de volgende zeven punten:

	globale x-coördinaat	globale y-coördinaat
FR1	162150	578400
HAR2	162380	577250
HAR4	164010	578300
HAR5	165280	576650
Gratingastate	159830	577380
Zweins	170350	578600
Ried2	168350	577150

waarvoor als gemiddeld te bereiken diepte mv - 22 m door de opdrachtgever was opgegeven.

Op grond van gegevens uit het archief van Grondmechanica Delft is per punt van onderzoek in detail onderzocht op welke diepte de weerstandbiedende laag mocht worden verwacht. Op grond van dit onderzoek is per locatie als voorlopige diepte van de vaste zandlaag gerekend met:

FR1	NAP - 24	m ± 24 m
HAR2	NAP - 25	m 21 m
HAR4	NAP - 24	m ± 24 m
HAR5	NAP - 25	m 20 m
Gratingastate	NAP - 18	m 1, m
Zweins	NAP - 24,5	m 15 m
Ried2	NAP - 25	m. 21,5 m

De werkelijke diepte is op basis van het terreinonderzoek bepaald.

GRONDMECHANICA DELFT

3. VELDONDERZOEK

De locatie van de punten van onderzoek is getekend op bijlage 1.
Per locatie is begonnen met een extra zware sondering met meting van de plaatselijke kleef en met hellingmeting. De resultaten en het berekende kleefgetal zijn afgebeeld op bijlage 2 t/m 8.
Bij het sonderen bleek het risico voor uitknikken van de buizenstreng dusdanig groot dat het niet verantwoord was de vaste laag over meer dan enkele meters te verkennen.
Op grond van de resultaten van de sonderingen is in overleg met de projectleider de definitieve geplande diepte vastgesteld, waarop de ondergrondse merken worden gefundeerd.

GRONDMECHANICA DELFT

4. CONSTRUCTIE EN WIJZE VAN PLAATSEN

Het principe van het systeem bestaat hieruit, dat de punt van de conus in een zettingsvrije laag staat. De punt is door middel van stangen met de oppervlakte verbonden, terwijl de omhullende buizen op en neer kunnen gaan met de bewegingen van het maaiveld of de daaronder liggende samendrukbare lagen, zonder dat de punt beweegt.

De constructie bestaat uit een roestvrije lange-slag sondeerconus met grote diameterpunt van gehard en verchroomd staal. De conus is samengesteld uit een vast en een telescopisch schuivend deel. O-ringen en een vuilschraapring zorgen ervoor, dat de in elkaar schuivende delen vrij van vuil blijven. De maximale slag die deze delen ten opzichte van elkaar kunnen maken, is 30 cm. In de punt worden de binnenstangen geschroefd. Het buitenste deel van de conus dat kan schuiven ten opzichte van de vaste punt, wordt met behulp van standaardsondeerbuizen verlengd tot de benodigde lengte.

Aan de hand van de gegevens wordt de vast-punt conus weggedrukt tot de geplande diepte. De eerste binnenstang wordt in de punt van de conus geschroefd. Vervolgens wordt de eerste sondeerbuis over de genoemde binnenstang geschoven en op de mantel van de conus geschroefd. Per meter worden binnenstang en sondeerbuis op de voorgaande geplaatst en wordt deze handeling herhaald totdat de gewenste diepte is bereikt. De schroefdraadverbindingen van de sondeerbuizen worden met een speciale pasta waterdicht afgesloten. Tevens dient deze pasta om de buizen aan elkaar te lijmen, zodat later bij het losdraaien van een dop niet de streng kan loskomen. Verder worden de borstaansluitingen van de sondeerbuisdraad voorzien van een anticorrosiemiddel. De ruimten tussen de sondeerbuis en de binnenstangen worden gevuld met een speciale olie. Dit is een milieuvriendelijk mineraal produkt, dat wrijving en roestvorming moet voorkomen. Als dit bij elke meter wordt gedaan, voorkomt men zoveel mogelijk luchtinsluiting.
Wanneer de vereiste diepte is bereikt, wordt de streng sondeerbuizen een gedeelte van de conusslag getrokken, bijvoorbeeld 20 cm van de slag van 30 cm. Hierbij wordt tijdens het trekken met een waterpasinstrument gecontroleerd of de aan de binnenstangen gekoppelde punt niet mee omhoogkomt. Daarna volgt de afwerking van het merk.

GRONDMECHANICA DELFT

5. UITVOERING

Bij het installeren van de vaste punten bleek dat het door de grote benodigde totaalkracht en de relatief weinig vaste bovenlagen in een aantal gevallen maar juist mogelijk was de definitieve geplande diepte te bereiken.
Gezien het risico voor knik en breuk van de buizenstreng zijn de punten daarom in enkele gevallen een of twee decimeter hoger blijven staan dan voorzien, zodat de afstand tussen bovenkant dop en putdeksel in die gevallen minder dan de theoretische maat van 0,5 m bedroeg.
Een doorsnede van alle punten is gepresenteerd op de bijlagen 9 t/m 15.

De uiteindelijke installatiediepte bedroeg voor de punten

FR1	mv - 30,2 m
HAR2	mv - 21,9 m
HAR4	mv - 31 m
HAR5	mv - 21,9 m
Gratingastate	mv - 22,9 m
Zweins	mv - 24,1 m
Ried2	mv - 23,3 m

dat wil zeggen in totaal 21,3 m meer dan was gepland.

Gezien de terreinomstandigheden moest het punt Gratingastate iets ten opzichte van de oorspronkelijke locatie worden verplaatst.

Bij het punt Zweins werd hinder ondervonden van de hoge grondwaterstand.

Na het installeren van de punten zijn op verzoek van de opdrachtgever de bovenkanten van de meetmerken conform de afspraken afgewerkt.

Het installeren van meetputten zal door de opdrachtgever in eigen beheer worden verzorgd.

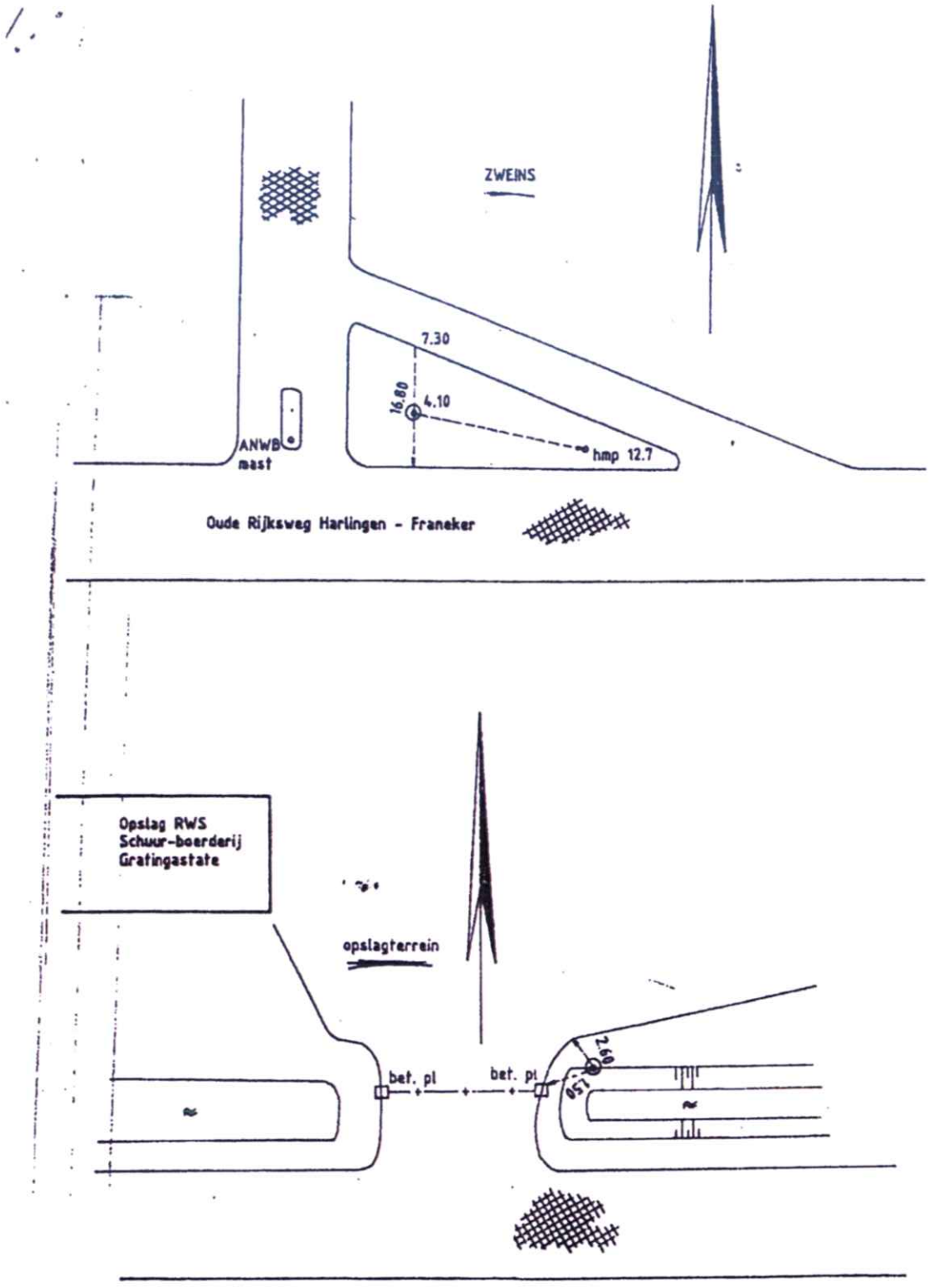
ZWEINS
7.30
16.80
4.10
hmp 12.7
ANWB
mast
Oude Rijksweg Harlingen - Franeker
Opslag RWS
Schuur-boerderij
Gratingastate
opslagterrein
bet. pl
bet. pl
2.90
1.50

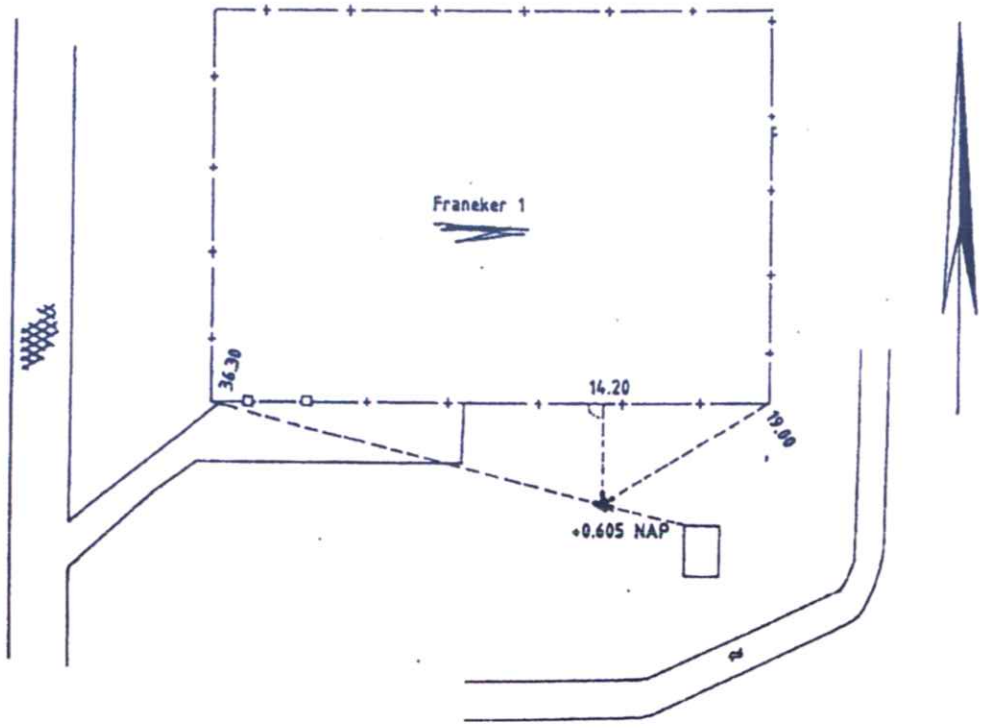
Franeker 1
36.30
14.20
19.00
+0.605 NAP

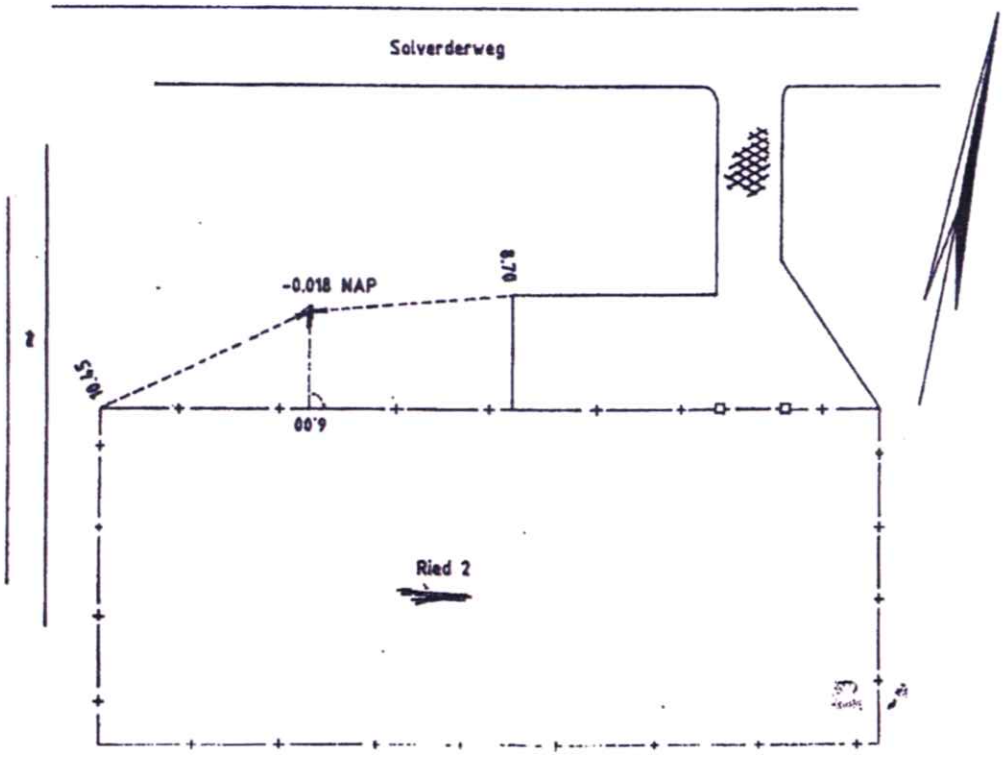
Solverderweg
-0.018 NAP
8.70
10.15
6.00
Ried 2

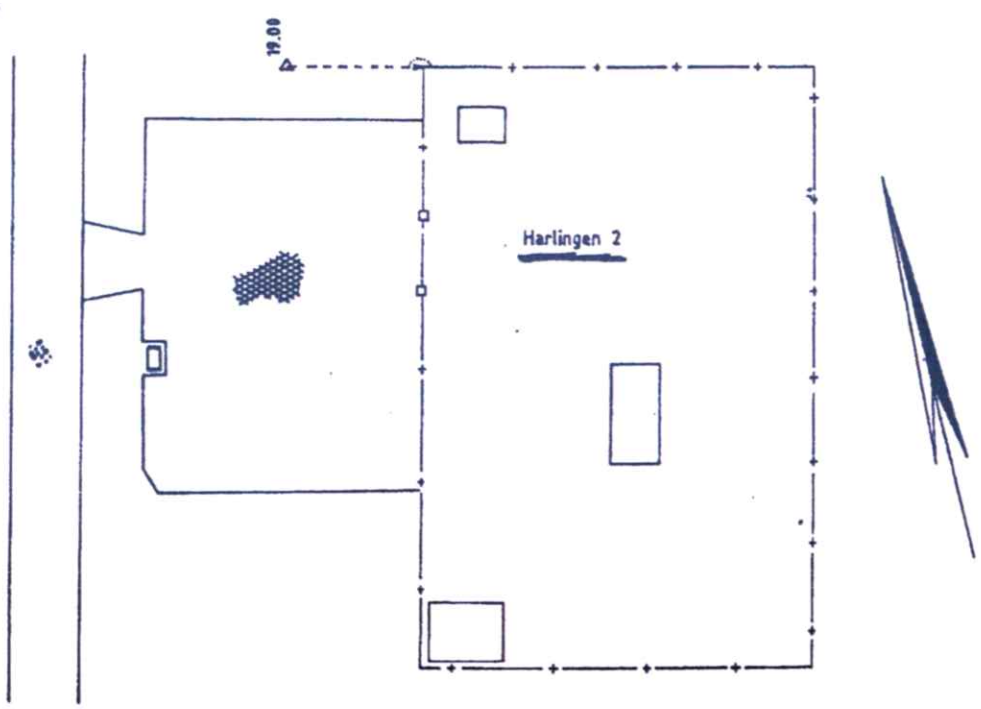
19.00
Harlingen 2

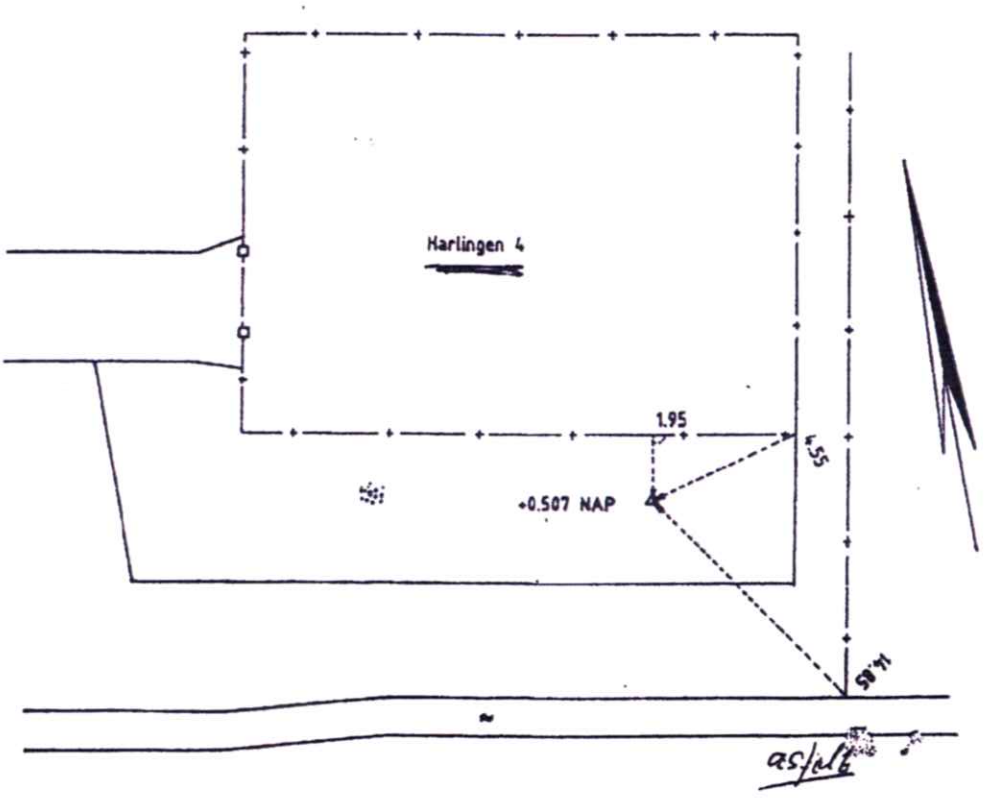
Harlingen 4
1.95
4.55
+0.507 NAP
asfalt

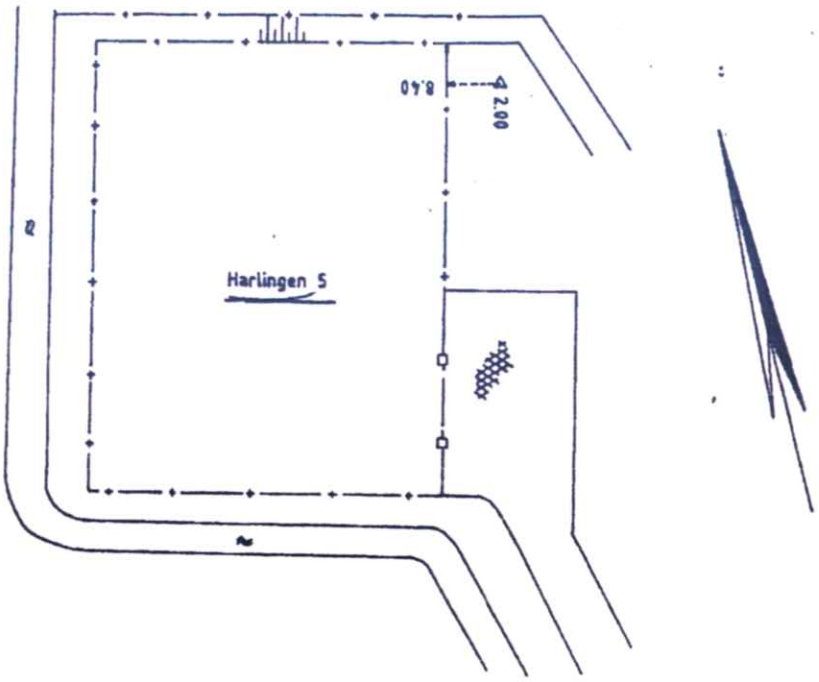
8.40
2.00
Harlingen S

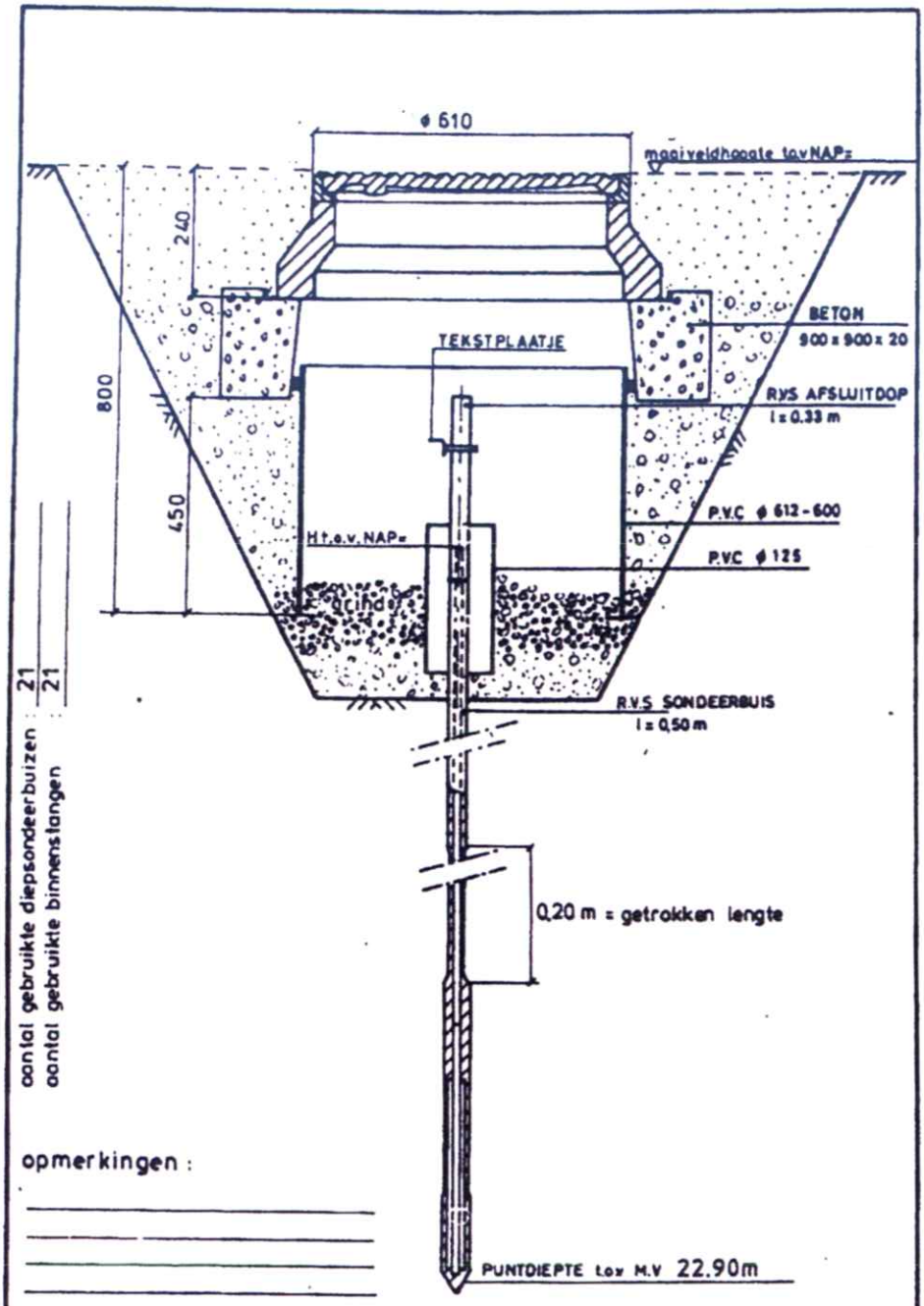

GRONDMECHANICA DELFT	Postbus 69, 2600 AB Delft Telefoon (015) 69 35 00	Telefax (015) 61 08 21 Telex 38234 soil nl	d.d. aug.'88
PLAATSINGSGEGEVENS ONDERGRONDS MERK STANDAARDAFWERKING MEETKUNDIGE DIENST RWS LOKATIE : GRATINGASTATE - 0A2748			CO-300770 BIJL.

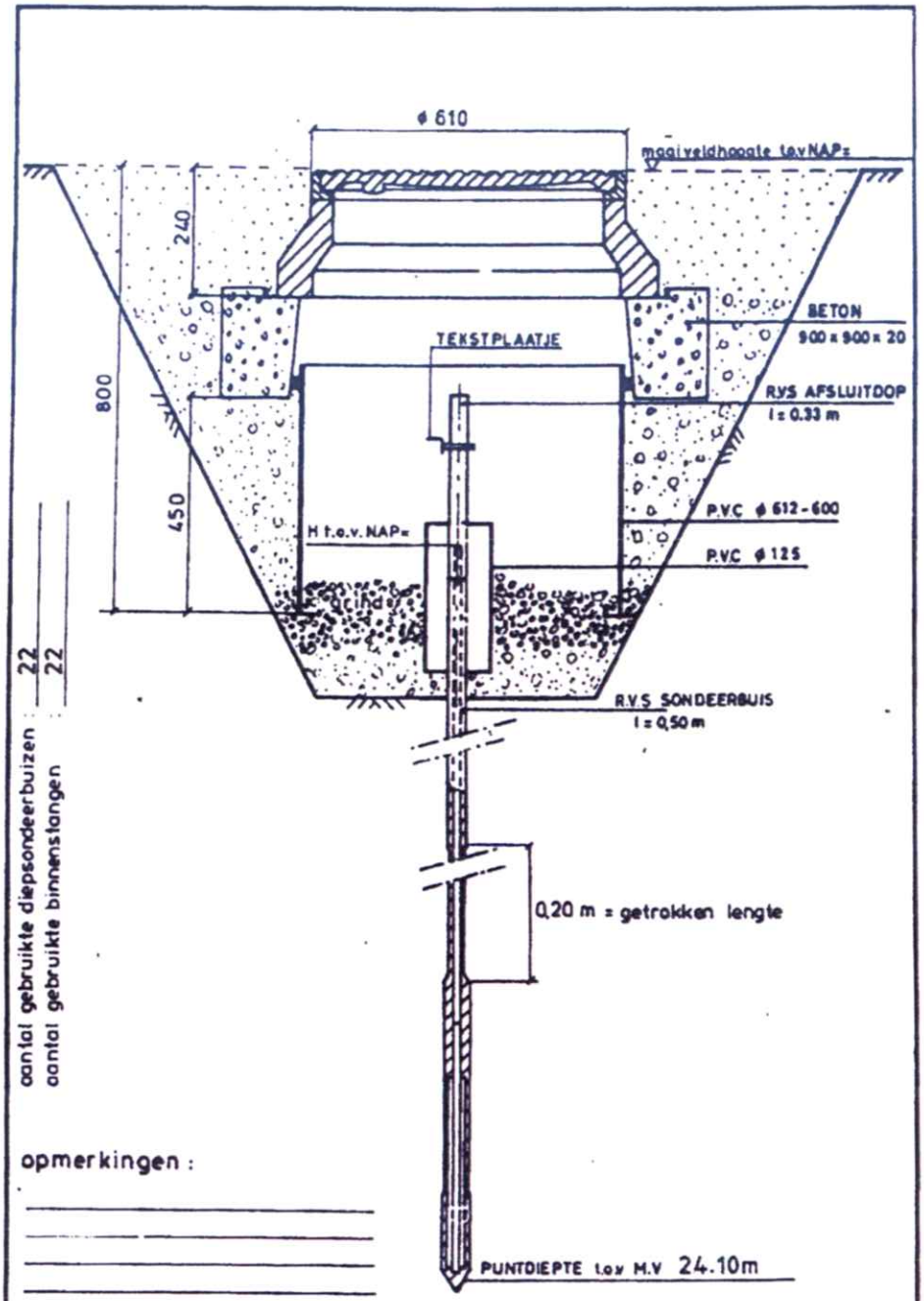

GRONDMECHANICA DELFT	Postbus 69, 2600 AB Delft Telefoon (015) 69 35 00	Telefax (015) 61 08 21 Telex 38234 soil nl	d.d. aug.'88	get.
PLAATSINGSGEGEVENS ONDERGRONDS MERK STANDAARDAFWERKING MEETKUNDIGE DIENST RWS LOKATIE : ZWEINS - 0 A2760			CO- 300770	gez.
			BIJL.	form. A4

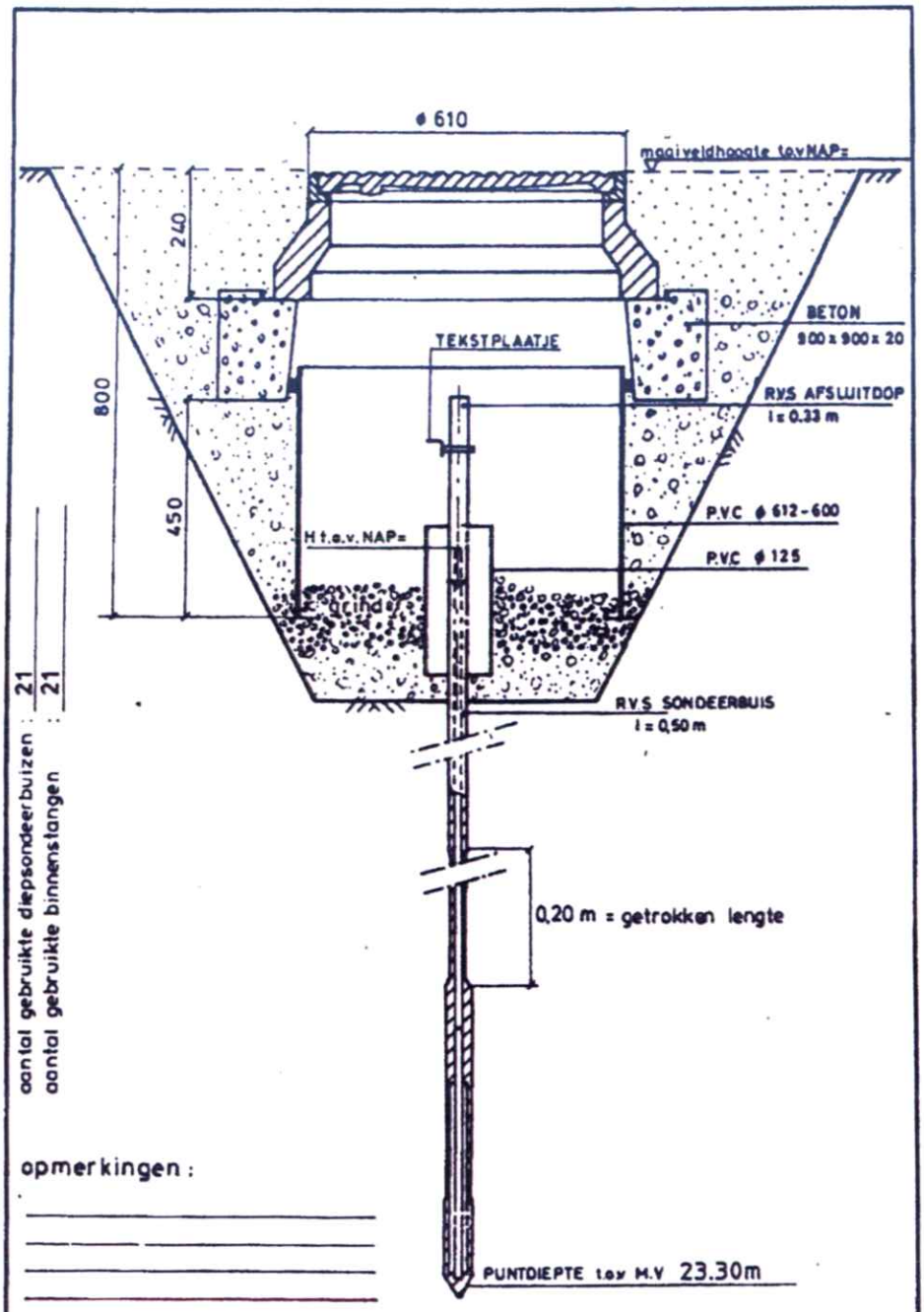

GRONDMECHANICA DELFT	Postbus 69, 2600 AB Delft Telefoon (015) 69 35 00	Telefax (015) 61 08 21 Telex 38234 soil nl	d.d. aug.'88	get.
PLAATSINGSGEGEVENS ONDERGRONDS MERK STANDAARDAFWERKING MEETKUNDIGE DIENST RWS LOKATIE : RIED 2 - 0A2758			CO-300770	gec.
			BUL.	form. A4


MASTEPUNTEN
SITUATIE
schaal: 1 25.000
CO-300770
Blz. 1

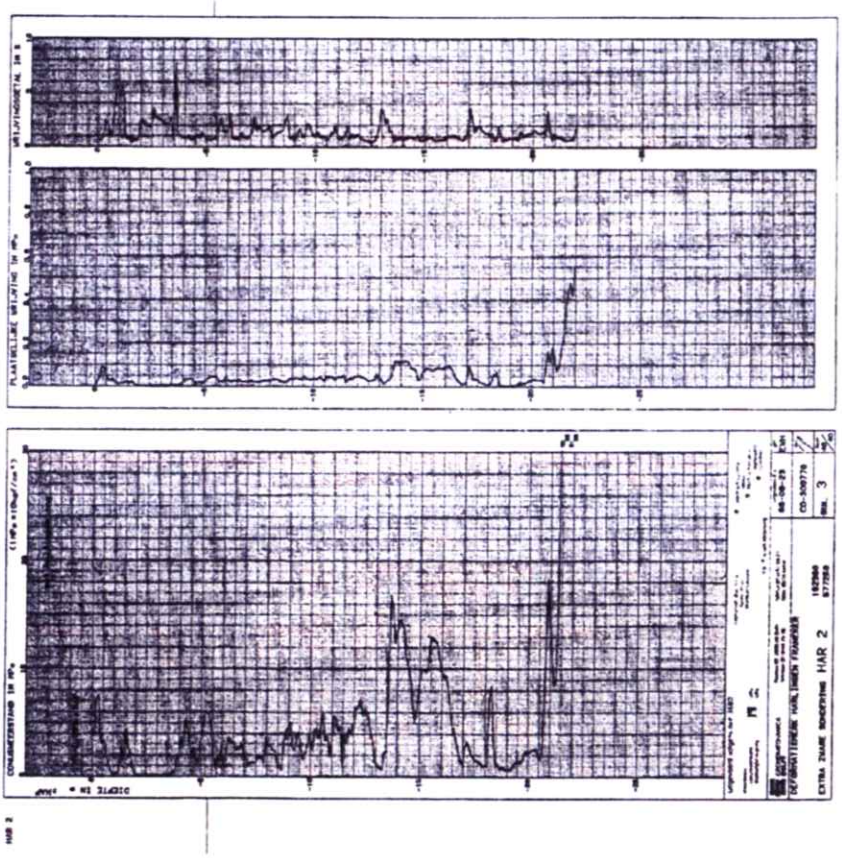
CO-300779
Blz. 3
HAR 2

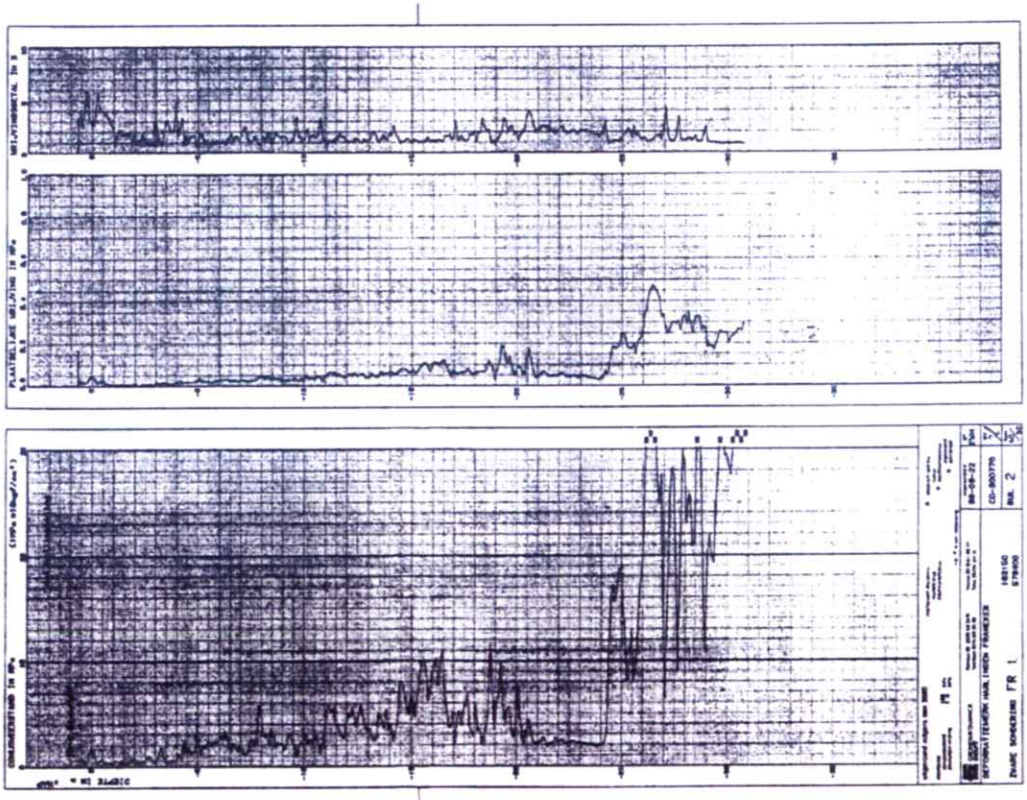

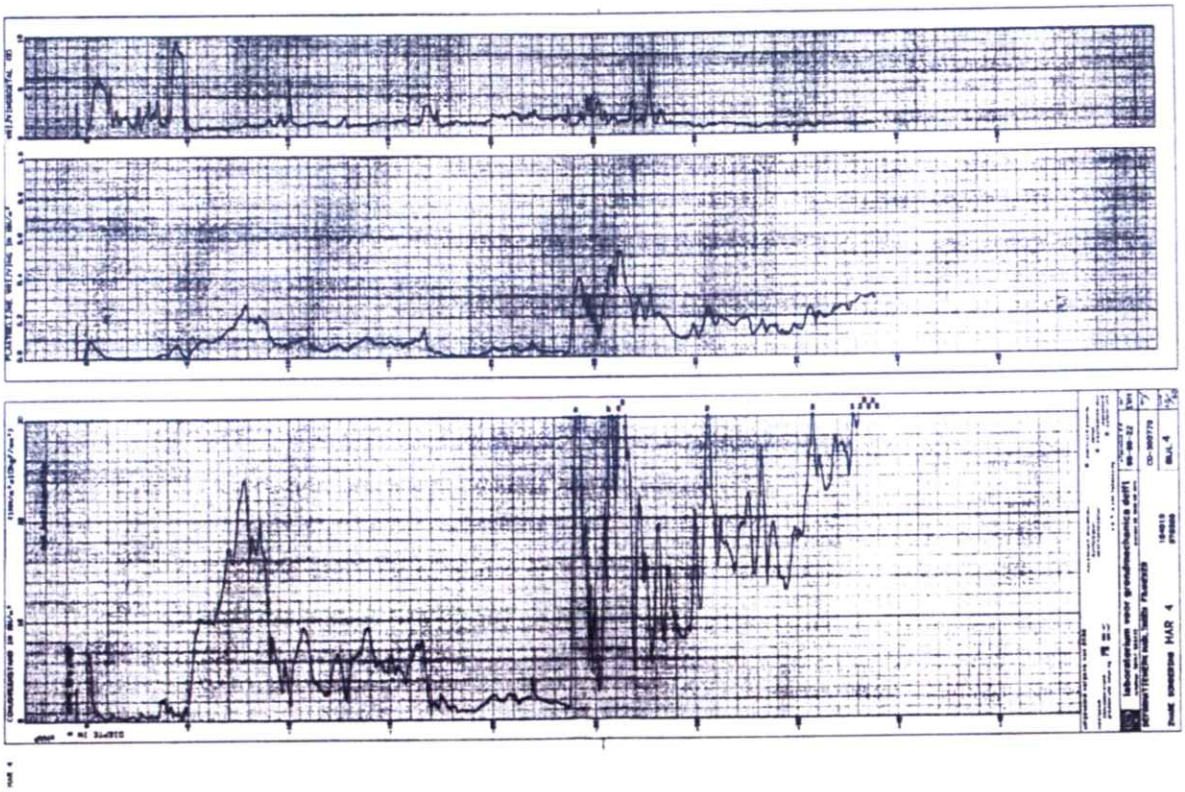

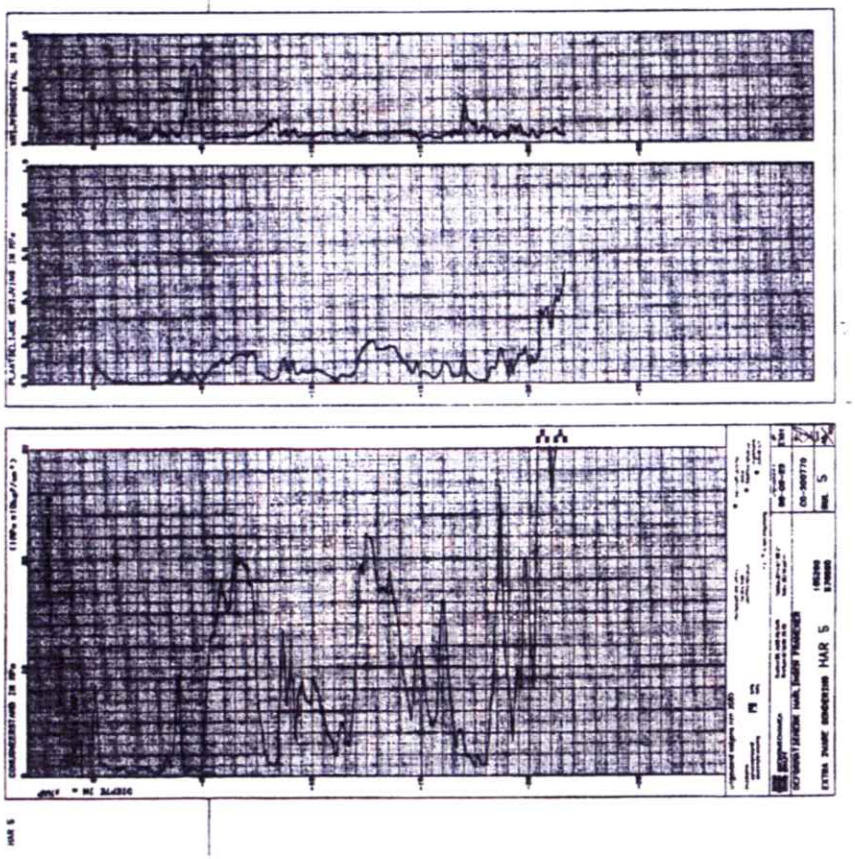

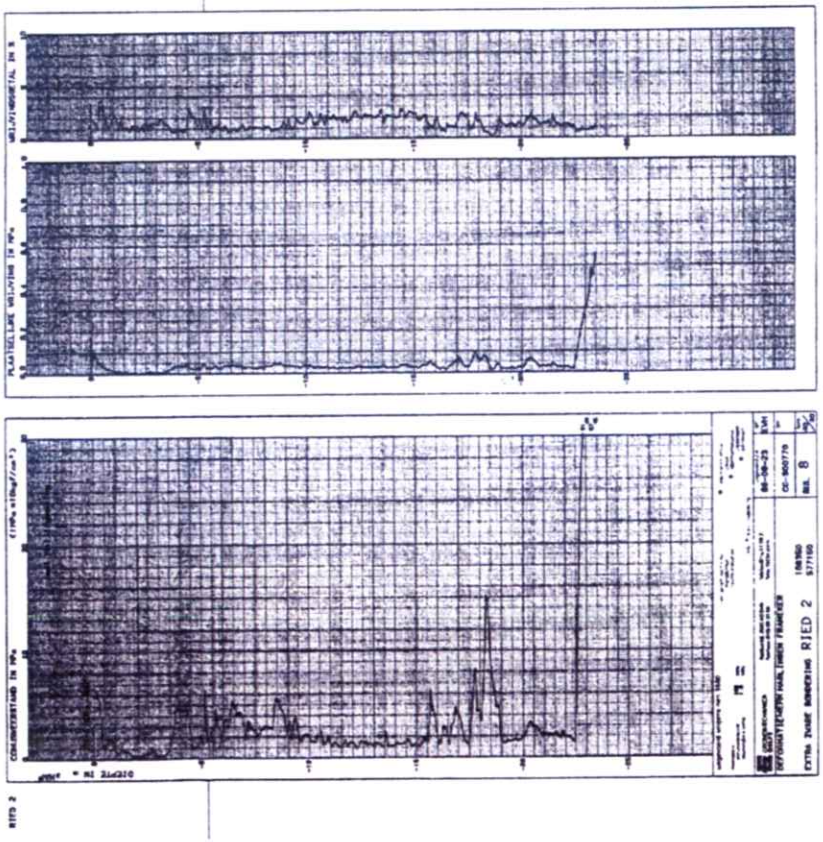
RIED 2
RIED 8
EXTRA ZWARE BOORSTANG
CD-900770
88-06-23

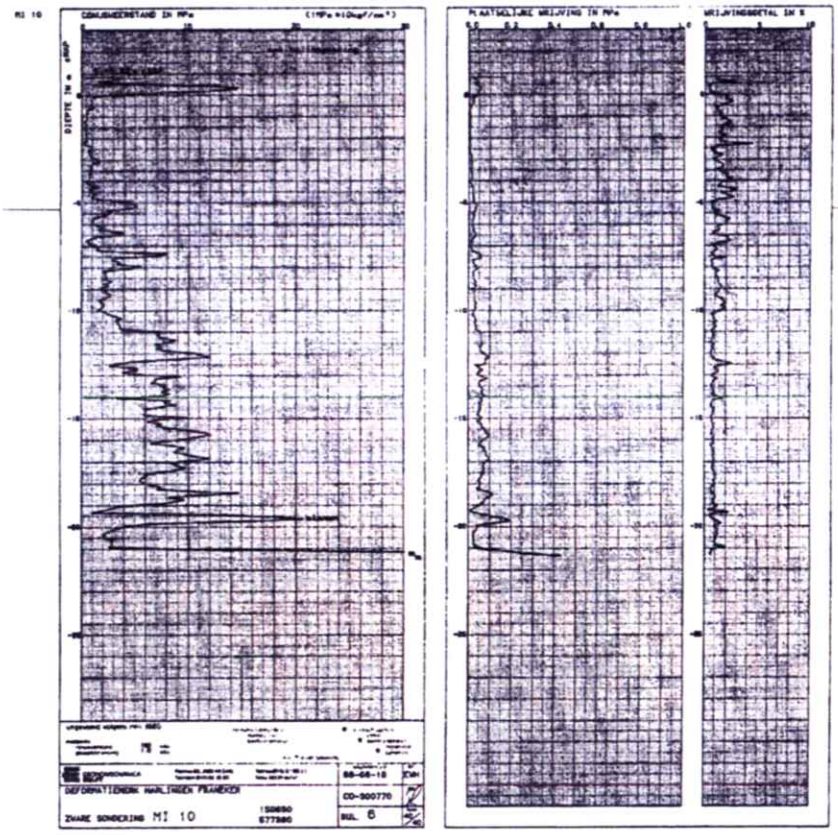
MI 10
DRUKWEERSTAND IN MPa
PLASTISCHE WRIJVING IN MPa
WRIJVINGSGETAL IN %
DIEPTE IN m
ZWARE SONDERING MI 10
CD-900770
88-08-10

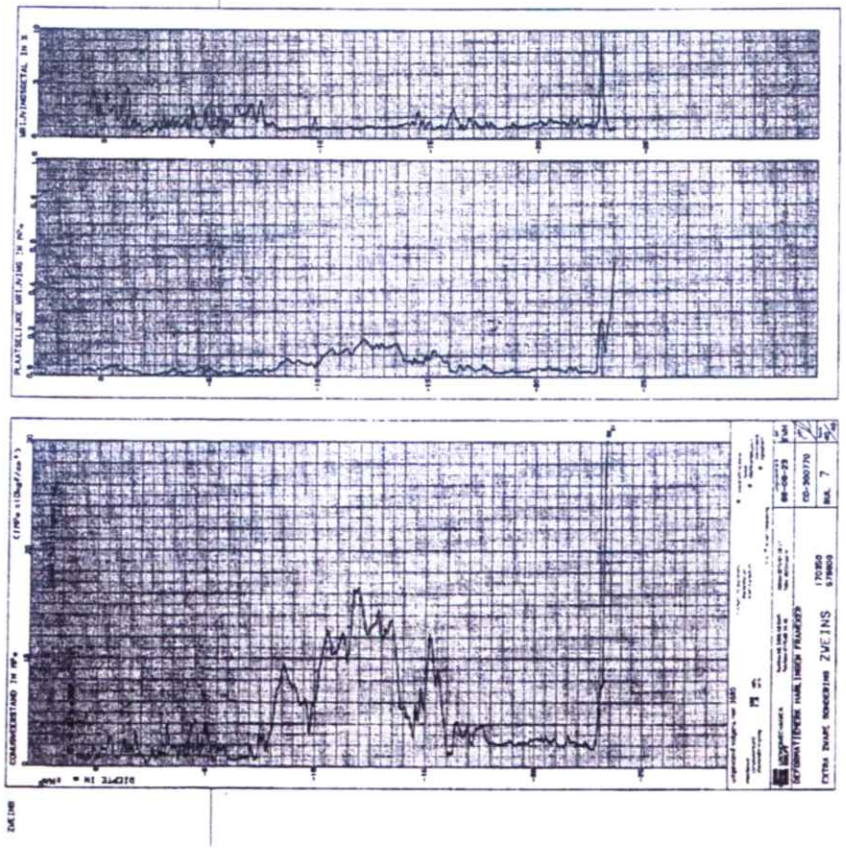

Addendum 1: Results of Modelling Review with State Supervision of the Mines, June – September, 2007

A review of the draft report submitted to State Supervision of the Mines in May, 2007 resulted in identification of a number of technical focus items that required further review. These focus items were:

1) The shape of the subsidence contours did not exactly match the shape of the reservoir structure map. A review of the reservoir model grid compared to the reservoir structure map was conducted, and subsequently a review of the transformation from reservoir model co-ordinates into Amersfoort X-Y coordinates.
2) The Compaction Coefficient, C_m, used in the draft report was the maximum value from the testing under load. A review of the derivation of a model C_m value from the rock mechanic testing results was conducted.
3) Previous studies had included the possibility of some depressurization of the water leg of the reservoir. This scenario was evaluated and incorporated into the revised model.
4) The surface subsidence data collected from the shallow founded markers should be included in comparison to model results, and the quality of these readings should be investigated. The modelling data has been compared to the surface measurements, but at this time, an assessment of the reliability of these readings is ongoing.

The results of the review of these technical focus items are shown in the following sections of this report. The resulting model does provide a more accurate depiction of the physical reservoir, most notably at the edges of the reservoir. This has caused the subsidence contours to become more natural in appearance but the current (2006) and ultimate (2016) maximum subsidence values are unchanged (9 – 10cm in 2006 and 12 – 13cm ultimate) from the May report.

Results of Coordinate Transformation Efforts

A comparison of the reservoir structure map to the reservoir model showed that some slight geometric differences occurred at the edges of the reservoir.

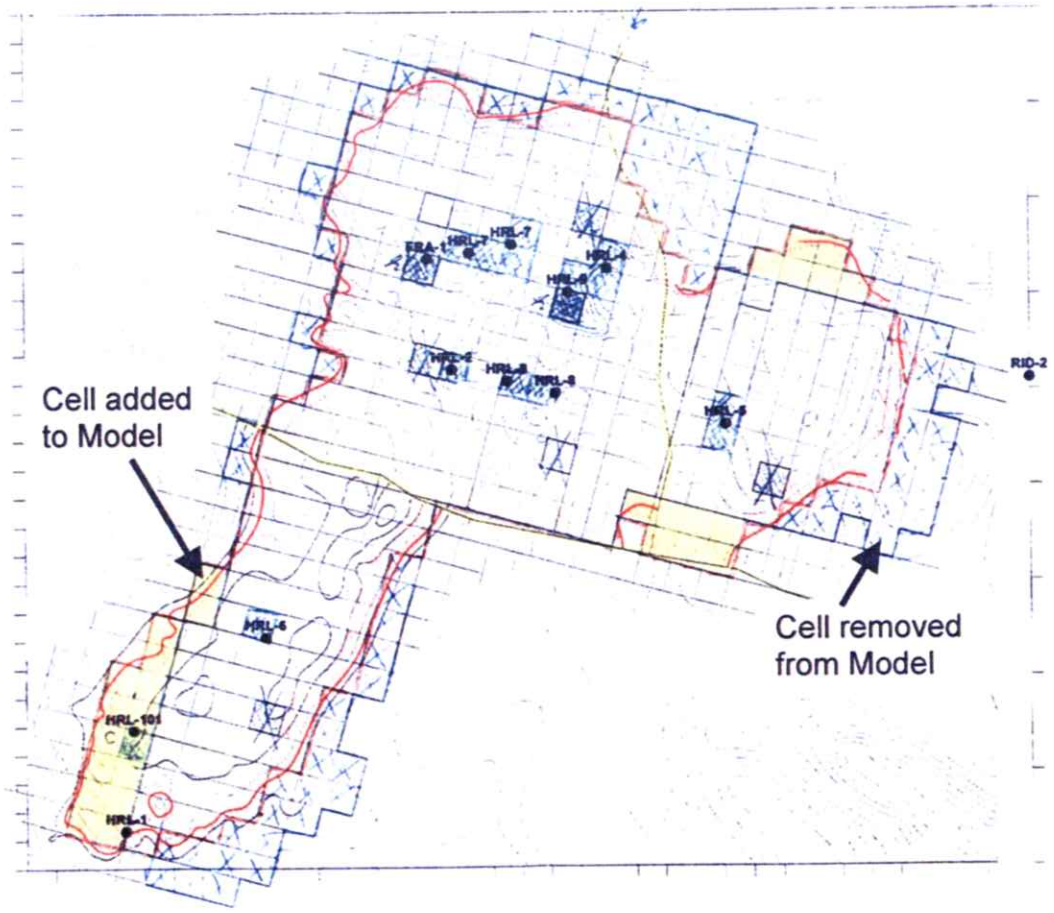

This grid revision also altered the placement of some of the wellbores to more accurately reflect the physical situation. The following pressure distributions (shown in bar) were generated using the updated reservoir model.

For 1997;

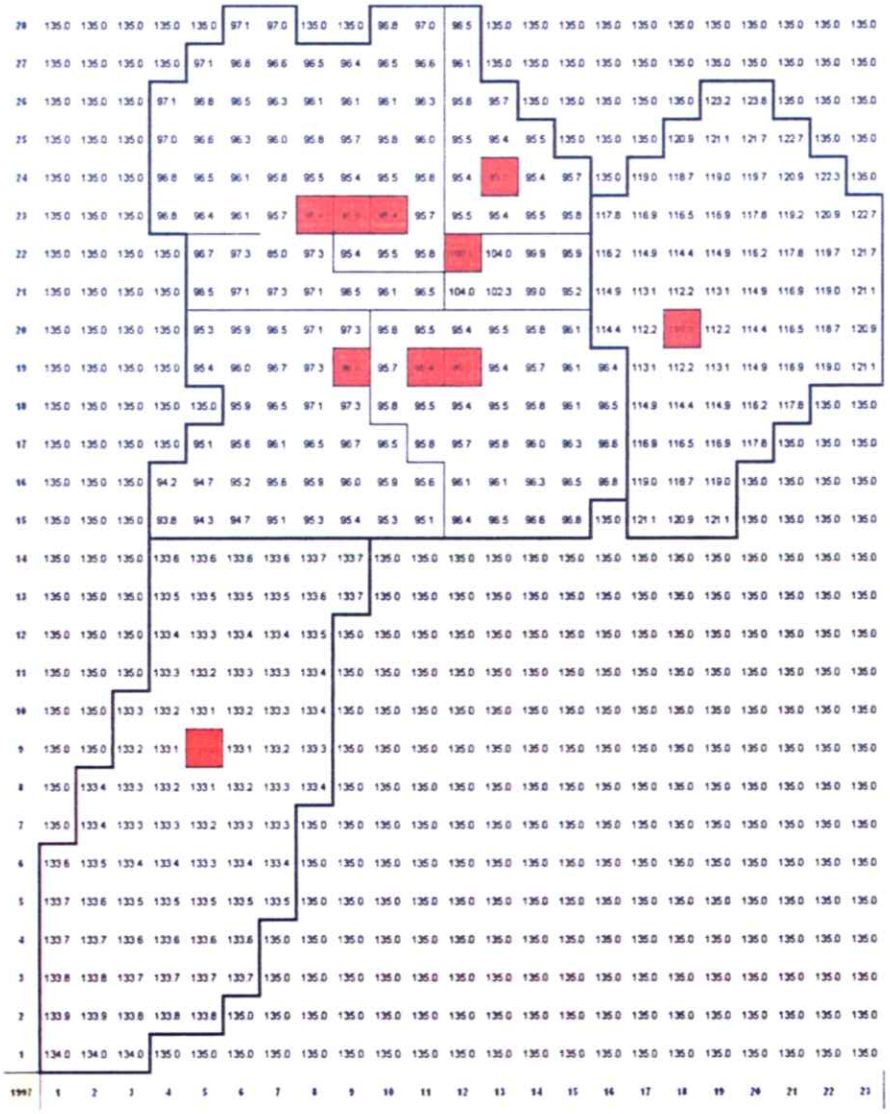

For 2000;

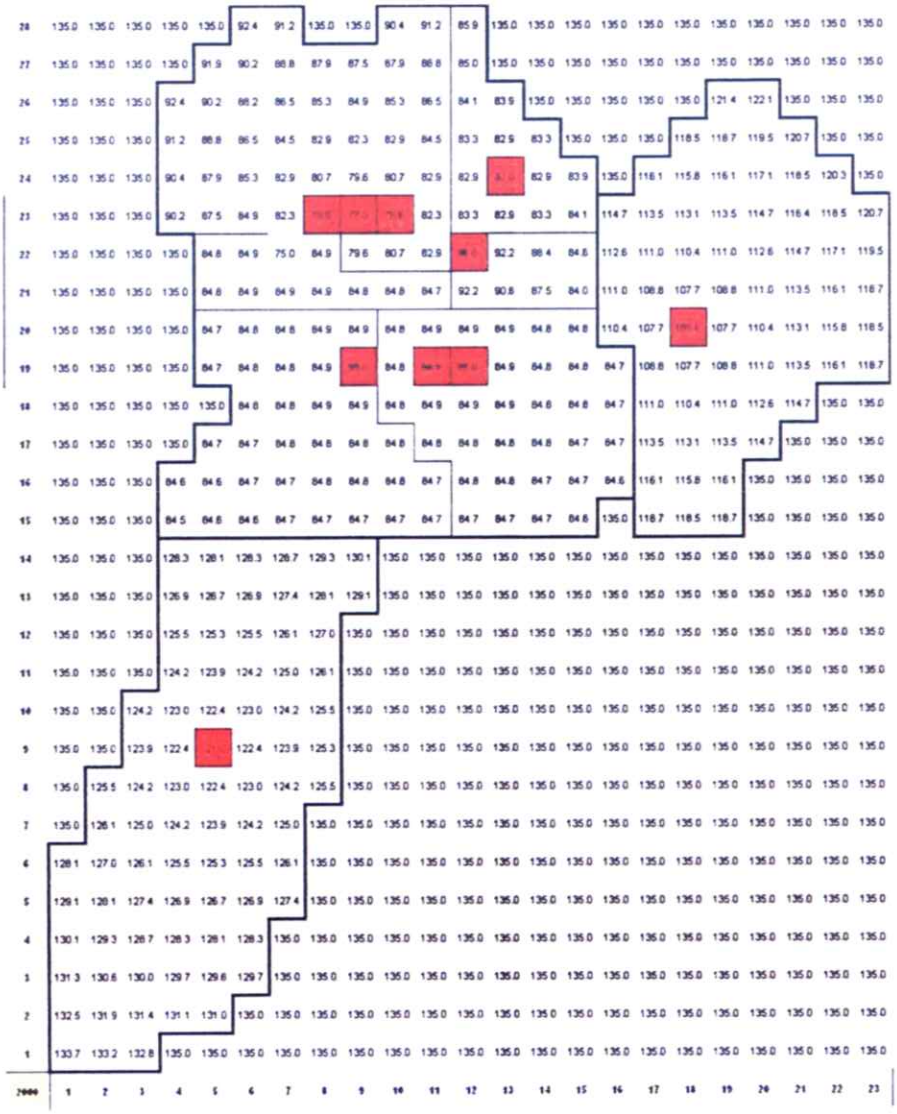

For 2003;

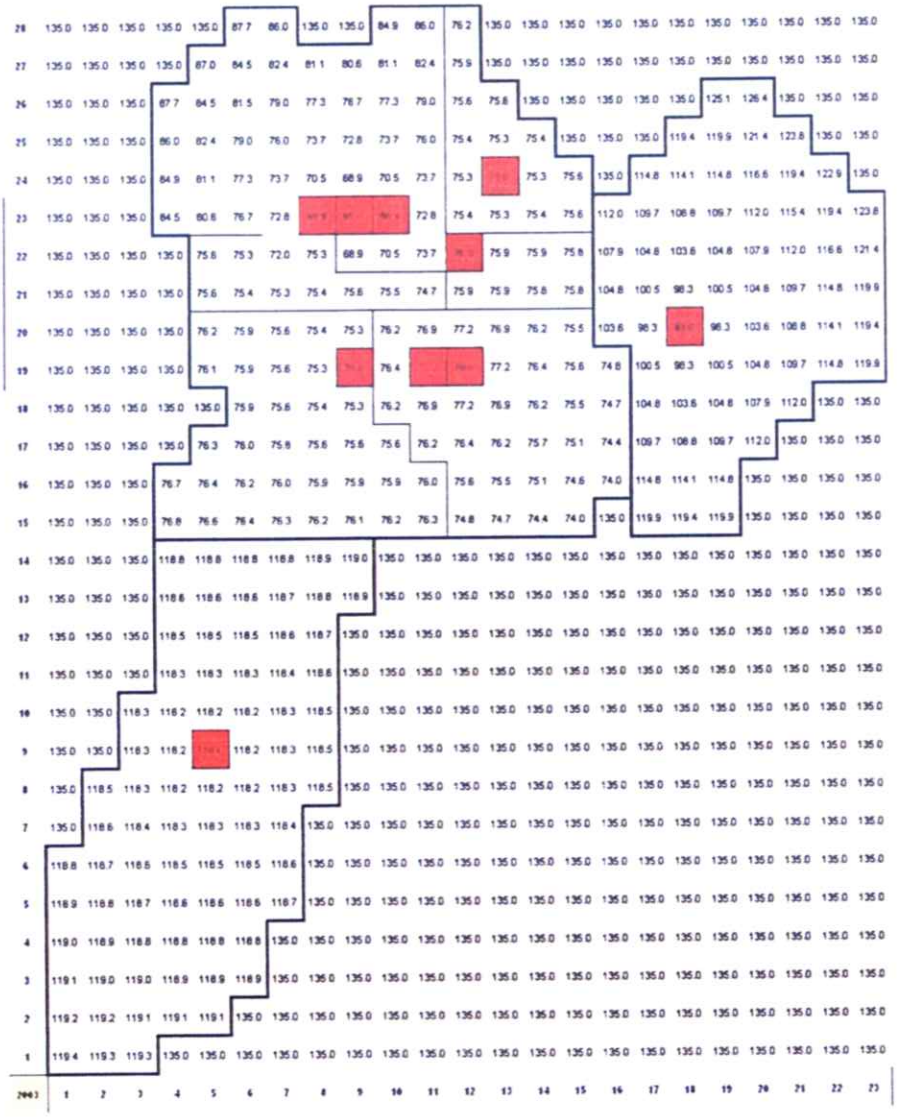

For 2006;

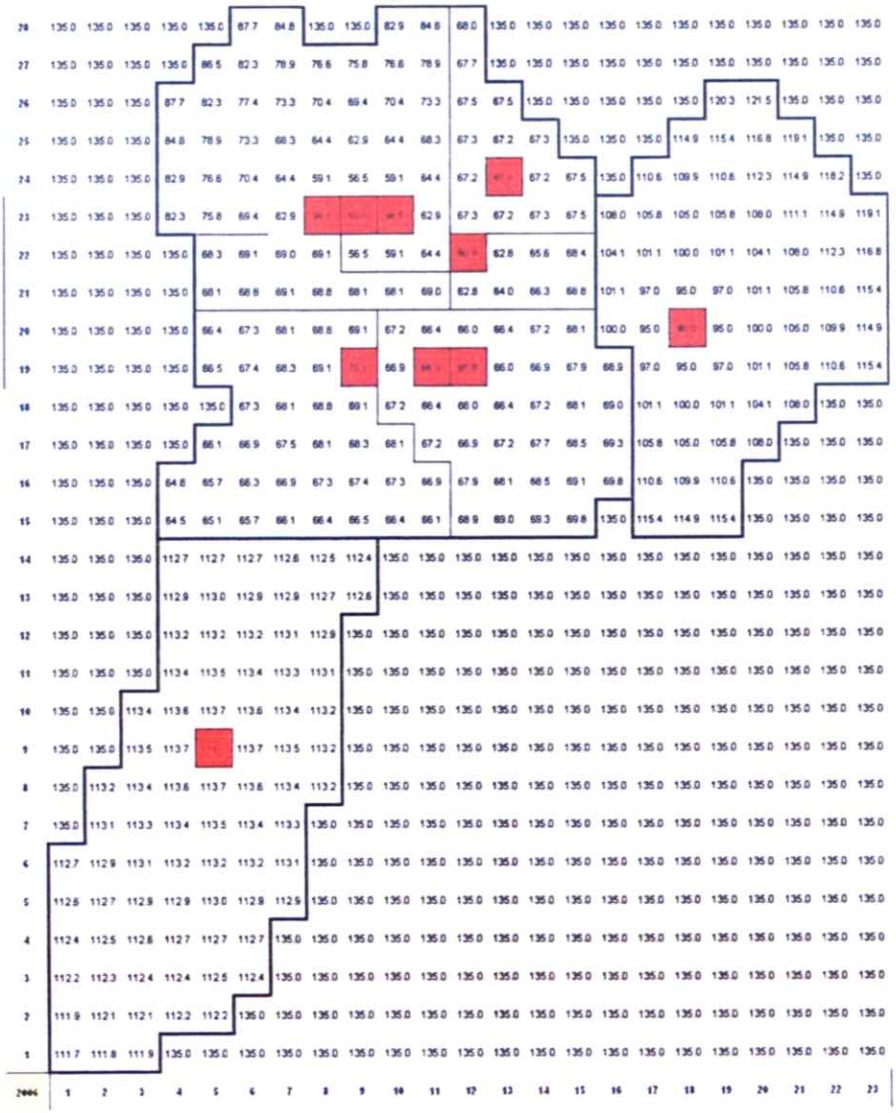

For 2016;

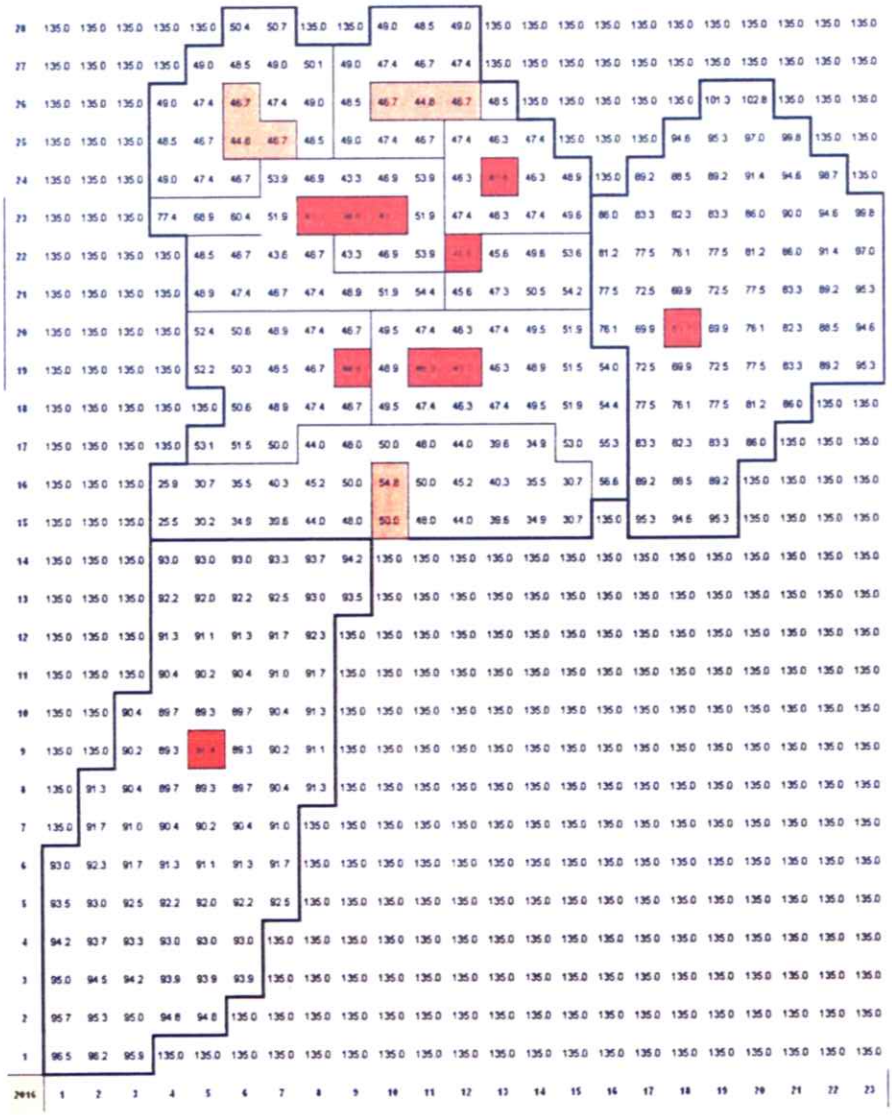

The review of the reservoir model geometry also indicated a need to alter the transformation from the reservoir grid co-ordinate system to the Amersfoort x-y co-ordinate system (the land co-ordinate system used in The Netherlands). The reservoir pressure distributions above are oriented North-South and East –West, but as can be seen by the reservoir structure map, the reservoir is actually rotated 15.5 degrees from the Amersfoort x-y system. The center of each reservoir grid was then represented by polar coordinates which was then converted to an 'Amersfoort x-y' polar coordinate system and then easily

converted to the actual Amersfoort x-y system. A sample calculation is shown below;

SimX	SimY			Sim Polar, h	Sim Polar, theta	Amersfoort Polar, h	Amersfoort Polar, gamma	90-Gamma	Amers X	Amers Y
1	1			219.20	45.00	219.20	60.50	29.50	158540.78	572507.94
1	1			=SQRT((A3-0.5)^2+(B3-0.5)^2)*310	=ATAN2(A3-0.5,B3-0.5)*180/PI()	=E3	=F3+15.5	=90-H3	=158350+G3*COS(I3*PI()/180)	=572400+G3*SIN(I3*PI()/180)

These changes in reservoir model geometry have provided a more accurate representation of the physical reservoir in the lateral extensions but have very little impact in the central area of the reservoir subjected to the highest pressure depletion. As such, the maximum calculated subsidence of each model year is unchanged from the previous model results, but the lateral extensions of the subsidence area are slightly affected with the impact of making more natural looking subsidence contours (less square or geometric as was evidenced in earlier models).

Results of Rock Compaction Coefficient, C_m, Review

As previously indicated in this report, the maximum value for C_m obtained in the rock mechanic laboratory testing was $4.86E^{-5}$/Bar and this was used in the previous modelling work. While this value was possible to achieve in the laboratory, the corresponding reservoir pressure to replicate this value is below the abandonment pressure of the reservoir. Such a high compaction coefficient was used in the earlier model to provide a cautious approach in simulating the gas caused subsidence (the result was forcing an over prediction of gas caused subsidence), but was not justified as it did not accurately represent the physical reality of what must be occurring in the reservoir. Therefore, the value of C_m used for the revised modelling was $3.92E^{-5}$/Bar corresponding to the maximum brine saturated compaction coefficient found in laboratory testing that is indicative of reservoir pressures above abandonment pressure.

Also, the concept of increasing the compaction coefficient over time was dropped and a constant C_m factor was used throughout the reservoir life. This reflects the idea that the actual change in pressure over the producing life of the reservoir changes the stress on the reservoir rock very slightly. Earlier iterations used almost the entire range of the laboratory testing, while the latest model honours the principle that stress induced by depressuring the reservoir to abandonment conditions actually occurs in a limited range on the strain-stress curve.

Results of Water Leg Depressurization Review

The former reservoir model had uniform reservoir thickness for each of the three pools (North, East, and South). The model was revised with varying gas zone thicknesses to more accurately reflect the reservoir structure map. The 'gas zone' is defined as having a water Saturation, S_w, of less than 50%. The resulting gas height map shows a tapering of height above the gas-water contact towards the edge of the reservoir, as one would expect to see in a net pay isopach.

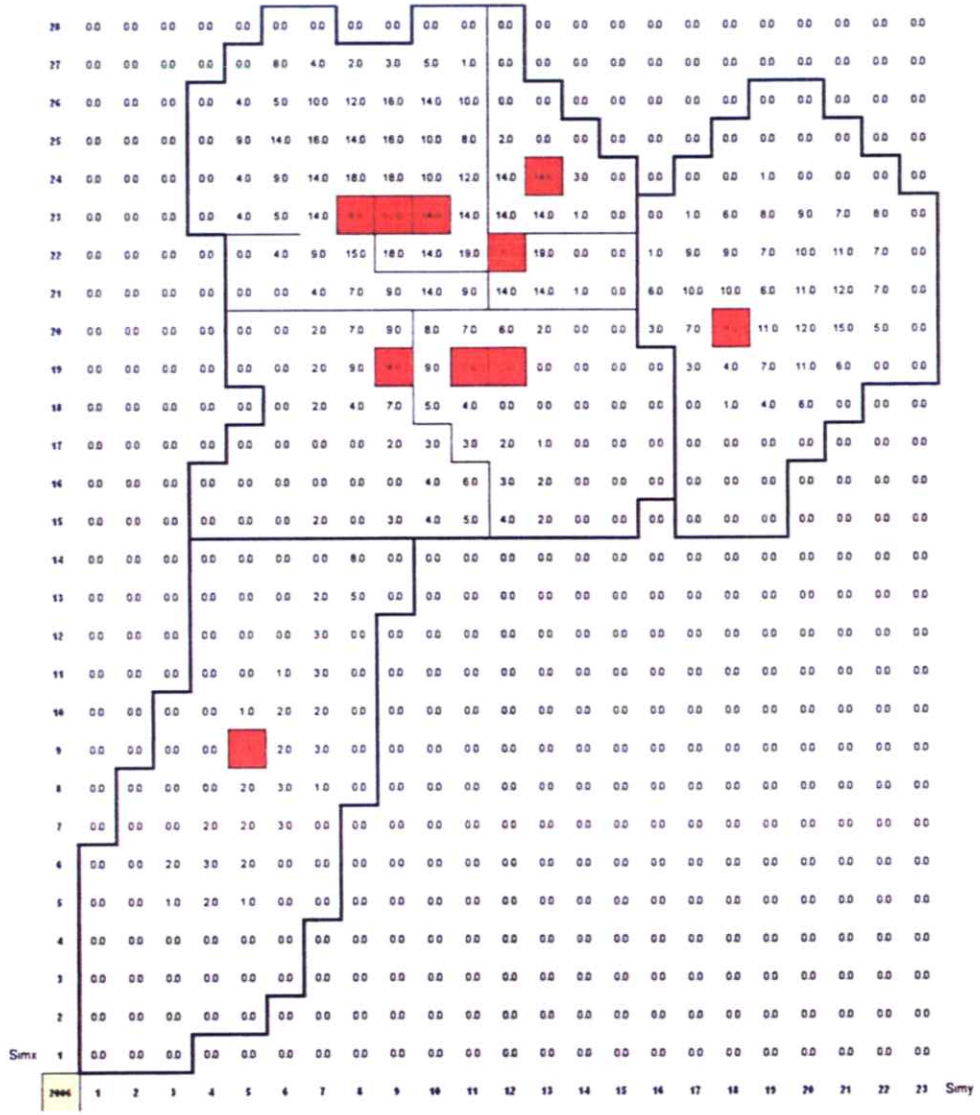

The transition zone is generated from the same structure map, but this time defined as being that region which is between 50 – 100% water saturation. This results in the following thickness distribution (in meters);

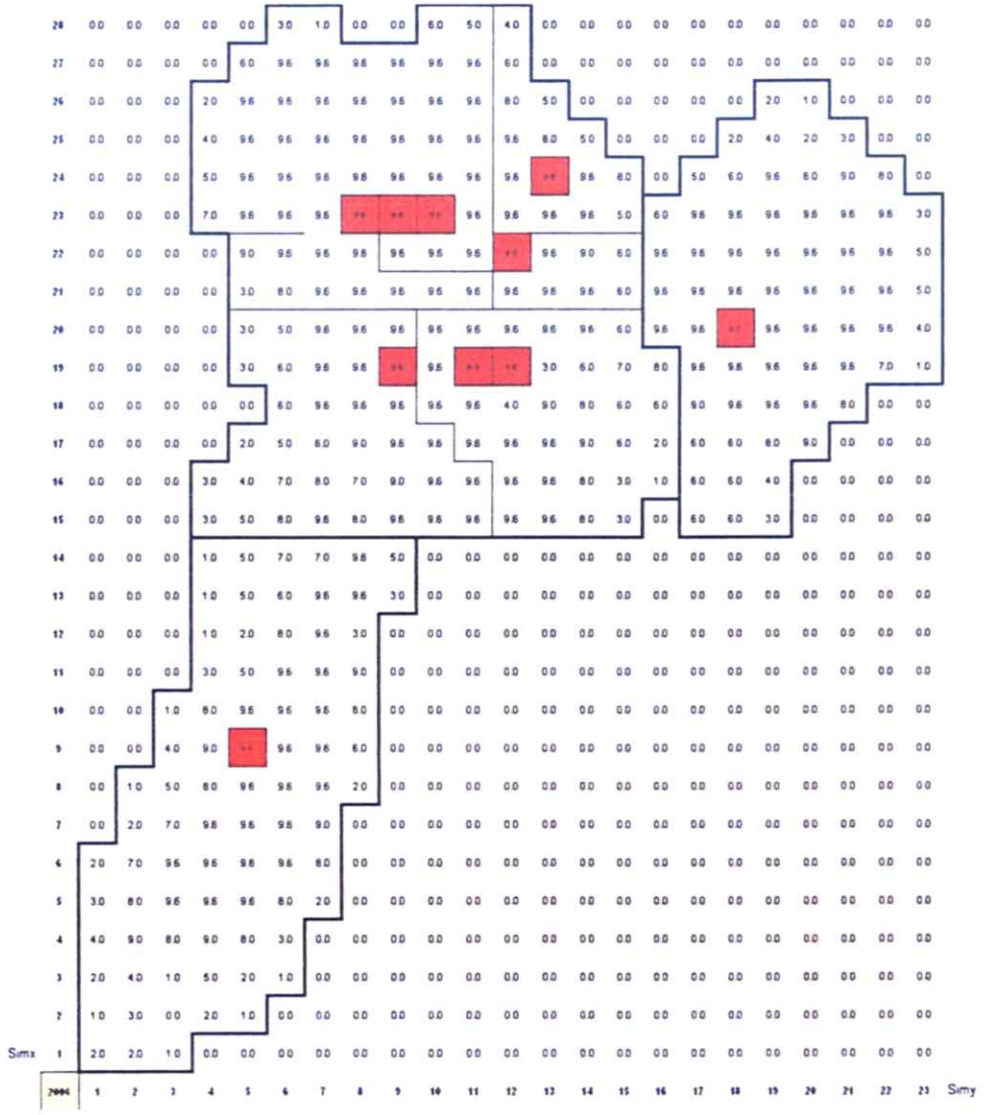

Previously, the water zone beneath the gas-water contact (defined, in the former model, at S_w=100%) was considered incapable of depressurization due to low porosity, low water rates, no evidence of pressure support on the P/z plots and the presence of tight unconformities in the chalk. The current model incorporates water leg depressurization since the low porosity below 100% water saturation provides a very small volume for depressurization, it is quite likely this effect would not be evident on a P/z plot. Also, the tight porosity would not provide much incremental water production, again as the affected volume is very low. The layers of tight unconformities will limit the

maximum depth of depressurization into the water leg, but it is possible to have some depressurization occur. The thickness of water leg depressurization is a function of the thickness of the transition zone – the area of the reservoir with the thickest, best developed pay zone would intuitively have the ability to depressurize deeper into the water leg.

The affected water zone thickness was iterated for each surface levelling surveying year to give the lowest root mean square value of the difference between modelled and measured for the surveyed data. The resulting water leg thicknesses for the relevant data sets are as follows;

For 1997;

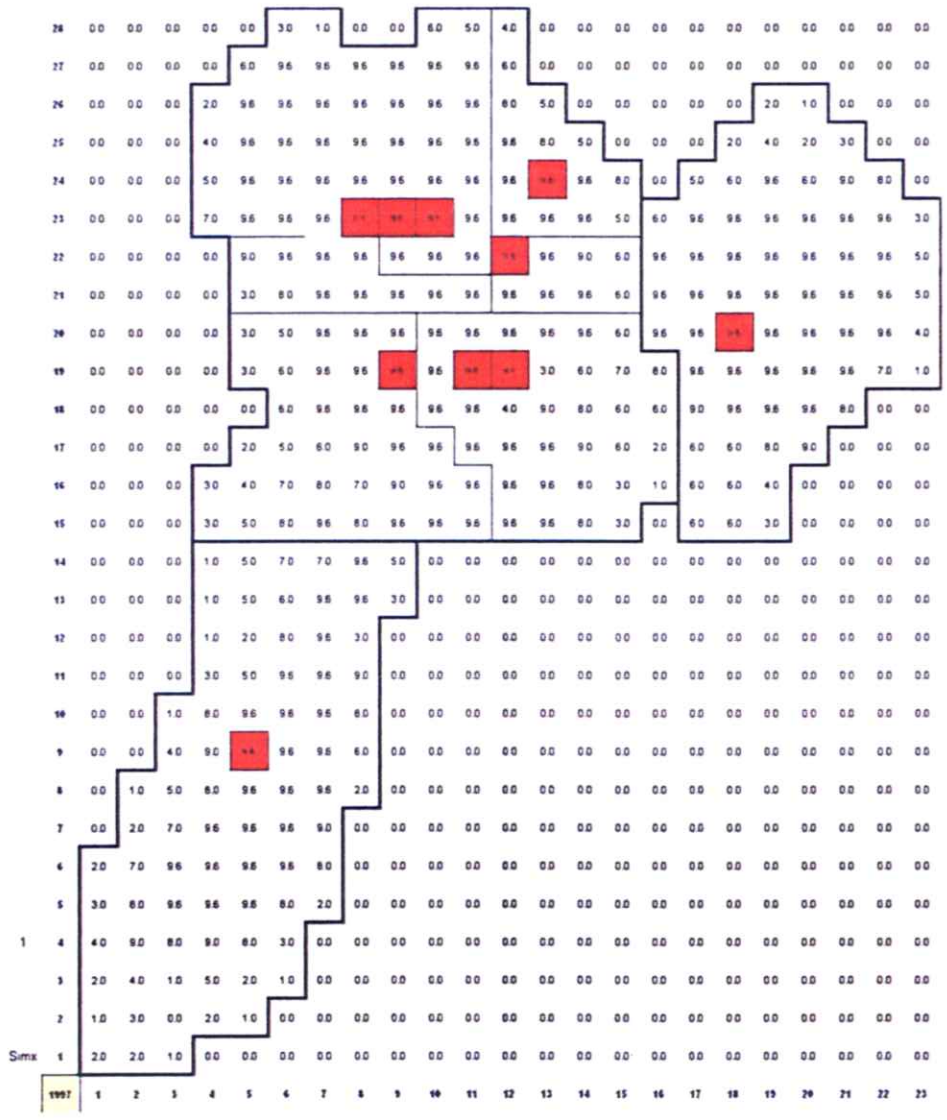

For 2000;

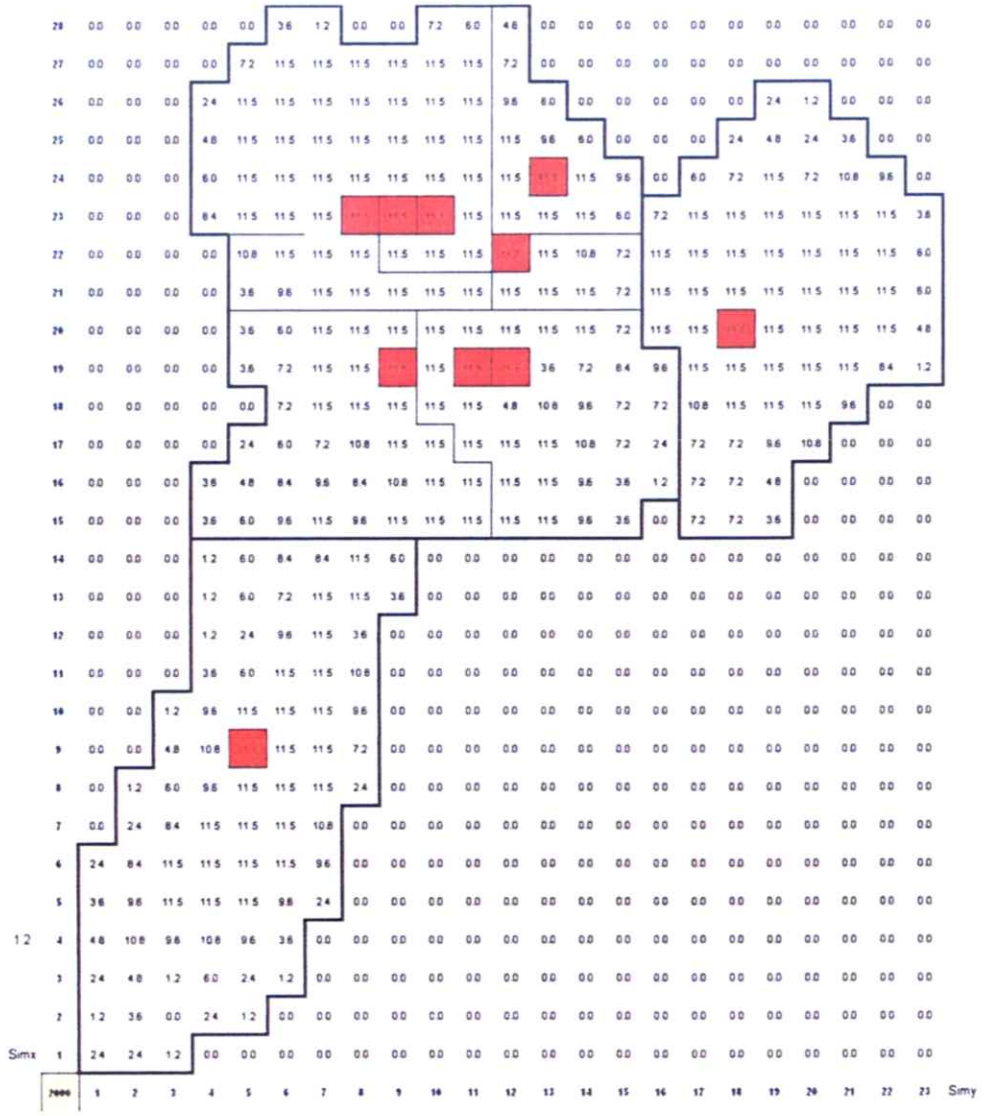

For 2003;

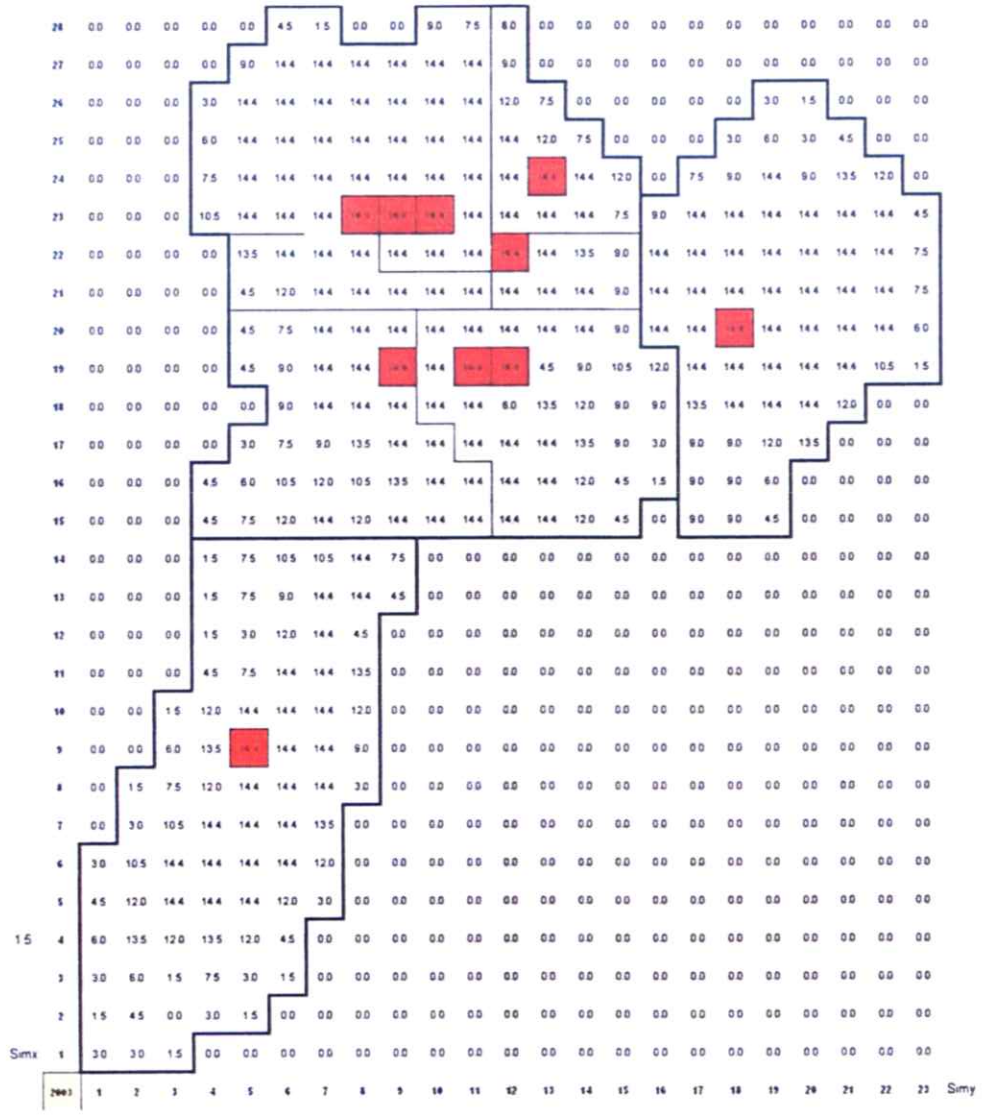

For 2006;

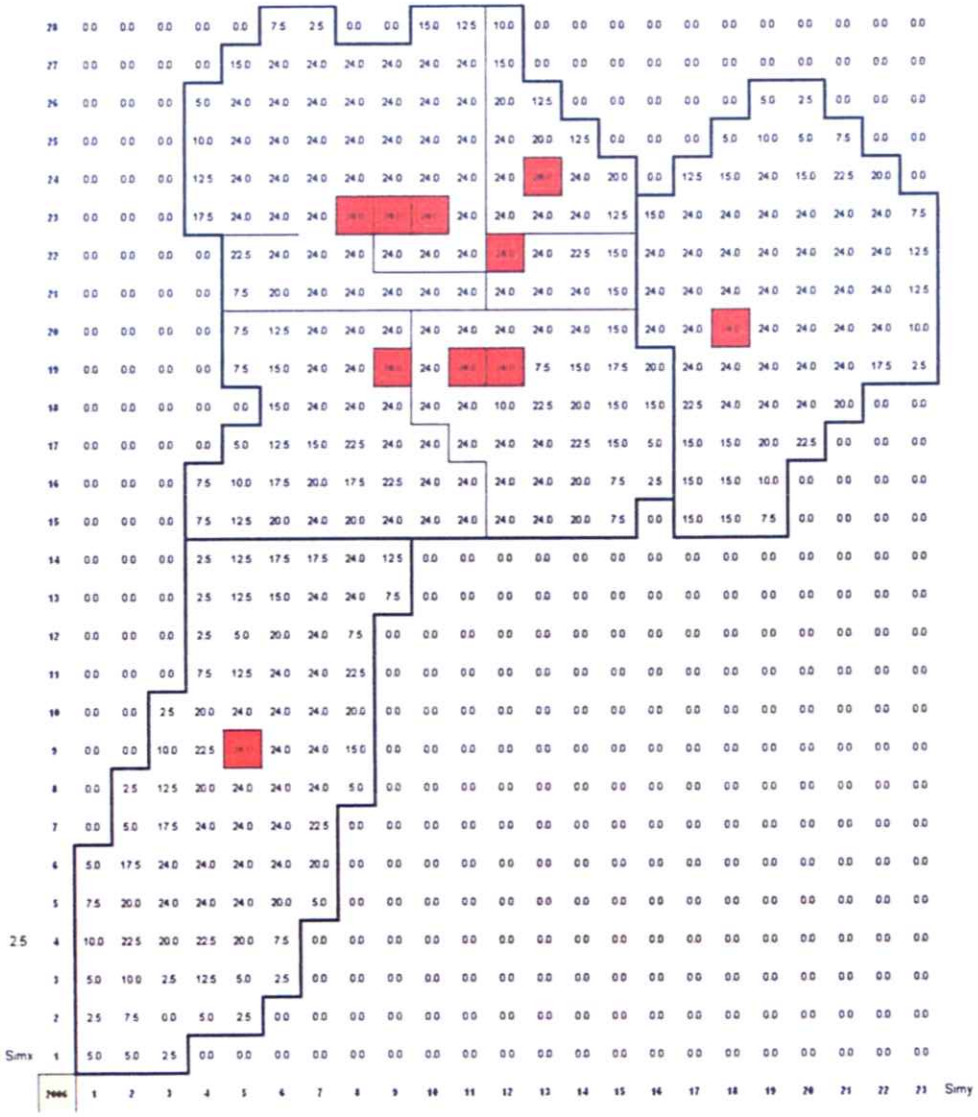

The 2006 data gives the following total affected thickness (gas, transition and water zone) distribution as follows;

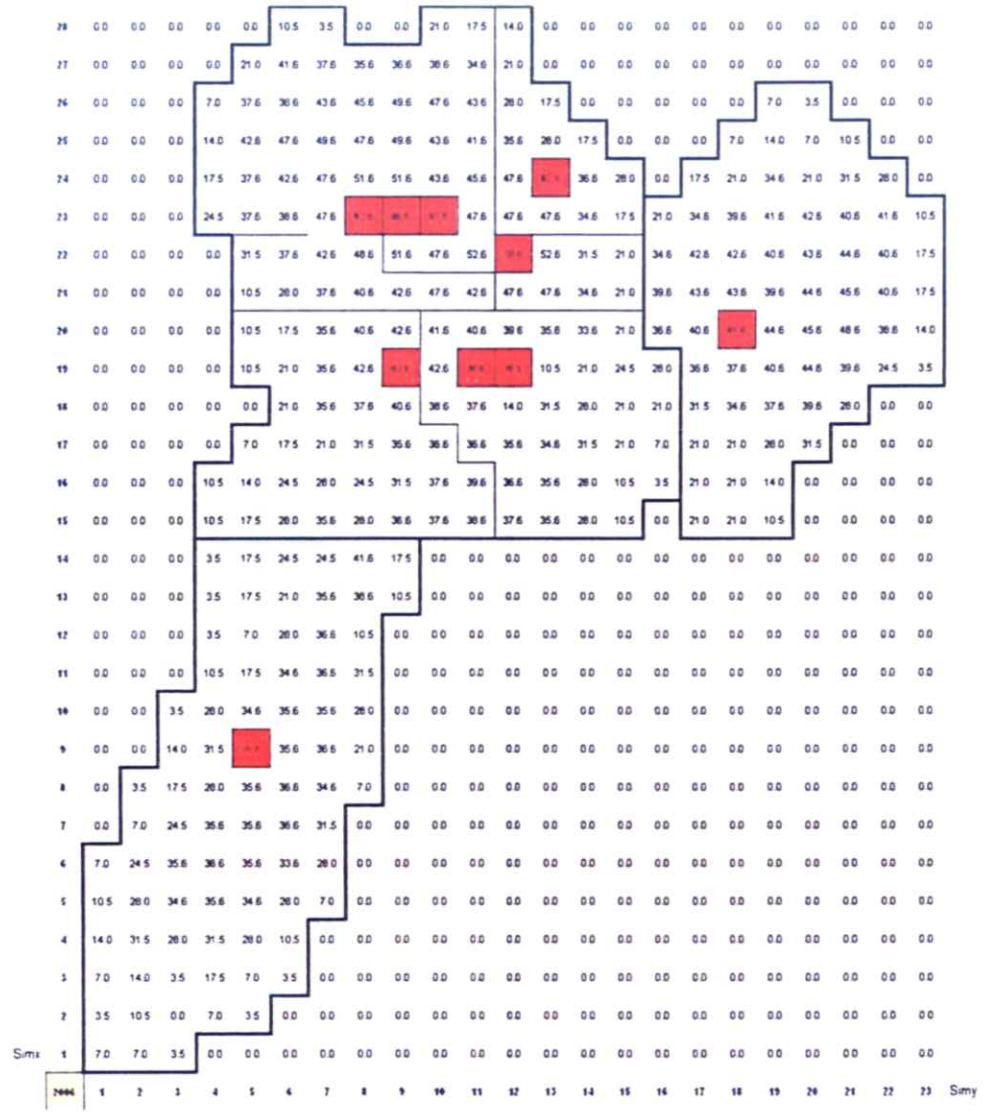

This gives a maximum thickness of 58.6m which log data would suggest is the maximum affected thickness due to tight unconformities and the very low porosity. This same thickness distribution is used for the 2016 prediction.

Surface Subsidence Measurement Quality Study (in progress)

The previous subsidence study had used the three deep founded survey markers of quality construction as a confirmation of the subsurface modelling work. The latest subsurface modelling has been compared to levelling points in the area (deep founded and shallow, regardless of construction quality) in an attempt to identify areas of concern for the surface benchmark surveying campaigns. A summary of the preliminary comparison is shown below.

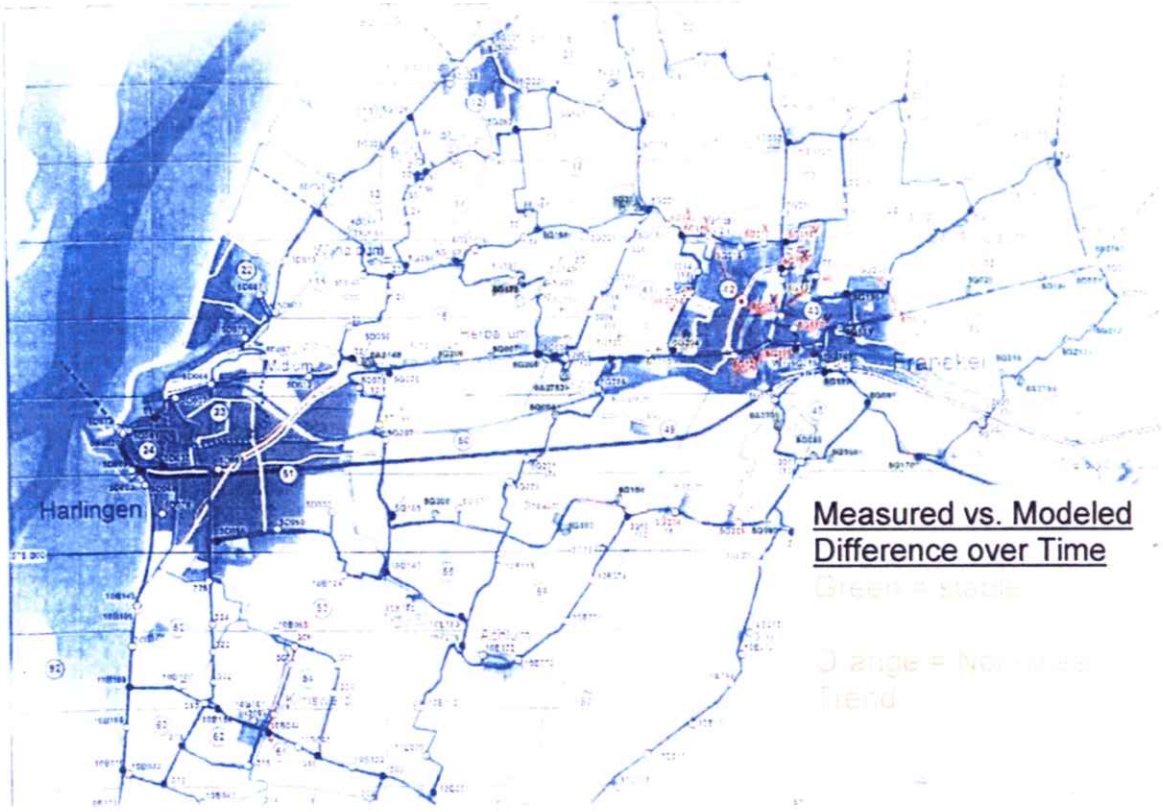

Measured vs. Modeled Difference over Time

The following graphs display the difference between measured subsidence (measured = surface benchmark survey value – theoretical salt caused subsidence) and modeled gas caused subsidence. The scale is in centimeters and positive values indicate measured is greater than modeled

subsidence.

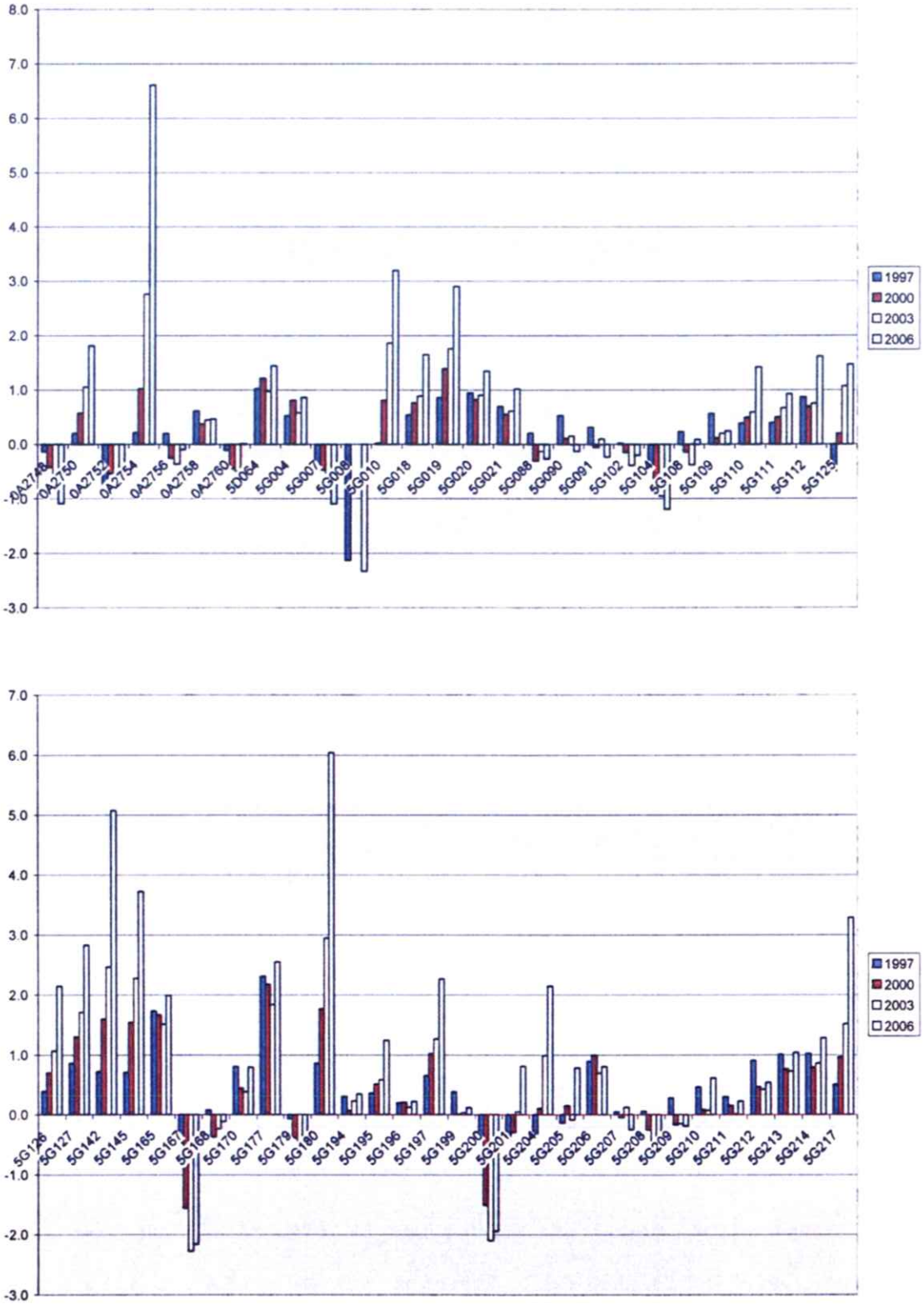

A study into the quality of surface benchmark surveying is currently ongoing.

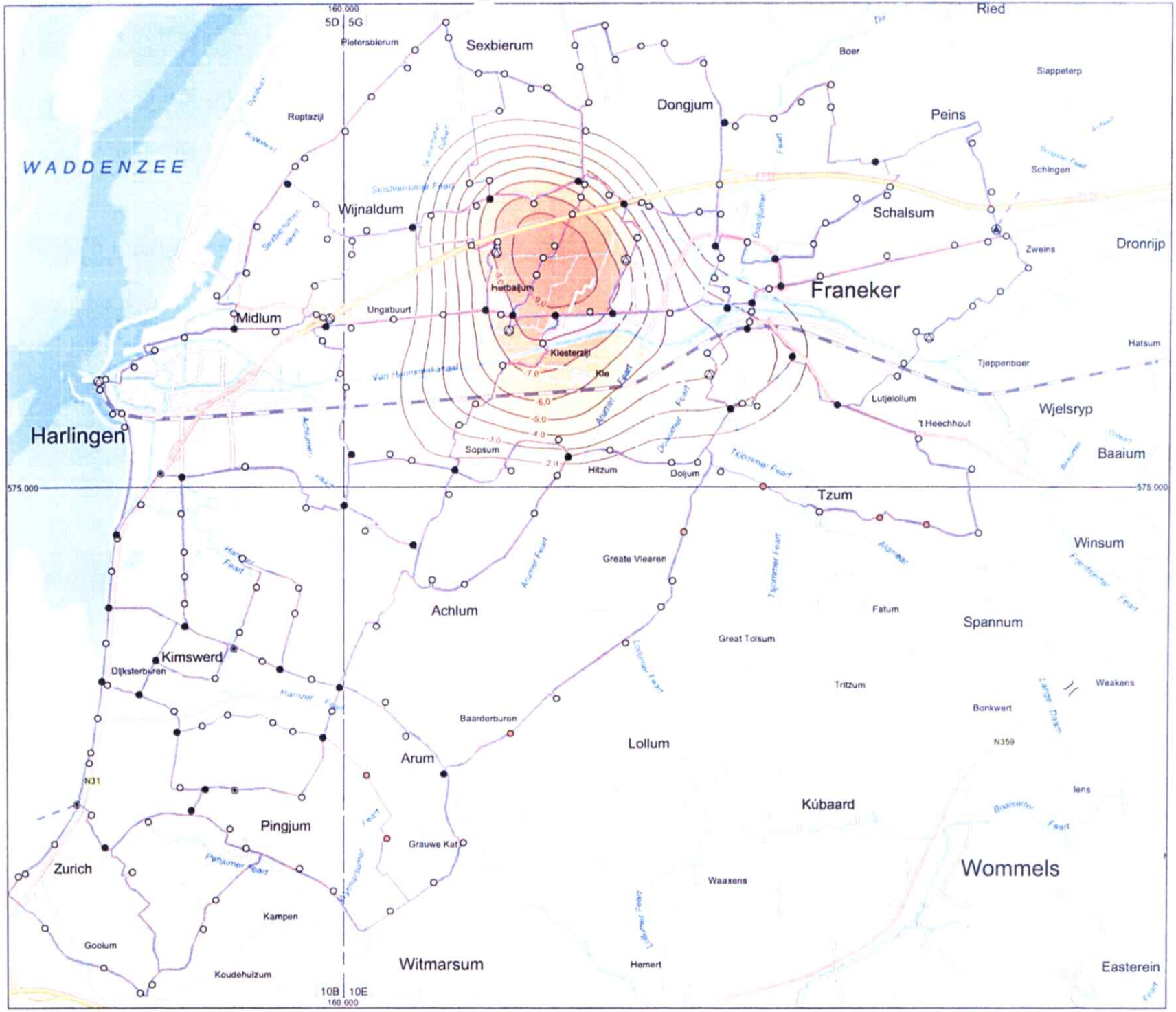
160.000
5D | 5G
Pietersbierum
Sexbierum
Ried
Boer
Slappeterp
Dongjum
Peins
Roptazijl
WADDENZEE
Schingen
Wijnaldum
Schalsum
Dronrijp
Zwelns
Franeker
Midlum
Ungabuurt
Hatsum
Tjeppenboer
Lutjelollum
Wjelsryp
't Heechhout
Harlingen
Sopsum
Hitzum
Doljum
Baaium
575.000
Tzum
Winsum
Greate Viearen
Achlum
Fatum
Spannum
Great Tolsum
Kimswerd
Dijksterburen
Tritzum
Weakens
Bonkwert
Baarderburen
N359
Arum
Lollum
N31
Iens
Kúbaard
Pingjum
Grauwe Kat
Zurich
Waaxens
Wommels
Kampen
Goolum
Witmarsum
Hemert
Easterein
Koudehulzum
10B | 10E
160.000
Verklaring
waterpastraject
hoogtemerk
hoogtemerk / knooppunt
hoogtemerk / aansluitpunt
ondergrondsmerk
nieuw te plaatsen meetpunt
5D bladnummer peilmerkenkaart RWS
575.000 RD-coördinaten (in meters)
bodemdaling in cm
0
1.0
2.0
3.0
4.0
5.0
6.0
7.0
8.0
9.0
10.0
11.0
12.0
13.0
VERMILION
150599-lwh-2006 0
BODEMDALINGSKOM DOOR GASWINNING 2006
Winningsvergunning Leeuwarden - West
Schaal 1:50.000

Conclusions and Revised Subsidence Contours

The current gas caused subsidence model is a more accurate depiction of the physical subsurface environment than the earlier model presented in May. The ultimate subsidence values are unchanged, as the former and current models have little net changes near the center of the subsidence bowl. However, the less affected radial edges of the reservoir are now better defined, resulting in smoother contours and a better conceptual model.

The revised gas caused subsidence contours for both 2006 and 2016 are attached below.

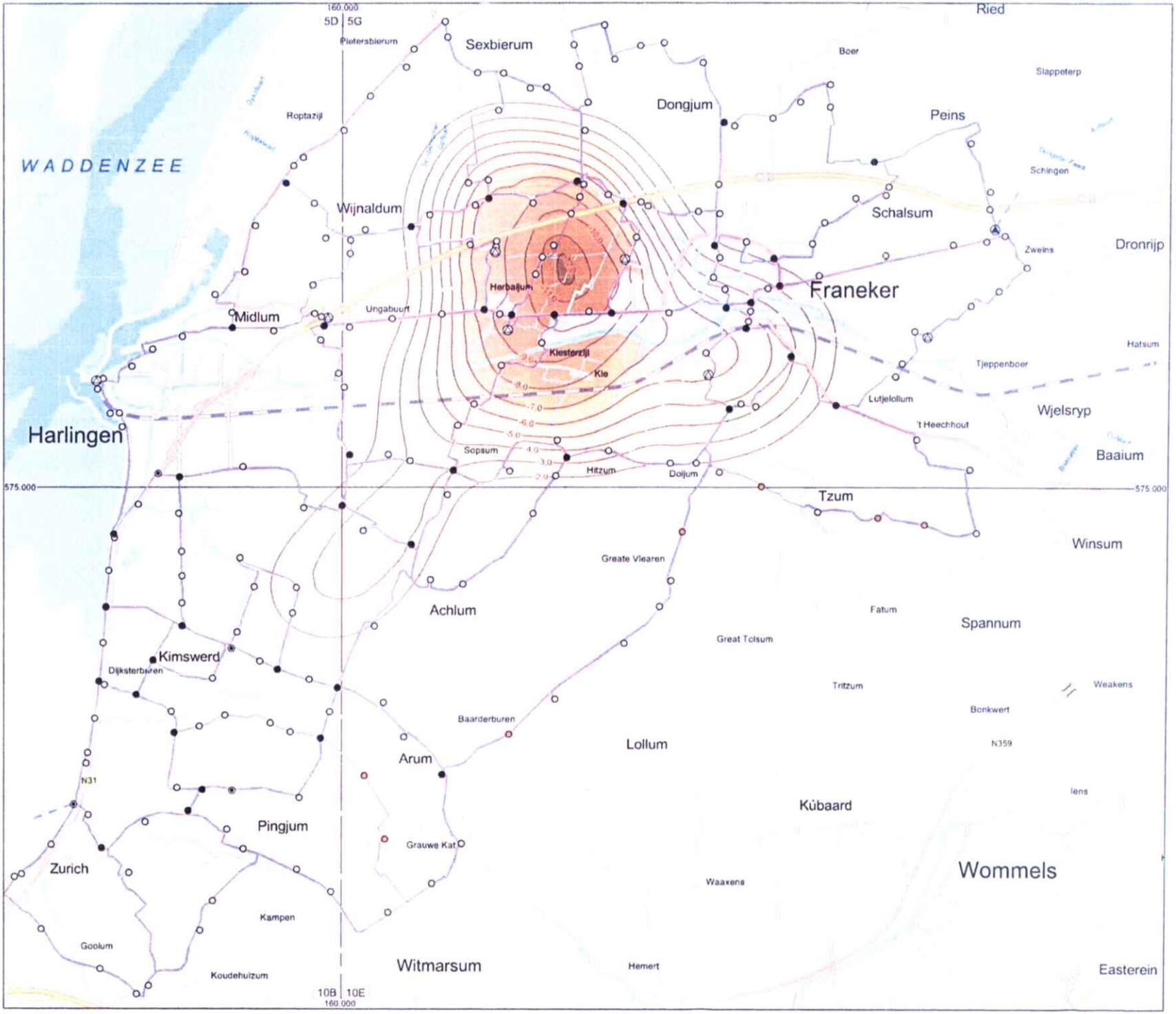
160.000
5D | 5G
Pietersbierum
Sexbierum
Ried
Boer
Slappeterp
Dongjum
Peins
Roptazijl
WADDENZEE
Schingen
Wijnaldum
Schalsum
Zweins
Dronrijp
Herbaijum
Franeker
Midlum
Ungabuurt
Hatsum
Kleasterzijl
Kle
Tjeppenboer
Lutjelollum
Wjelsryp
't Heechhout
Harlingen
Sopsum
Hitzum
Doljum
Baaium
575.000
575.000
Tzum
Winsum
Greate Vlearen
Achlum
Fatum
Spannum
Great Tcisum
Kimswerd
Dijksterburen
Tritzum
Weakens
Bonkwert
Baarderburen
N359
Lollum
Arum
N31
Iens
Kûbaard
Pingjum
Grauwe Kat
Zurich
Wommels
Waaxens
Kampen
Goolum
Witmarsum
Hemert
Easterein
Koudehuizum
10B | 10E
160.000
Verklaring
waterpastraject
hoogtemerk
hoogtemerk / knooppunt
hoogtemerk / aansluitpunt
ondergrondsmerk
nieuw te plaatsen meetpunt
5D bladnummer peilmerkenkaart RWS
575.000 RD-coördinaten (in meters)
bodemdaling in cm
0
1.0
2.0
3.0
4.0
5.0
6.0
7.0
8.0
9.0
10.0
11.0
12.0
13.0
150599-lwh-2016 0
VERWACHTE BODEMDALINGSKOM DOOR GASWINNING 2016
Winningsvergunning Leeuwarden - West
Schaal 1:50.000